Ohio Department of Transportation
Library
1980 West Broad St.
Columbus, OH 43223
614-466-7680

14702

Pavement Performance Testing

Final Report
December 2001

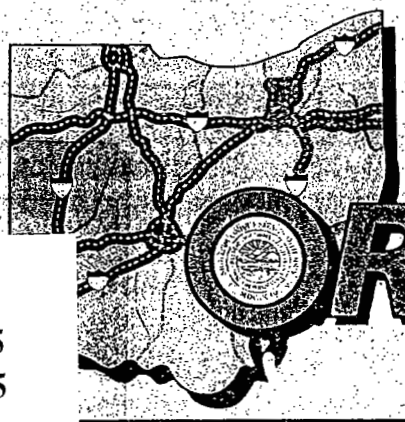

Ohio Research Institute
for Transportation
and the Environment

ORITE

TE
251.5
.S425
2001x

Stocker Center
Ohio University
Athens, OH
45701-2979

1. Report No.	2. Government Accession No.	3. Recipient's Catalog No.
FHWA/OH-2001/14		3 1980 00025 8042

4. Title and subtitle.	5. Report Date
Pavement Performance Testing	December, 2001
	6. Performing Organization Code
7. Author(s)	8. Performing Organization Report No.
Dr. Shad Sargand and Dr. Sang-Soo Kim	
	10. Work Unit No. (TRAIS)
9. Performing Organization Name and Address	11. Contract or Grant No.
Ohio University Department of Civil engineering College of Engineering & Technology Stocker Center Athens, Ohio 45701	State Job No. 14702(0)
	13. Type of Report and Period Covered
	Final Report
12. Sponsoring Agency Name and Address	14. Sponsoring Agency Code
Ohio Department of Transportation 1980 W Broad Street Columbus, OH 43223	

15. Supplementary Notes

16. Abstract

The objectives of this study were to evaluate the effects of aggregate gradation and polymer modification on rutting and fatigue resistance of Superpave mixes. Asphalt mixes were prepared using three different gradations (above, through, and below the restricted zone) and three PG 70-22 binders (unmodified, SBS and SBR modified), and were evaluated using a triaxial repeated load test, a static creep, the Asphalt Pavement Analyzer, and the flexural beam fatigue test. When aggregates meeting Superpave angularity requirements was used, the effects of gradation on the rut and fatigue resistance of Superpave mixes were relatively small and the effects of the restricted zone was not significant. Even though binders used in this study had similar dynamic shear moduli, mixes containing polymer modified binders showed significantly lower resilient moduli than the unmodified mixes when measured in the indirect tensile and triaxial compressive modes. All laboratory test results indicated that the polymer modified mixes were significantly more rut resistant and fatigue resistant than the unmodified mixes with the same PG grading. Improvement in rut resistance due to polymer modification was shown to be most significant in the triaxial repeated load test, especially at a higher temperature. Accelerated Pavement Load test results showed the similar trends regarding rutting performance. At higher test temperature or at a fast wheel speed, mixes with polymer modified binder performed better than mixes with an unmodified binder.

17. Key Words	18. Distribution Statement
Superpave, restricted zone, polymer modified, gradation, rutting, fatigue, accelerated load test, triaxial repeated load test, creep, flexural beam fatigue test, APA	No Restrictions. This document is available to the public through the National Technical Information Service, Springfield, Virginia 22161

19. Security Classif. (of this report)	20. Security Classif. (of this page)	21. No. of Pages	22. Price
Unclassified	Unclassified		

PAVEMENT PERFORMANCE TESTING

Report No. FHWA/OH-2000/14

FINAL REPORT

Shad M. Sargand
Sang-Soo Kim

Prepared in cooperation with the Ohio Department of Transportation
and the U.S. Department of Transportation, Federal Highway
Administration

"The contents of this report reflect the views of authors who are responsible for the facts and the accuracy of the data presented herein. The contents do not necessarily reflect the official views or policies of the Ohio Department of Transportation or the Federal Highway Administration. This report does not constitute a standard, specification or regulation."

OHIO RESEARCH INSTITUTE FOR TRANSPORTATION AND THE ENVIRONMENT
CIVIL ENGINEERING DEPARTMENT
OHIO UNIVERSITY

December, 2001

ACKNOWLEDGEMENTS

The support of this research by the Ohio Department of Transportation (DOT) is gratefully acknowledged. The authors wish to extend sincere appreciation to the engineers of the Ohio DOT, especially David Powers, Roger Green, Brad Young, and Monique Evans for their support, cooperation, and counsel. The authors would also like to thank Roger Hayner and Steve Jones, Marathon-Ashland Petroleum LLC. and Larry Shively, Shelly Co., for supplying the asphalts and aggregates used in this study. Kalyan-Reddy Asam, William Edwards, Issam Khoury, Michael Krumlauf, and Alan Moran contributed to this project in various capacities.

TABLE OF CONTENT

LIST OF TABLES

LIST OF FIGURES

CHAPTER 1

INTRODUCTION

1-1 Overview

Recently, Ohio Department of Transportation (ODOT) adopted Superpave in their asphalt mix design procedure. The newly introduced Superpave is a comprehensive asphalt mixture design system intended to ensure good field performance of long-lasting asphalt pavements under various traffic loading and climatic conditions. However, there are some concerns in implementing Superpave because this new design procedure has not been rigorously validated. Aggregate gradation criteria and the applicability of Superpave to modified asphalt mixture systems are two important issues that need to be addressed.

One of the characteristics of the aggregate gradation criteria in Superpave is the restricted zone. This is a zone lying on the maximum density curve between the 300 μm sieve and the 2.36 mm sieve size through which it is considered undesirable for the gradation to pass [1]. The restricted zone is intended to discourage the use of fine sand or natural sand, in order to achieve adequate voids in mineral aggregate (VMA). However, the restricted zone criteria were developed through a Delphi Method, a consensus process among a group of individuals without experimental work and validation. In some states it has been indicated that some of their standard mixes with acceptable field performance are passing through the restricted zone and are considered to be undesirable according to the Superpave criteria [2]. To prevent systematic rejection of good economical mixes by the restricted zone criteria, the effects of the restricted zone on the performance of asphalt pavement need to be determined.

Due to increased traffic loading and traffic volume, the use of modifiers in hot mix asphalt has become a very popular practice. ODOT requires the use of polymer modified binders in construction of high stressed asphalt pavements. However, the applicability of Superpave to the modified asphalt mix has not been properly validated through field tests. Results of recent laboratory studies suggest that binders with the same Superpave Performance Grade (PG grade) but prepared using different modifier types and methods could result in different field performance [3,4].

1-2 Research Objectives

This research project has the following three objectives.

1. To determine the effect of aggregate characteristics and gradation and polymer modifier on pavement rutting and fatigue performance.
2. To obtain data for the development and verification of the mechanistic empirical design approach for flexible pavement.
3. To determine the correlation of predicted performance of pavement system by laboratory methods with accelerated load test.

Seven laboratory test methods, the Asphalt Pavement Analyzer (APA), a triaxial repeated load test, a uniaxial static creep test, a flexural beam fatigue test, the indirect tensile resilient modulus test, the indirect tensile strength test, and a moisture susceptibility test, were employed to evaluate the rutting resistance, fatigue cracking resistance, and moisture susceptibility of the mixtures. Two types of aggregate, 3 aggregate gradations, and 3 types of asphalt binder were used to prepare test specimens. Following the laboratory evaluation and based on its results,

three mixes were chosen in cooperation with ODOT personnel. Using these mixes, three test pads were constructed at the Accelerated Pavement Load Facility located at the Ohio University Lancaster campus and loaded with a super-single wheel to determine rut resistance and pavement responses under various wheel loading.

CHAPTER 2

LITERATURE REVIEW

The Superpave system is a comprehensive asphalt mix design procedure introduced as a major final product of the Strategic Highway Research Program (SHRP). It includes performance graded (PG) binder specifications, aggregate specifications, a mix design procedure using a gyratory compactor, performance based testing, and performance prediction of mixes. In Superpave, performance of unmodified and modified asphalt binder is assured by determining temperatures at which certain rheological properties of binder are within the critical limit values. Specifications of Superpave aggregate include gradation requirement, consensus, and source properties. Consensus properties include coarse and fine aggregate angularity, flat and elongated particle and clay content. The coarse and fine aggregate angularity is specified to achieve a high degree of internal friction and high shear strength to resist rutting. The flat and elongated particle criteria are to avoid the breaking of aggregates during handling, construction, and later by traffic. By placing limitations on the amount of clay in aggregates, the bond between the aggregates and the asphalt binder is strengthened. The properties related to the aggregate source in the Superpave are toughness, soundness, and deleterious materials [5].

Performance of asphalt pavements is usually measured against four major distress modes: rutting, fatigue cracking, low temperature cracking and moisture damage. In this chapter, factors affecting asphalt pavement performance including the four major distress modes are reviewed.

2.1 Factors Affecting Rutting

Rutting or permanent deformation of a pavement is caused by the repeated application of heavy traffic load at high temperatures and appears as longitudinal depressions in wheel paths accompanied by small projections to the sides [6-8]. The pavements that undergo rutting pose serious safety problem due to the trapping of water by the ruts, which would cause hydroplaning and accumulation of ice [9]. The lack of shear resistance of mixes and heavy loading (high traffic volume, tire pressures, and axle loads) are major cause of rutting [10-15]. Densification of insufficiently compacted pavement by traffic also contribute to rutting. Rutting is a complex phenomenon in which aggregate, asphalt and asphalt-aggregate mixture properties play an important role. Use of stiff asphalt binders and aggregate of rough surface texture, cubical shape, and proper gradation for stone-on-stone contact minimizes rutting [7,16]. An important mix property contributing to the rutting phenomena is the amount of air void content in the asphalt mix. When air void content is too low either due to too high asphalt content or too low void in mineral aggregate, the pavement may experience severe rutting [10]. At this level of air void, the asphalt binder reduces the contact between the aggregate particles by acting as a lubricant between them [13].

2.2 Factors Affecting Fatigue Cracking

Fatigue cracking is a failure mode caused by the repeated application of traffic load. This type of cracking is also known as "alligator cracking", because the crack pattern is similar to the pattern on an alligator's back [16,17]. The initial stages of fatigue cracking can be recognized by the presence of periodic longitudinal wheel path cracks, i.e., the cracks occurring in the direction

of traffic. The cracks occupy a small area initially but gradually propagate and become large cracks due to repeated application of the traffic loading [18].

Fatigue cracking is affected by various mix characteristics such as asphalt type, aggregate type, and air voids [18,19]. In order to minimize fatigue cracking, soft elastic binders [7,16,20,21] and crushed fine aggregates [22] should be used. Lower air void content or higher asphalt content in the mix will also reduce fatigue cracking [20,23]. Since fatigue cracking is a load related problem, the insufficient thickness of the pavement for the given loading condition may also cause fatigue cracking. Fatigue cracking is further worsened by a lack of pavement drainage facilities that may lead to the saturation of pavement sub layers and, therefore, a loss of strength [17]. The saturated pavement experiences excess amounts of strain and undergoes premature cracking. Also, moisture may cause asphalt to strip off of aggregate possibly forming potholes.

2. 3 Factors Affecting Low-Temperature Cracking

Low temperature cracks appear in a transverse direction to the pavement (perpendicular to the direction of traffic) at regular intervals [16]. Cracks form when the thermal shrinkage stress caused by the temperature drop exceeds the tensile strength of the asphalt mix [7,17,24]. This cracking can occur from a sustained low temperatures [4] or repeated fluctuations in temperature [24,25]. Once low temperature cracking occurs, it spreads from the top of the pavement to the bottom layers. Stiffness of asphalt binder at low temperatures is the single most important material's property controlling low temperature cracking. A soft asphalt binder releases stresses

and prevent thermal cracking [26,27]. Use of asphalt binder of low age hardening potential is desirable to minimize low temperature cracking.

2.4 Factors Affecting the Moisture Susceptibility

Moisture-induced damage or stripping is another major concern when asphalt pavement related distresses are considered. The strength of hot mix asphalt pavement (HMA) comes from the strong interlock between aggregate and good adhesion between the aggregate and asphalt cement. Moisture damage occurs when water weakens the adhesion or bond between the asphalt cement and aggregate surface [17,28,29,30]. The stripping failure can be prevented by properly understanding the physicochemical aggregate-asphalt adhesion phenomena. Water may penetrate through the asphalt film and displace it from the aggregate [30]. Although both aggregate and asphalt binder are important, aggregate properties play a major role in stripping [29,30]. The hydrophilic aggregates (water loving, siliceous aggregates) are more prone to stripping problems. Binders with high stiffness better resist displacement by water than the low stiffness binders [17]. Where stripping is a problem, many antistripping agents are available to reduce the stripping potential of asphalt mixes [31,32].

2.5 Aggregate Gradation

Aggregate gradation plays a significant role in providing stability and durability to the asphalt mix [34]. In the Superpave mix design process, two requirements introduced for aggregate gradations are control points and the restricted zone. Figure 2.1 shows the 0.45-power-gradation chart consisting of control points, restricted zone and the maximum density line. Superpave requires that all gradations should pass between the control points and at the same

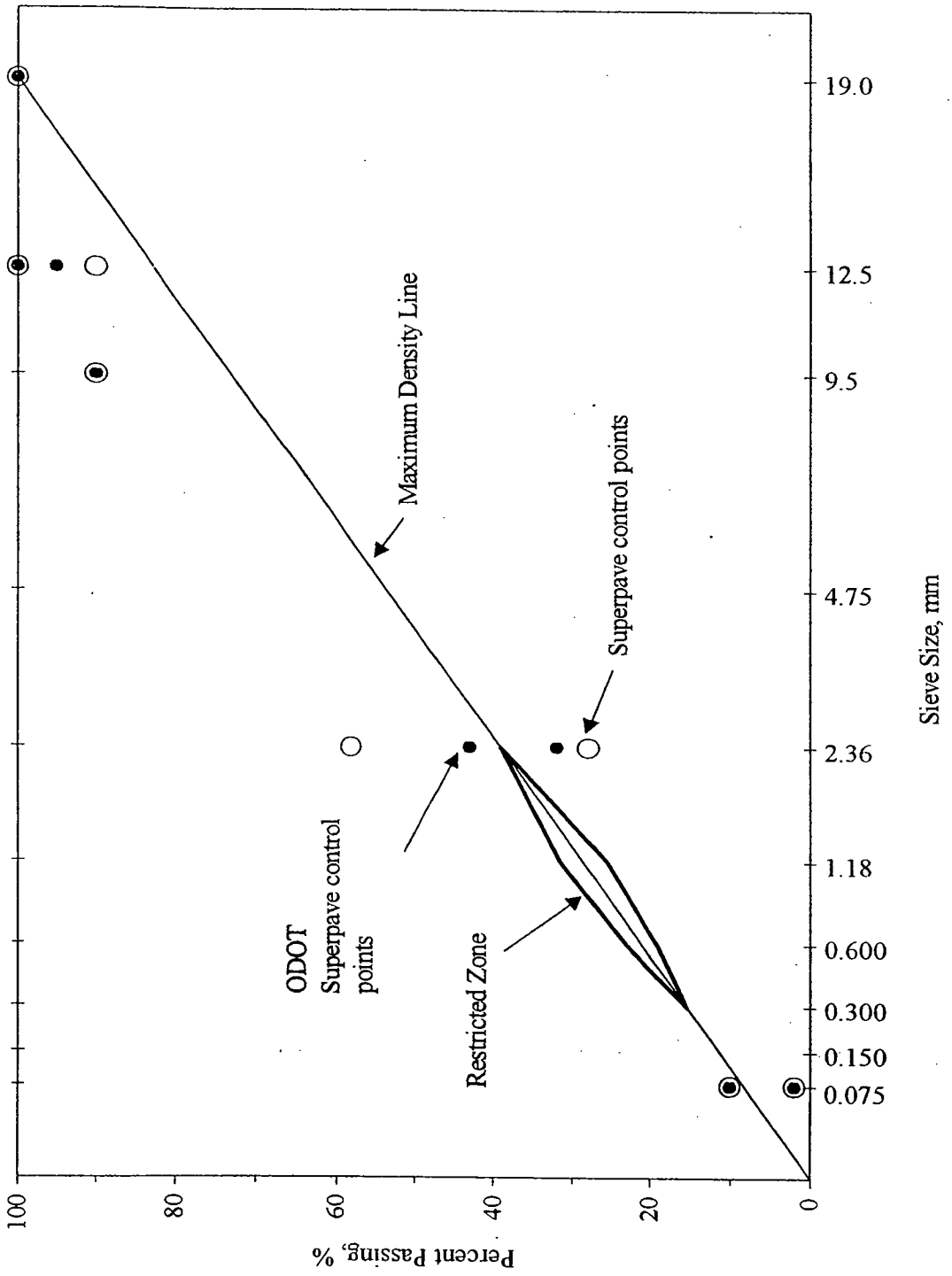

Figure 2.1 Gradation chart raised to 0.45 power of the Superpave mix design

time avoid the maximum density line and the restricted zone [5,34]. This provides a good aggregate structure that enhances rutting resistance and also achieves sufficient void space for mixture durability. These points control the top size of the aggregate, relative proportion of coarse and fine aggregates, and the amount of dust [34]. The purpose of the restricted zone is to discourage the use of fine natural sand in an aggregate blend [5]. The presence of excessive natural sand results in a mix that causes compaction problems during construction, contributing to reduced resistance to rutting. Also, the restricted zone prevents a gradation from following the maximum density line and having inadequate voids in mineral aggregates (VMA) [5,35]. Mixtures having insufficient VMA lack durability [5]. Superpave generally recommends that the gradations pass below the restricted zone (coarse gradation) to achieve improved mix performance [5,33]. However, recent studies [2,33,36,37] reported that the gradations passing above the restricted zone (fine gradation) could perform better than the gradation passing below the restricted zone. Also, gradations passing through the restricted zone could perform the same or even better than the other gradations that were not passing through the restricted zone.

2.6 Polymer-Modified Asphalts

In order to improve HMA performance, the practice of modifying the asphalt binder became common and polymers in particular have received widespread attention as the performance improvers of the asphalt binder [38]. Polymers significantly increase the stiffness of asphalt at high temperatures preventing permanent deformation, increase the strain tolerance improving the fatigue resistance at ambient temperatures, and soften binders at low temperature minimizing low temperature thermal cracking [39-45].

Polymers can be classified into two categories: elastomers and plastomers. Elastomers add only little strength to the binder at initial low strain level, but they can be stretched out and get stronger at higher strain level and recover when the applied load is removed. Plastomers form a rigid three dimensional network and provide tensile strength under heavy load but crack at higher strains. Two of the most commonly used elastomeric polymers are styrene-butadiene rubber (SBR) and styrene-butadiene styrene (SBS). SBS is a block copolymer and has a higher tensile strength than a randomly reacted SBR. For laboratory evaluation, use of dynamic tests which measure accumulated strain over a number of cycles is generally recommended, because the tensile strength of the elastomer varies as the strain level varies [46].

CHAPTER 3

MATERIALS AND TEST PROCEDURES

3.1 Aggregates

The aggregates used in this study were obtained from Ostander Quarry in Ohio. These aggregates were crushed limestone and were supplied in three sizes (#7, #8, and #10) by Shelly Company, Ohio. Three 12.5 mm nominal maximum size gradations (coarse, intermediate, and fine gradations) were chosen, in consultation with ODOT, to study the effects of gradations and the restricted zone. The limestone aggregates received from the quarry were dried, sieved separately, and recombined to form the three gradations. The gradations and properties of the combined limestone aggregates are given in Table 3.1. The gradations are also shown in Figure 3.1 together with the original Superpave control points and the ODOT Superpave control points. When drawn on the gradation chart raised to the 0.45 power, the coarse, intermediate and fine gradations pass below, through and above the restricted zone, respectively. The percent passing from 19.0 mm to 4.75 mm particle size were kept the same for all three gradations, while the percent passing for the particle sizes smaller than 4.75 mm varied. In this study, gravel aggregate was also used for a few additional laboratory tests. The gravel blend consisted with #8 rounded gravel, #10 screening, and natural sand -- all from Xenia Ohio and supplied by Martin Marietta Aggregate. The aggregates were blended in proportions of 60%: 20%: 20% (gravel: screening: sand). The gradation of the gravel aggregate meeting ODOT 441, Type 1 specification but not

Table 3.1. Gradation and aggregate properties

Sieve	Percent passing			
	Crushed Limestone			Gravel
	Coarse Aggregate	Intermediate Aggregate	Fine Aggregate	
3/4 "(19.0 mm)	100.0	100.0	100.0	100.0
1/2 "(12.5 mm)	97.0	97.0	97.0	100.0
3/8 "(9.5 mm)	88.0	88.0	88.0	92.2
#4 (4.75 mm)	62.0	62.0	62.0	48.0
#8 (2.36 mm)	32.0	39.1	46.0	32.8
#16 (1.18 mm)	19.0	28.6	35.0	22.2
#30 (0.600 mm)	14.0	21.1	26.0	14.6
#50 (0.300 mm)	10.0	15.5	19.0	7.0
#100 (0.150 mm)	7.0	9.0	10.0	4.0
#200 (0.075 mm)	5.0	4.0	4.0	2.9
Bulk specific gravity	2.568	2.568	2.568	2.620
Coarse Aggregate Angularity	100/100	100/100	100/100	--
Fine Aggregate Angularity	47	47	47	--

the Superpave specifications is also shown in Figure 3.1. It can be seen from Figure 3.1 that ODOT Superpave specifications require tighter control of aggregate gradation.

3.2 Asphalt Binders

For this study, two polymer modified binders (SBS and SBR modified PG 70-22), typically used for construction of the interstate systems and other heavy-duty pavements in Ohio, were supplied by Marathon Ashland Petroleum LLC, North Bend, Ohio. The unmodified PG 70-

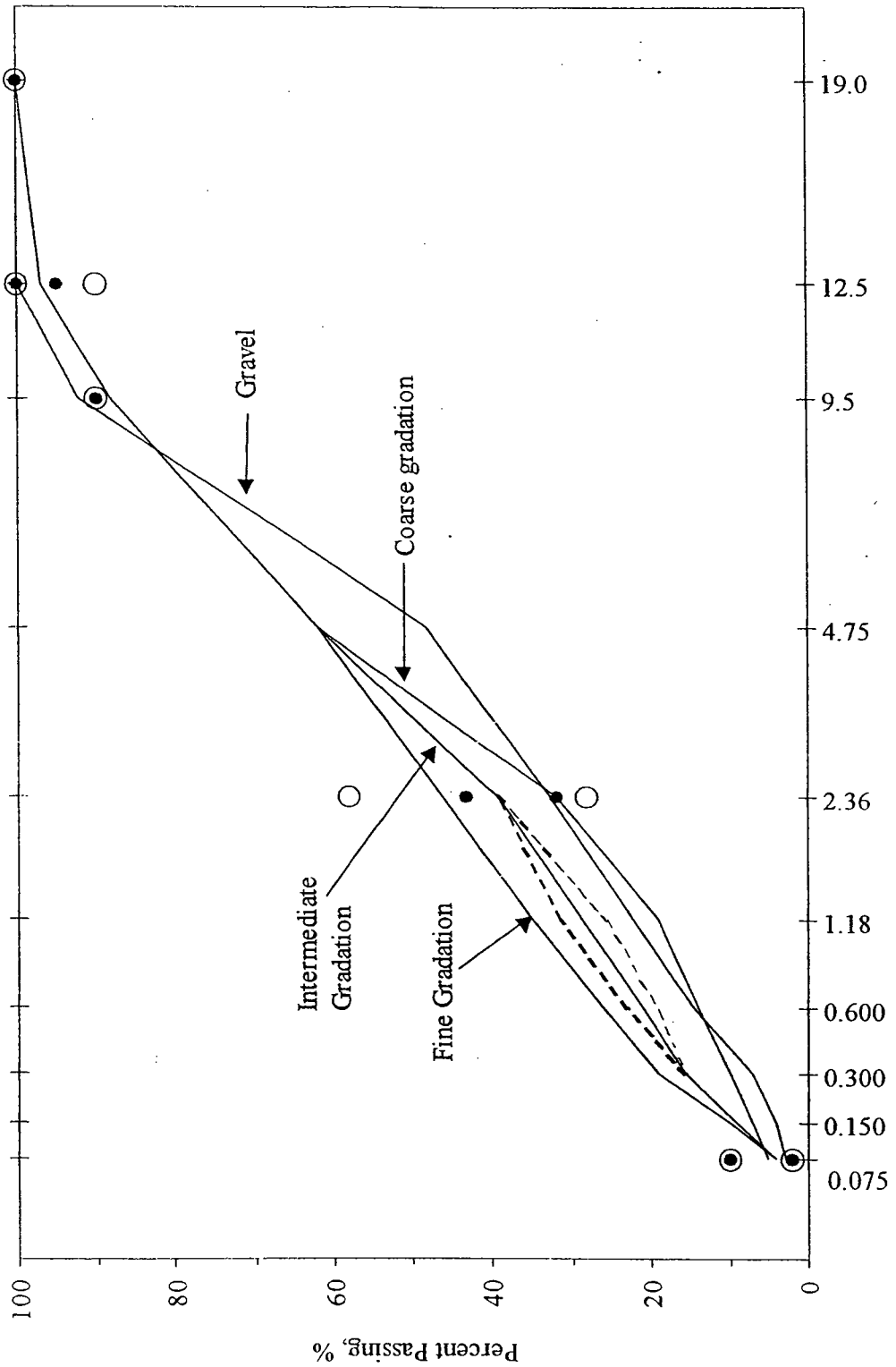

Figure 3.1 Gradations chart raised to 0.45 power of the aggregate

22 asphalt was also used in this study as a control. All three binders were prepared from the same base asphalt. The SBS modified binder was prepared by adding 3% radial SBS with intermediate molecular weight, while the SBR modified binder was modified with 3% high molecular weight SBR latex from Ultrapave. Rheological properties of the binder used in the grading process were given in Table 3.2. Even though these three asphalt binders were sold as the same PG grade, the actual grade was estimated to differ slightly. The actual continuous PG grades of the unmodified, SBS, and SBR modified binders were estimated to be PG 72-25, PG 77-23, and PG 76-26, respectively.

3.3 Test Procedures

This section describes the laboratory preparation of the specimens and test methods used in this study. Mix design followed the Superpave procedure. The cylindrical and beam test specimens were prepared using the Superpave Gyratory Compactor (SGC) and a static compression machine, respectively. Except the Asphalt Pavement Analyzer (APA) test, all laboratory mix tests were performed using a closed-loop electro-hydraulic material testing system from MTS. The test system utilized TestStar II control system and TestWare SX software to command the tests and collect data. Figure 3.2 shows the MTS test set-up for the triaxial repeated load test. From left to right, the 250 kN (55 kip) load frame with triaxial cell, computer, and controller are shown.

Table 3.2 Rheological properties asphalt binder

Binder Properties	Base PG 64-22	Unmodified PG 70-22	SBS PG 70-22	SBR PG 70-22
Original Binder				
Pass DSR Temp, °C	64	70	76	76
G*/Sinδ (Minimum 1.00 kPa)	1.927	1.345	1.671	1.268
Fail DSR Temp, °C	70	76	82	82
G*/Sinδ (Minimum 1.00 kPa)	0.880	0.650	0.927	0.689
Brookfield @ 135C, Pa.s	0.513	0.628	2.172	1.735
Brookfield @ 165C, Pa.s	0.148	0.0168	0.602	0.500
COC Flash Point, C (Minimum 230 ^{O}C)	322	332	354	336
RTFO Residue				
% Wt. Loss/Gain (Maximum 1%)	-0.127	-0.04	-0.077	-0.039
Pass RTFO Temp, °C	64	70	76	70
G*/Sinδ (Minimum 2.20 kPa)	4.629	2.989	2.542	4.306
Fail RTFO Temp, °C	70	76	82	76
G*/Sinδ (Minimum 2.20 kPa)	2.002	1.388	1.395	2.187
PAV Residue				
Pass PAV Temp, °C	25	25	19	19
G*Sinδ (Maximum 5000 kPa)	3636	4928	4479	4904
Fail PAV Temp, °C	22	22	16	16
G*Sinδ (Maximum 5000 kPa)	5225	6902	6365	6825
BBR Pass Temp, °C	-12	-12	-12	-12
Creep Stiffness (Maximum 300 MPa)	155.5	206.0	103.5	120.0
m-value (Minimum 0.300)	0.321	0.306	0.340	0.317
BBR Fail Temp, °C	-18	-18	-18	-18
Creep Stiffness (Maximum 300 MPa)	314.5	394.0	232.0	259.0
m-value (Minimum 0.300)	0.272	0.248	0.293	0.266
Actual Continuous PG Grade	--	PG 72-25	PG 77-23	PG76-26

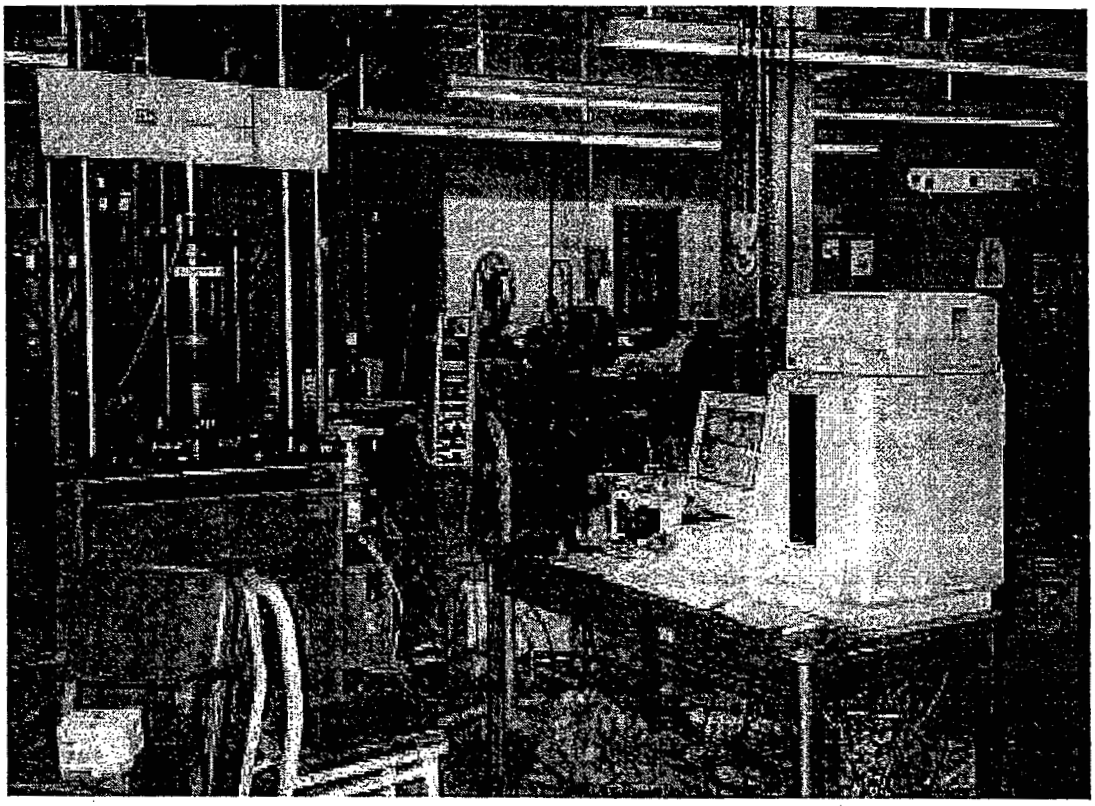

Figure 3.2 MTS load frame with triaxial cell, computer, and controller

3.3.1 Mix Design

The mix design of the unmodified and polymer modified mixtures followed the Superpave procedure. For unmodified mixtures, the equi-vicous temperatures were used for mixing and compaction. For SBS and SBR modified mixtures, the mixing and compaction temperatures suggested by the supplier were followed (156-170°C for mixing and 140-156°C for compaction). The number of gyrations were selected from ODOT Supplemental Specification 858 (1997) (N_{ini} = 8, N_{des} =109, and N_{max} = 174). The volumetric properties of the unmodified mixtures are shown in Table 3.3. In this table, it can be noticed that the intermediate and fine gradation mixes did not meet the Superpave VMA requirement. Several mixes for each gradation type were investigated at the beginning of this study. However, all of the intermediate and fine gradation mixes investigated did not meet the minimum Superpave VMA requirements. Subsequent discussion between ODOT and OU research personnel led to a decision that distinctively different gradations as shown in Figure 3.1 were to be used in this project to study the effects of

Table 3.3 Volumetric properties of design mixes

Mix Property	Coarse	Intermediate	Fine	Gravel (non-Superpave)	Superpave Criteria
Asphalt Content, %	6.4	5.7	5.7	5.3	5.4 minimum
Air Voids, %	4.0	4.0	4.0	4.0	4.0
VMA, %	14.1	12.7	12.4	15.5	14 minimum
VFA, %	68.0	69.0	67.5	64.0	65-75
Dust Proportion	1.2	1.1	1.1	0.7	0.8-1.6 or 0.6-1.2
% G_{mm} @ N=8	83.8	86.6	87.8	85.4	89 maximum
% G_{mm} @ N=109	96.0	96.0	96.0	96.0	96.0
% G_{mm} @ N=174	97.5	97.3	97.0	96.5	98 maximum

gradation on pavement performance. For the unmodified asphalt mixes, the aggregates showed high absorption (2.3-2.1%) and required thorough remixing before compaction. The optimum asphalt content of the unmodified asphalt mixes were 6.4%, 5.7%, and 5.7% for coarse, intermediate, and fine gradation samples, respectively. For the polymer modified mixes, the optimum asphalt content was reduced, because the absorption of the aggregates with modified asphalts was lower (1.8-1.5% for SBS and 1.6-1.1% for SBR mixtures). Optimum asphalt content of the SBS mixes were 6.4%, 5.4%, and 5.4% for the coarse, intermediate, and fine gradation samples, respectively. Optimum asphalt content of the SBR mix were 6.0%, 5.1%, and 5.1%; for the coarse, intermediate and fine gradation samples, respectively. For the gravel mixtures, the absorption ranged between 1.1-0.8%. An optimum asphalt content of 5.3% was determined for all three asphalt binders.

3.3.2 Specimen Preparation

Test specimens of controlled air void contents were prepared in the laboratory using the optimum binder contents discussed previously. For statistical analysis of results, minimum duplicate specimens were prepared and tested for each testing condition. For the Asphalt Pavement Analyzer (APA) test, specimens 150 mm in diameter x 76.2 mm in height with 7 ± 0.5% air void contents were prepared using a Pine Superpave Gyratory Compactor (SGC). For the triaxial repeated load test, the uniaxial static creep test, the diametral resilient modulus test, and the indirect tensile strength test, specimens 150 mm in diameter x 115 mm in height with N_{des} = 109 to have 4 ± 0.5 % air void contents were prepared using SGC following AASHTO TP4. For the flexural fatigue test, a set of beam specimens were compacted to 8 ± 0.5 % air void

contents using a static press with a 534 kN (120,000 lb) load. Before applying the load, loose mix in the beam mold was thoroughly rodded and carefully finished to have uniform surface elevation and thus uniform density. The prepared specimens were tested according to the testing program illustrated in Table 3.4

3.3.3 Asphalt Pavement Analyzer (APA)

The Asphalt Pavement Analyzer (APA) is an automated version of Georgia Loaded Wheel Tester (GLWT) used to evaluate the rutting characteristics of asphalt mixes. In an APA test, beams or cylindrical test specimens are subjected to repeated stresses via loaded wheels riding back- and-forth on a pressurized hose placed lengthwise on top of the specimens (Figure

Table 3.4 Summary of laboratory testing program

	Mix Type											
Binder Type	Unmodified				SBS				SBR			
Gradation/Aggregate	C	I	F	G	C	I	F	G	C	I	F	G
APA	X	X	X	X	X	X	X	X	X	X	X	X
Triaxial Repeated Load	X	X	X	✓	X	X	X	✓	✓	✓	✓	✓
Uniaxial Static Creep	X	X	X		X	X	X					
Diametral Resilient Mod	X	X	X		X	X	X					
Indirect Tensile Strength	X	X	X		X	X	X					
Flexural Fatigue	X	X	X		X	X	X					

C = Coarse graded limestone; I = Intermediate graded limestone;
F = Fine graded limestone; G = Gravel blend;
X = tested; ✓ = tested only at 60°C, not at 40°C.

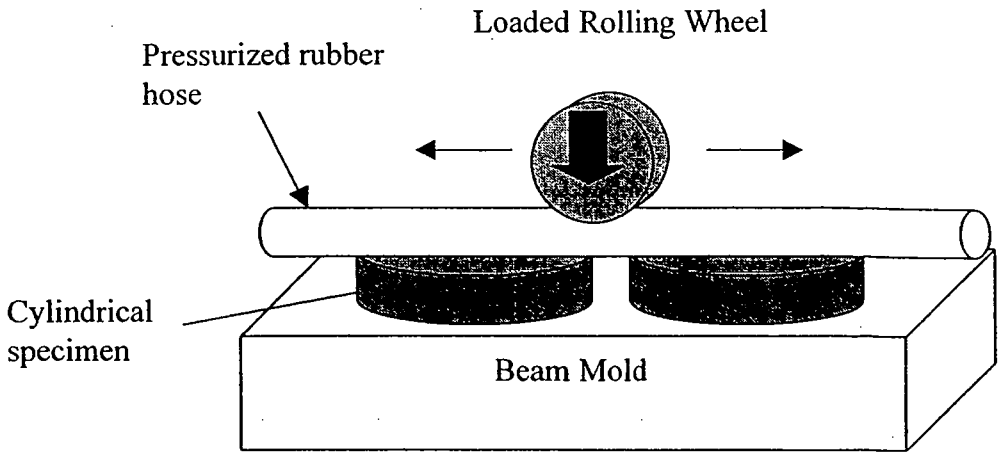

Figure 3.3 Schematic diagram of the APA loading system

3.3). The test can be performed in dry or wet conditions. Results from an APA test are empirical and often used as an accept/reject criterion to supplement the Superpave volumetric mix design that does not have any strength test at the moment [47,48]. In the current ODOT specification, an APA test is required if more than 15% of fine aggregate is not meeting fine aggregate angularity (FAA) criteria in Superpave specifications; standard test method is listed in Supplemental Specification 1057 "Loaded Wheel Tester Asphalt Mix Rut Testing Method". In this study, the samples were conditioned at 60°C in the APA chamber for a minimum of 12 hours prior to dry APA tests. For wet tests, the specimens were subjected to 55-80 % vacuum saturation with water and then kept immersed in 60°C water for 12 hours before testing. In both dry and wet tests, specimens were tested at 60°C with a 511.5 N (115-lb) wheel load and 689.4 kPa (100 psi) hose pressure. Test temperature 60°C was higher than the temperatures specified in the ODOT specification because of very low rutting potential of the heavy-duty mixes used in this study. Rut depths were measured at 5, 500, 1000, and 8000 cycles at two locations at the middle of each specimen using a digital measuring guage.

3.3.4 Triaxial Repeated Load Test

Triaxial repeated load tests have been used to evaluate the rutting potential of asphalt mixes [10,12,49-55]. As shown in Figure 3.4, this test closely simulates loading condition typical in pavement. The repeatedly applied deviator stress simulates a fast moving traffic load and the confining pressure represents confinement of the loaded pavement area by surrounding pavement materials. The level of confinement in a triaxial repeated load creep test is important, because confinement affects the state of stress in the test specimen, influencing ranking mixtures [55]. In the triaxial repeated load test, a pulse load is repeatedly applied to the sample and deformation is measured as shown in Figure 3.5. During the loading period, the specimen is deformed, and during the unloading and rest period, only a portion of the strain is recovered,

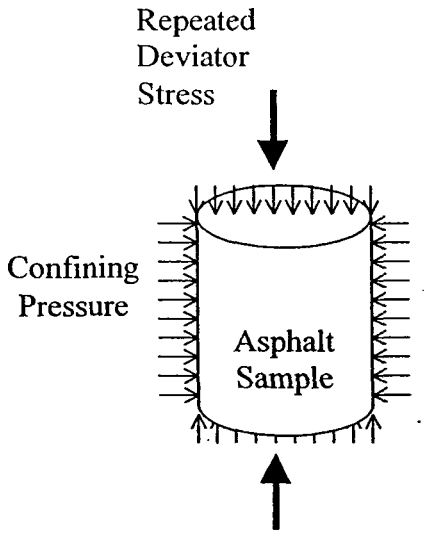

Figure 3.4 Schematic diagram of the loading in triaxial repeated load test

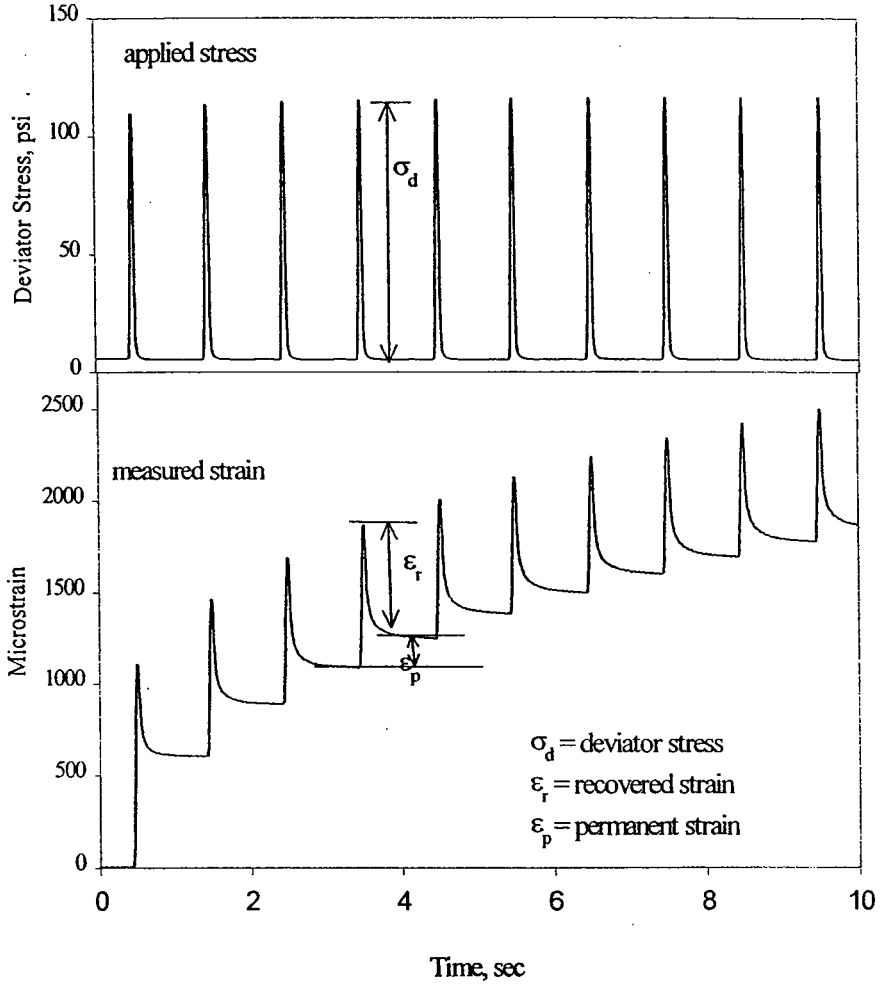

Figure 3.5 Applied stress and measured strain during a triaxial repeated load test

leaving permanent strain. Rutting potential of asphalt mixes is closely related to the permanent strain [10]. As the deviator stress or temperature increases, the permanent strain increases. Increases in the confining pressure cause decreases in the permanent strain. The relationship between the permanent strain, ε_p, and the number of load application, N, is usually described by a power law [56]:

$$\varepsilon_p = aN^b$$

where a, b ; materials parameters or intercept and slope of log ε_p- log N curve, respectively

These materials parameters, a, b, or their derivatives are being used in pavement analysis and performance prediction models such as FHWA's VESYS [57]. Resilient modulus can also be determined from the triaxial repeated load test result.

$$MR = \sigma_d/\varepsilon_r$$

where MR; resilient modulus
σ_d; deviator stress
ε_r ; recovered strain

A repeated load creep test is more suitable than a uniaxial static creep test for evaluating the rutting potential of asphalt mixes, especially elastomeric polymer modified asphalt mixes [52,55]. Valkering et al. [52] showed that polymer (SBS) modification significantly improved rutting resistance of asphalt mixes in their indoor test track study, and repeated load creep test results. However, a static creep test did not show any improvement in rutting resistance due to

the polymer modification. These observations were attributed to the enhanced ability to recover strain in the polymer modified mixtures. During each unloading and rest period in the repeated load test, polymer increases the amount of recovered strain, resulting in less permanent strain However, in the static creep test where load is applied on the sample continuously, the enhanced ability to recover due to the polymer modification can not be measured.

In laboratory creep tests of HMA, the use of a realistic stress level similar to field loading conditions is important for two reasons. First, when the applied stress is too low, yield strength of asphalt plays a major role in the strain response of the specimen, and the contribution of aggregates in rutting resistance may become insignificant. For example, a comprehensive triaxial repeated load creep study was performed to evaluate the effects of mix variables on rutting with 20 psi deviator stress. While all the binder related parameters showed significant influence on the permanent strain, the aggregate type (crushed stone vs. gravel) did not show any significant difference. Authors attributed the insignificance of aggregate type on rutting in the test to the low stress level that could not fully mobilize the friction between aggregate particles [56]. Second, at stresses approaching the strength of the mix or at strain near failure, creep response is not always linear. In such cases, use of linear viscoelastic superposition principle can not be applied to predict rutting potential under high field stress from result of low stress creep tests [58]. In this study, 827 kPa (120 psi) deviator stress and 138 kPa (20 psi) confining pressure were used based on a similar study [10]. This level of deviator stress is within the upper range of real heavy traffic loading on pavement.

Figure 3.6 show a test specimen placed inside the triaxial cell with heated silicon oil. Prior to testing, the sample was placed in the triaxial cell filled with silicon oil for a minimum of

12 hours at test temperature. The confining pressure on the sample was controlled by pressurized air supplied to the top surface of the silicon oil. The silicon oil also served the purpose of heating medium to control temperature. After temperature conditioning, a confining pressure of 20 psi was applied before preconditioning load. Then, a preconditioning stress of 83 kPa (12 psi) was applied for 30 cycles. Next, the specimen was subjected to a 827 kPa (120 psi) deviator stress for 10,000 cycles. The deviator stress was applied 0.1 seconds in a haversine form and had a rest period of 0.9 seconds. The axial displacement of the specimen was measured using two LVDTs placed opposite each other. The confining pressure was applied continuously throughout the test. After loading 10,000 cycles, the axial load was withdrawn, while the confining pressure was held at 138 kPa (20 psi), and the sample was allowed to recover for 15 minutes. After completion of the test, percent air void of the sample was measured again. Tests were performed at 40°C and 60°C, the temperatures range over which rutting resistance is critical.

3.3.5 Uniaxial Static Creep Test

The uniaxial static creep test is a simpler test than the triaxial repeated load test, in which the deformation of specimen due to the uniaxial static compressive load without confinement is measured as a function of time. Because of its simplicity, this test has been used for many years with reasonable correlation with the rutting of the asphalt pavements [58]. However, cyclic or dynamic test results correlate better with the performance of asphalt mixes in the field [12, 53]. The uniaxial static creep test identifies the rutting resistance of the asphalt mixes when performed at a temperature and stress level related to that existing in the real pavements [28,58].

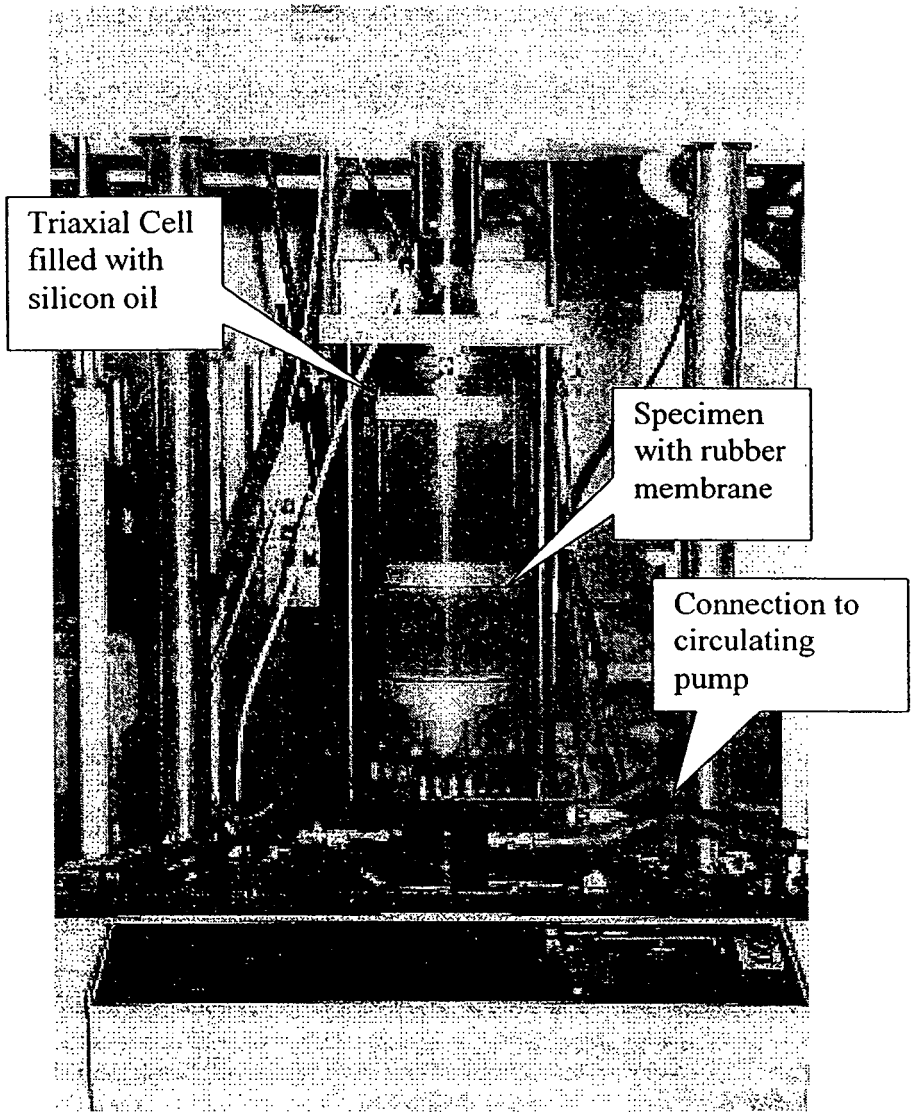

Figure 3.6 Triaxial repeated load test set-up

A static load of 414 kPa (60 psi) was suggested to be a realistic stress level for field traffic loading and adopted in this project [58].

Figure 3.7 shows the MTS static creep test set-up together with the environment conditioning chamber. Prior to the static creep testing, a specimen was placed in the environmental chamber for a minimum of 12 hours for temperature equilibrium. The environmental chamber provided a stable thermal environment maintaining temperatures in the range of –30 to 100°C. The 414 kPa (60 psi) of static creep stress was applied for 3,600 seconds (1 hour) followed by 3,600 seconds (1 hour) of recovery. The total axial compressive deformation of the sample was measured using two LVDTs at predetermine time intervals. After the test, the percent air voids of the sample was measured. In this test, duplicate samples were tested at 60°C and 40°C. In this test, permanent strain, creep stiffness after 1 hour, total strain after 1 hour, percent recovery, and steady state slope were determined to evaluate rutting potential of mixes.

3.3.6 Flexural Beam Fatigue Test

The flexural beam fatigue test estimates the cracking potential of asphalt pavement due to repeated heavy traffic loading. A schematic loading configuration of the beam is shown in Figure 3.8. In this test, the beam specimen is subjected to four point bending with free rotating beam-holding fixtures at all loading and reaction points. For symmetrical loading, the middle third of the beam will be in pure bending allowing easy calculation of flexural stress, strain and stiffness. The number of cycles to failure (fatigue life) and dissipated energy (area within hysteresis loop) are commonly used as indicators of fatigue cracking potential [20, 59]. The

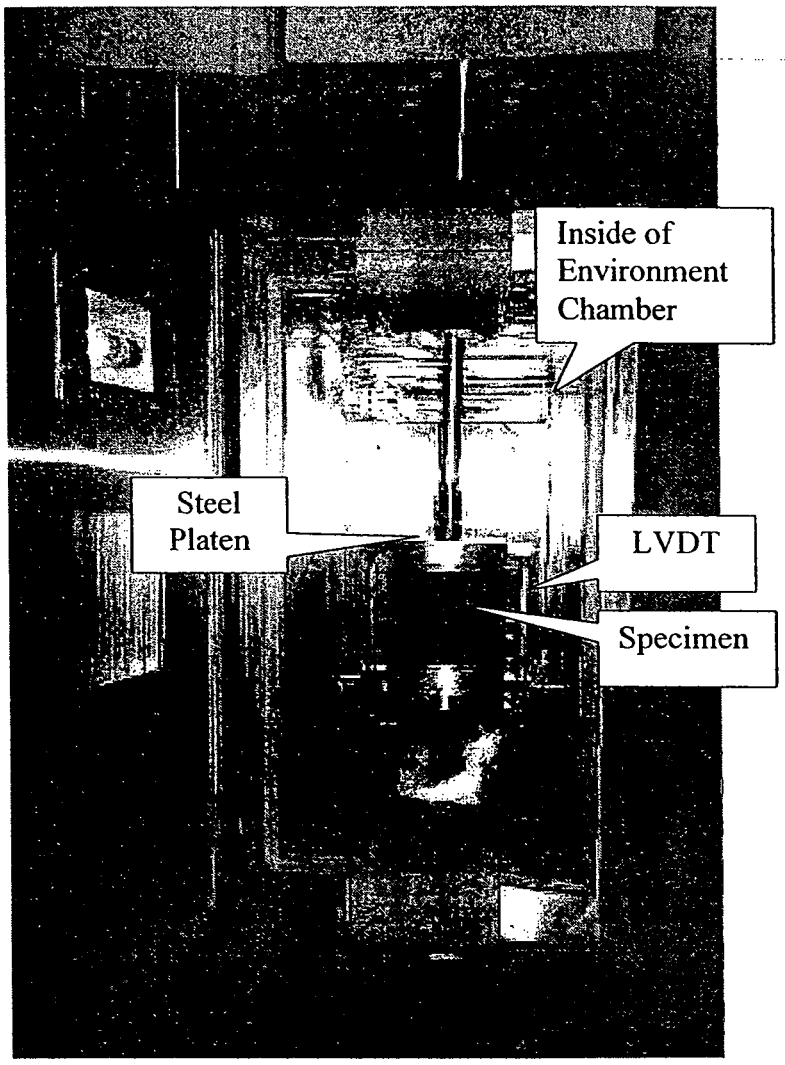

Figure 3.7 Static creep test set-up inside the environment chamber

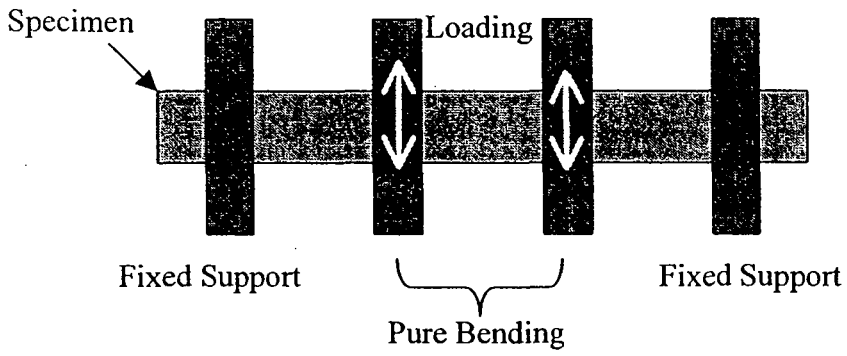

Figure 3.8 Schematic diagram of the loading applied in flexural beam fatigue test

flexural beam fatigue test can be performed either in controlled strain mode or controlled stress mode. In the controlled stress mode, the stress or load remains constant throughout the experiment, whereas in controlled strain test, the deformation or strain is maintained at a constant value. For the strain-controlled test, the failure point is commonly defined as the load cycle where the flexural stiffness of the beam sample become 50% of the initial stiffness. It is believed that controlled strain testing might be more suitable for evaluating mixes for thin pavements on stiff foundation and the controlled stress test better for thick pavement structures [20]. This flexural beam fatigue test was found to be sensitive to asphalt type, aggregate type, air void content, and temperature [19]. As the magnitude of the applied flexural strain increase, fatigue life decrease. One of the common relationships between fatigue life, N_f, and the applied initial tensile strain, ε_o, is given as;

$$N_f = K1\ (\varepsilon_o)^{K2}$$

where, N_f = fatigue life
ε_o = initial tensile strain, and
K1 and K2 = experimentally determined regression coefficients

K1 and K2 are materials properties which depend on asphalt, aggregate, and mix properties. This form of relationship is commonly used in the pavement fatigue performance models.

In this study, the flexural beam fatigue test was performed following AASHTO TP8-94, "Method for Determining the Fatigue Life of Compacted Bituminous Mixtures Subjected to Repeated Flexural Bending." To prepare the beam specimens for this test, loose mixes were compacted by a static press with a load of 534 kN (120,000 lb). The original sample had a dimension of approximately 381 mm, 76 mm, and 50 mm and was trimmed on both sides of the beam length-wise using a diamond saw as required in the procedure, bringing the final dimensions to 381 mm, 63 mm, and 50 mm. All the beam specimens had percent air voids close to 8%. A piece of aluminum block was glued onto the middle of the neutral axis of the beam, so that a LVDT could be positioned to measure deflection. Figure 3.9 shows the flexural beam fatigue test set-up together with the environmental chamber.

Prior to testing, the beam specimen was kept in the environmental chamber at a temperature of 20 ± 1°C for a minimum of 12 hours. Then, the beam was mounted in a flexural bending beam fixture within the environmental chamber. Controlled strain mode of cyclic loading was applied to the sample until failure. As previously discussed, the failure is defined as the load cycle at which the sample showed a 50% reduction in stiffness compared to the initial stiffness. The strain applied on the samples was 275 microstrain at a frequency of 5 Hz. At this strain level, all the specimens showed fatigue lives larger than 10,000 cycles as recommended in

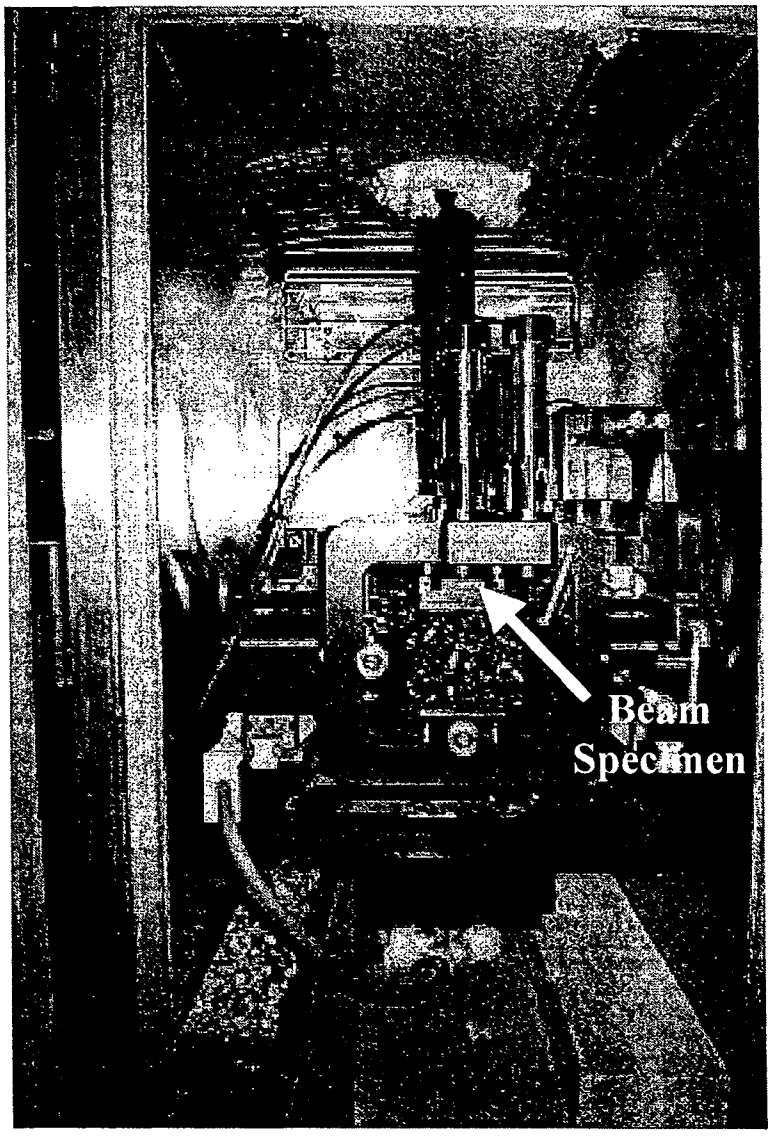

Figure 3.9 Flexural beam fatigue test set-up in the environmental chamber

AASHTO TP8. Duplicate samples of the three limestone gradations using two asphalt binders (unmodified and SBS) were used in this test. Gravel and SBR samples were not used in this test. From this test, flexural stiffness, phase angle, cumulative dissipated energy and steady-state slope were determine.

3.3.7 Indirect Tensile Resilient Modulus Test

Because of its simplicity, the indirect tensile resilient modulus test has been popularly used to determine the elastic modulus of the bituminous mixtures. In this test, a repeated load is applied to the vertical diametral axis to induce tension along the diametral axis in line with the applied load [17]. Then, the resilient modulus is determined from following equation;

$$M_{Rt} = P \frac{(\mu_{RT} + 0.27)}{t \Delta H_t}$$

where, M_{Rt} = resilient modulus of elasticity, MPa,
P = cyclic load, N
μ_{RT} = total resilient Poisson's ratio
t = thickness of specimen, mm
ΔH_t = total recoverable horizontal deformation, mm

The resilient modulus is commonly used in analysis of pavement response due to traffic loading and in the design of pavement structures.

In this study, the resilient modulus of asphalt mixtures was determined following AASHTO TP31 "Method for Determining the Resilient Modulus of Bituminous Mixtures by Indirect Tension." Specimens of 150mm diameter by about 115mm height were kept in the

environmental chamber for minimum of 12 hours at the test temperature prior to testing. A load of fixed magnitude was applied to a cylindrical specimen along its diametral axis. Tests were performed at three temperatures (5, 25, and 40°C) with a repeated load of haversine wave form (0.1 second loading time and 0.9 seconds rest period). Extensometers and LVDTs were used to measure the horizontal and vertical deformation, respectively. The total loads applied to the samples at 5, 25, and 40°C were 7,000 N (1,573 lb), 4,000 N (900 lb), and 2,000 N (450 lb), respectively.

3.3.8 Indirect Tensile Strength Test

In the indirect tensile strength test, a specimen is loaded along the diametral axis at a constant rate of deformation until failure. The indirect tensile strength of the sample is calculated from the maximum load endured by the sample before failure.

$$S_t = \frac{(50.127 \times P_o)}{t}\left[\sin\left[\frac{1455.313}{D}\right] - \left[\frac{12.7}{D}\right]\right]$$

where S_t = indirect tensile strength, kPa
P_o = maximum load sustained by the specimen, N
t = specimen thickness, mm
D = specimen diameter, mm

This test measures the strength or relative resistance to cracking due to fatigue or temperature. High strength values indicate greater resistance to fracture. Mixes with high strength have the ability to absorb energy without fracture [60].

In this study, the same specimens used to measure the indirect tensile resilient modulus were used to determine the indirect tensile strength. After temperature conditioning for 12 hours at 25°C, compressive loads were applied on the asphalt specimen along the diametral axis at a deformation rate of 50 mm per minute until failure.

3.3.9 Moisture Susceptibility Test

The moisture susceptibility of asphalt mixes were determined following AASHTO T 283 "Standard Test Method of Test for Resistance of Compacted Bituminous Mixture to Moisture Induced Damage". One of the commonly used moisture susceptibility tests for asphalt mixes is the Lottman test (AASHTO T283). This is a quantitative strength test in which six samples having 6-8 percent of air voids are compacted. Among them, three samples are used as control samples and the remaining three samples are subjected to vacuum saturation of 55-80 percent with water and then subjected to freezing and thawing conditions. Finally, the samples are tested for the indirect tensile strength (ITS), and the retained tensile strength (TSR) is calculated. Retained tensile strength is the ratio of the ITS of the conditioned specimens to the ITS of the dry unconditioned specimens and is used as a moisture susceptibility indicator. A minimum TSR value of 0.80 is required in the Superpave mix design [5]. This test procedure is considered to be the most appropriate method, at present, for determining the moisture damage in asphalt mixes [17, 61].

In this test, two aggregates (limestone coarse gradation and gravel blend) and two asphalt binders (unmodified and SBS) were used. The specimens of about 63.5 mm height were prepared with the Superpave gyratory compactor with 100 mm diameter mold. Neither aggregates nor

asphalt binders were known to have moisture damage problems. For ultimate comparison, TSRs were determined after 1, 2, and 3 cycles of freeze/thaw conditioning for limestone mixes and only after 3 freeze/thaw conditioning for gravel mixes.

CHAPTER 4

TEST RESULTS AND DISCUSSION

4.1 Asphalt Pavement Analyzer

Use of angular crushed limestone aggregate resulted in highly rut resistant mixes for all gradations and asphalt binder types studied, having APA rut depths well below the ODOT specification requirement (maximum 5 mm). The results of the dry and wet APA tests are presented in Table 4.1 showing measured rut depths at 500, 1,000, and 8,000 cycles of loading. The final rut depths measured at 8,000 cycles are shown in Figure 4.1 and are used for the following data analysis.

Analyses of variance (ANOVA) were conducted to determine if the APA rut depths of mixes were affected by aggregate type, aggregate gradation (the restricted zone), or asphalt binder type. As shown in Table 4.2-A, analysis of limestone dry APA test results indicated that asphalt binder type was statistically significant (p-value < 0.05), while aggregate gradation was not ($p > 0.05$). When compared with unmodified PG 70-22 and SBR PG 70-22 mixes, SBS PG 70-22 mixes exhibited lower rutting. Overall average rut depths for unmodified, SBS, and SBR mixes were 0.89, 0.65, and 0.95mm, respectively. This ranking was not the same as the ranking of their $G^*/\sin\delta$, the binder rutting criteria at high temperatures; SBS had highest $G^*/\sin\delta$, followed by SBR, and unmodified. For gravel mixes, due to insufficient number of data, a meaningful statistical analysis was not possible. Qualitative comparison was made for rut depths among the three mixes of different binders. Mixes with both SBS and SBR modified binder

Table 4.1 Results of dry and wet APA tests

Gradation	Asphalt Type	Rut Depth, mm				Dry/Wet Ratio
		5 cycles	500 cycles	1000 cyc	8000 cyc	
Dry Test						
Coarse	Unmodified	0.00	0.31	0.42	0.86	0.76
	SBS	0.00	0.27	0.36	0.72	0.75
	SBR	0.00	0.36	0.56	1.12	1.03
Intermediate	Unmodified	0.00	0.31	0.41	0.99	1.25
	SBS	0.00	0.31	0.39	0.68	0.76
	SBR	0.00	0.35	0.52	0.95	0.90
Fine	Unmodified	0.00	0.09	0.18	0.81	1.17
	SBS	0.00	0.23	0.29	0.54	0.53
	SBR	0.00	0.27	0.42	0.81	0.61
Gravel	Unmodified	0.00	2.08	2.82	6.11	1.36
	SBS	0.00	1.36	1.98	4.73	1.48
	SBR	0.00	1.65	2.21	4.86	1.17
Wet Test						
Coarse	Unmodified	0.00	0.53	0.67	1.13	
	SBS	0.00	0.42	0.51	0.96	
	SBR	0.00	0.43	0.54	1.09	
Intermediate	Unmodified	0.00	0.33	0.40	0.79	
	SBS	0.00	0.40	0.48	0.90	
	SBR	0.00	0.41	0.54	1.06	
Fine	Unmodified	0.00	0.34	0.41	0.69	
	SBS	0.00	0.39	0.50	1.01	
	SBR	0.00	0.70	0.78	1.33	
Gravel	Unmodified	0.00	1.48	2.37	4.49	
	SBS	0.00	1.09	1.63	3.19	
	SBR	0.00	1.22	1.79	4.16	

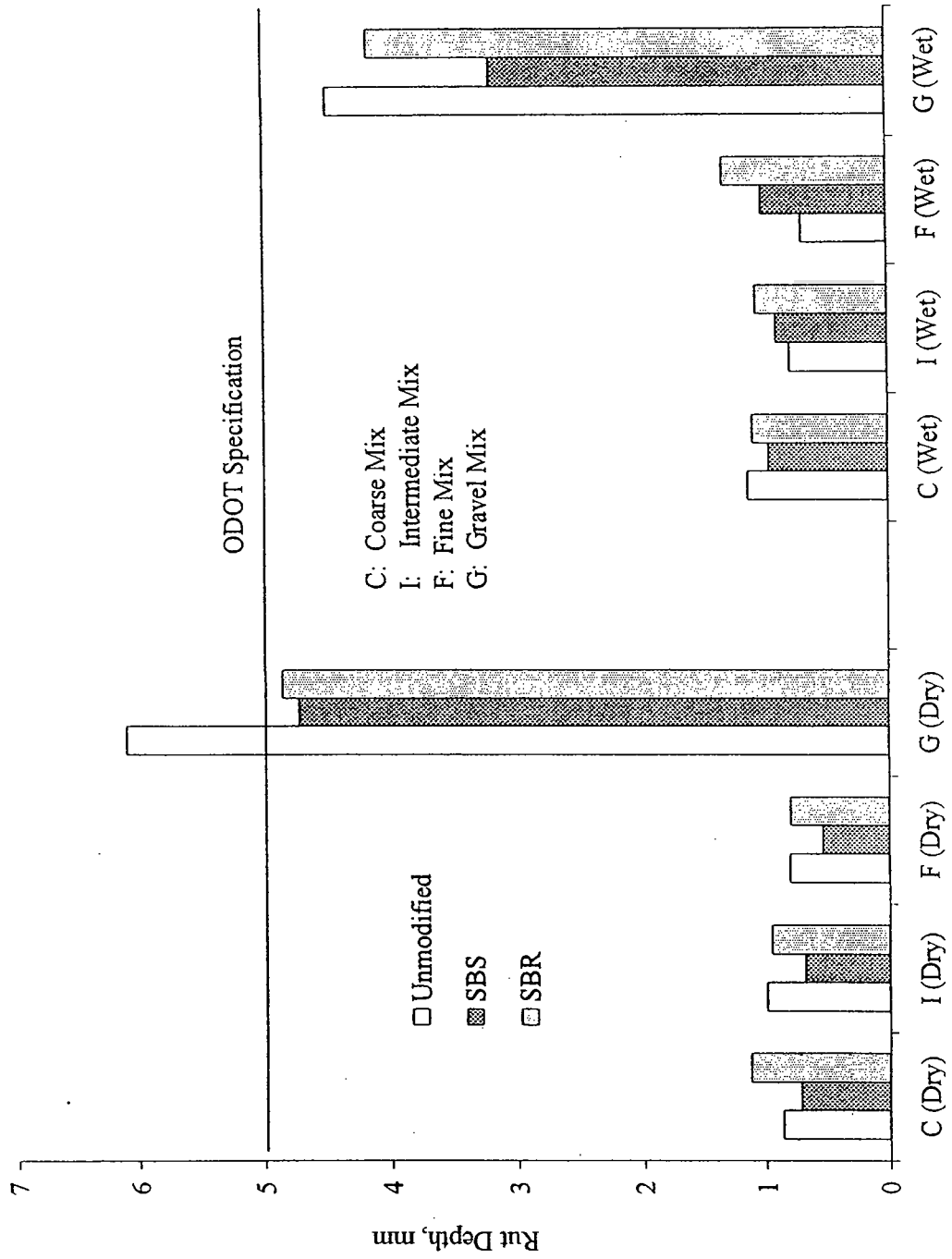

Figure 4.1 Results of dry and wet APA tests

Table 4.2 Analysis of Variance for APA rut depth

A. Effect of Gradation & Asphalt (Limestone Dry Data) $R^2 = 26.4\%$

Source	DF	Seq SS	Adj SS	Adj MS	F	P
Gradation	**2**	**0.28052**	**0.28052**	**0.14026**	**1.92**	**0.159**
Asphalt	**2**	**0.84314**	**0.84314**	**0.42157**	**5.78**	**0.006**
Error	43	3.13724	3.13724	0.07296		
Total	47	4.26090				

B. Effect of Aggregate (All Dry Data) $R^2 = 94.6\%$

Source	DF	Seq SS	Adj SS	Adj MS	F	P
Aggregate	**1**	**104.184**	**103.460**	**103.460**	**867.05**	**0.000**
Asphalt	2	1.348	1.348	0.674	5.65	0.006
Error	50	5.966	5.966	0.119		
Total	53	111.498				

C. Aggregate - Wet Test Interaction (All Data) $R^2 = 93.5\%$

Source	Seq SS	df	MS	F	P
Test Type	2.963	1	2.963	21.84	0.0000
Aggregate	132.742	1	132.742	978.39	0.0000
TestType*Agg	**5.236**	**1**	**5.236**	**38.60**	**0.0000**
Error	10.039	74	0.135		
Total	156.577	77			

D. Dry APA test vs. Wet APA Test

ANOVA for Rut Depth (Limestone Data) $R^2 = 27.1\%$

Source	DF	Seq SS	Adj SS	Adj MS	F	P
Gradation	2	0.21315	0.21315	0.10657	1.58	0.215
Asphalt	2	0.94085	0.86098	0.43049	6.37	0.003
Test Type	**1**	**0.35118**	**0.35118**	**0.35118**	**5.20**	**0.026**
Error	60	4.05502	4.05502	0.06758		
Total	65	5.56019				

ANOVA for Rut (Gravel Data Only) $R^2 = 86.6\%$

Source	DF	Seq SS	Adj SS	Adj MS	F	P
Asphalt	2	3.5887	3.5887	1.7944	10.86	0.005
Test Type	**1**	**4.9408**	**4.9408**	**4.9408**	**29.90**	**0.000**
Error	8	1.3220	1.3220	0.1653		
Total	11	9.8516				

showed a noticeably lower dry rut depth than mixes with unmodified binder.

Magnitude of rut depth in limestone mixes was relatively small in comparison with the magnitude of errors in APA measurement. This was manifested as a low R^2 for the ANOVA of limestone only data (Table 4.2-A & D). Lower R^2 indicates a larger portion of measurement variability comes from errors not from the factors used in the statistical model. This relatively large magnitude of error obsecures the difference among aggregate gradations. An ANOVA was performed again after careful review of the data and removal of three outliers (deviation from mean > 2 standard deviations) from the 48 data points. Then, gradation was statistically significant ($p = 0.024$), but less than asphalt binder type ($p = 0.006$). Mixes with fine gradation showed the least rut depth (0.71 mm), and mixes with coarse gradation showed the largest rut depth (0.88 mm).

ANOVA performed on all dry APA data indicated aggregate type had a significant effect on rut depth (Table 4.2-B). Mixes with crushed limestone showed much lower rutting (average rut = 0.81mm)than rounded smaller size gravel mixes (average rut = 5.23mm), as expected.

Studies conducted at the National Center for Asphalt Technology (NCAT) [33] and Texas [62] using APA support these findings. They concluded that APA was sensitive to aggregate type and gradation. When high quality aggregates were used, the restricted zone did not have a significant effect on rutting performance. In general, coarse gradations that passed below the restricted zone showed the highest rut depths. NCAT study also found that APA rut depth had correlated somewhat with asphalt binder film thickness. For limestone and granite mixes, rut depth increased with an increase in film thickness. To compare with this finding, surface areas of three limestone gradations used in this study were calculated from gradations

[17], and asphalt binder film thicknesses were estimated. The estimated film thickness for coarse, intermediate, and fine mixes were 13.9, 10.7, and 9.6μm; the same order as rut depth.

In addition to the dry APA test, a wet APA test was performed to evaluate moisture susceptibility of mixes. As a moisture susceptibility parameter, APA rut ratio was defined as average rut depth form dry APA test divided by average rut depth from wet APA test. The results are presented in Table 4.1. As shown in Table 4.2-C, there was strong interaction between aggregate type and dry/wet test ($p < 0.05$ for TestType*Agg). ANOVA of each aggregate with limited data shows that APA moisture conditioning significantly affected rut depth (Table 4.2-D). For limestone mixes, overall average rut depth increased from 0.81 mm to 1.00 mm due to APA moisture conditioning, whereas overall rut depth of gravel mixes decreased from 5.23 mm to 3.95 mm. For limestone, mixes with SBS showed the lowest wet/dry rut ratio (highest susceptibility), whereas for gravel mixes with SBS showed the highest wet/dry ratio (lowest susceptibility). The reduction of rut depth after vacuum saturation and warm water soaking is believed to be due to excess pore water pressure [62]. Under dynamic loading, excess pore water pressure can be developed and reduces effective stress between aggregate particles. Thus, some of the APA wheel load can be supported by excess pore water pressure. Originally, moisture susceptibility was thought to be evaluated by conducting dry and wet APA tests. However, the moisture conditioning procedure used our study may need further refinement to evaluate moisture susceptibility, according Cross and Voth [62]. They investigated three moisture conditioning procedures; (1) soaking in 40°C water for 2 hours, (2) vacuum saturation followed by 24 hours at 60°C water and 2 hours at 40°C water, and (3) vacuum saturation followed by freeze/thaw conditioning, 24 hours at 60°C water and 2 hour at 40°C water. About half of the

mixes treated with vacuum-saturation showed a decrease in rut depth. None of the three moisture conditioning procedures correlated with the tensile strength ratio (TSR) measured following AASHTO T 283 procedure. Correlation of these conditioning procedures with field performance is yet to be determined.

In summary, aggregate type, gradation, and binder type were statistically significant factors affecting APA rutting performance. Mixes with crushed limestone exhibited much smaller rutting than mixes with rounded gravel. Intermediate gradation passing through the restricted zone performed as good as other gradations. In general, coarse gradation passing below the restricted zone showed the highest rut depth. Mixes with polymer modified binders showed smaller rut depth than mixes with unmodified binder. Differences between unmodified and modified binders were more noticeable in gravel mixes that have weaker aggregate structures. From a practical prospective, all gradation and all binder types of crushed limestone mixes studied performed very well, having an average rut depth of 0.81mm.

4.2 Triaxial Repeated Load Test

From triaxial repeated load test data, rate of permanent strain per load cycle, rut rates were determined after 1,000 and 10,000 cycles of loading using the slope of the creep curve, in addition to permanent strain at 10,000 load cycle, resilient modulus and percent recovery. The results of the triaxial repeated load test are summarized in Tables 4.3 and 4.4, and correlations among parameters are listed in Tables 4.5 and 4.6. Asphalt binders and asphalt mixtures are viscoelastic materials that exhibit dramatic changes in their rheological and physical properties with temperature changes. To separate the overshadowing temperature effect from other effects,

Table 4.3 Results of triaxial repeated load test

Test Temp	Mix Type	Asphalt Type	After 10,000 Cycles				Rut rate@ 1K cycle με/cycle	Rut rate @ 10K cycle με/cycle
			Void Change* %	Resilient Modulus GPa	Permanent Strain % strain	Recovery %		
60°C	LS Coarse	Unm	--	1.25	0.9920	2.1	1.344	0.144
		Unm	0.0	1.26	0.9909	--	1.289	0.159
		SBS	-0.2	1.26	0.6417	4.0	0.755	0.061
		SBS	-0.2	1.34	0.6602	3.9	0.812	0.071
		SBR	-0.3	1.10	0.7378	3.7	0.930	0.088
		SBR	-0.2	1.05	0.7811	3.6	0.970	0.091
	LS Inter	Unm	-0.2	1.28	0.7544	3.0	0.990	0.108
		Unm	-0.2	1.26	0.8150	--	1.010	0.104
		SBS	-0.1	1.24	0.5415	--	0.620	0.090
		SBS	-0.2	1.29	0.5218	5.1	0.629	0.053
		SBR	-0.2	1.14	0.5386	5.0	0.655	0.063
		SBR	-0.3	1.09	0.5731	4.8	0.697	0.069
	LS Fine	Unm	-0.2	1.21	0.7819	2.9	0.999	0.101
		Unm	-0.2	1.34	0.7650	--	0.977	0.078
		SBS	-0.2	1.23	0.4407	6.2	0.482	0.039
		SBS	-0.2	1.33	0.4161	6.5	0.492	0.046
		SBR	-0.3	1.12	0.5752	5.0	0.666	0.062
		SBR	-0.2	1.12	0.5082	4.5	0.596	0.055
	Gravel	Unm	-0.3	0.94	1.6027	1.8	2.084	0.245
		Unm	-0.1	0.98	1.5691	1.7	2.053	0.241
		SBS	-0.1	1.00	1.0990	2.4	1.354	0.130
		SBS	-0.2	0.98	1.0991	2.2	1.332	0.132
		SBR	-0.1	0.95	1.1751	2.3	1.468	0.152
		SBR	-0.1	0.97	1.3400	2.2	1.684	0.177
40°C	LS Coarse	Unm	-0.1	4.6	0.3611	5.4	0.49	0.05
		Unm	-0.2	3.1	0.3516	5.3	0.51	0.03
		SBS	-0.1	2.2	0.3096	6.5	0.44	0.04
		SBS	-0.1	2.2	0.3308	6.2	0.41	0.03
	LS Inter	Unm	-0.2	4.5	0.3095	6.1	0.44	0.03
		Unm	-0.2	5.0	0.2710	6.9	0.32	0.02
		SBS	-0.1	2.6	0.2785	7.7	0.32	0.02
		SBS	-0.1	2.4	0.2612	8.4	0.30	0.02
	LS Fine	Unm	-0.1	2.9	0.2435	7.7	0.24	0.02
		Unm	-0.1	3.5	0.2630	7.0	0.42	0.02
		SBS	-0.1	2.8	0.2165	10.0	0.27	0.02
		SBS	-0.1	2.5	0.2326	8.8	0.28	0.02

* Negative value means decrease in voids; -- Not measured

Table 4.4 Average resilient modulus determined from triaxial repeated load test at 40°C and 60°C

Mix Type	Asphalt Type	Resilient Modulus, GPa	
		40°C	60°C
LS Coarse	Unmodified	3.85	1.26
	SBS	2.20	1.30
	SBR	--	1.08
LS Intermediate	Unmodified	4.75	1.27
	SBS	2.50	1.27
	SBR	--	1.12
LS Fine	Unmodified	3.20	1.28
	SBS	2.65	1.28
	SBR	--	1.12
Gravel	Unmodified	--	0.96
	SBS	--	0.99
	SBR	--	0.96

-- Not measured

Table 4.5 Pearson correlations (r) among mix properties determined from 60°C triaxial repeated load test (limestone only, n = 18)

	Permanent Strain	%Recovery	Rut Rate @ 1000 Cycle	Rut Rate @ 10,000 cycle
%Recovery	-0.951			
Rut Rate @ 1000 Cycle	0.996	-0.945		
Rut Rate @ 10,000 Cycle	0.924	-0.913	0.927	
Log MR	0.076	0.067	0.098	0.086

Table 4.6 Pearson correlations (r) among mix properties determined from 40°C triaxial repeated load test (limestone only, n = 12)

	Permanent Strain	%Recovery	Rut Rate @ 1000 Cycle	Rut Rate @ 10,000 cycle
%Recovery	-0.926			
Rut Rate @ 1000 Cycle	0.896	-0.868		
Rut Rate @ 10,000 cycle	0.808	-0.688	0.754	
Log MR	0.228	-0.391	0.282	0.196

correlations were determined at each test temperature using limestone data only. At 60°C, permanent strain, percent recovery, rut rates at 1,000 and 10,000 cycles were very strongly correlated with each other ($|r| > 0.91$) but not with the resilient modulus ($|r| < 0.1$). This was due to the fact that the permanent strain, percent recovery, and rut rates are governed by the viscous nature of asphalt mixes while resilient modulus is governed by elastic nature of mixes. Permanent strain and rut rates had very strong positive correlation with each other, i.e., larger permanent strain was associated with larger rut rates. Permanent strain had a significant negative correlation with percent recovery. Mixes showing large permanent strain tended to have low percent recovery after repeated load tests. At 40°C, similar trends, but with weaker correlations than at 60°C, were observed. It is speculated that at 40°C relaxation behavior of the asphalt mix was slow, and during the 0.9 second rest period in the triaxial repeated load test, the asphalt mix did not recover fully. The permanent strain for a loading cycle used in rut rate calculation would include not only plastic strain but also a significant level of elastic and delayed elastic strain. It would also affect the accumulated permanent strain and percent recovery, resulting in less correlation at lower temperatures.

Analyses of variance were performed to determine the effects of aggregate type, gradation, asphalt binder type, and temperature on permanent strain, rut rate, percent recovery, and resilient modulus. The results of permanent strain, percent recovery, and rut rate were expected to be similar because of their strong correlation. Analysis of whole data set (n=36) indicated a significant effect of aggregate type, asphalt type, and gradation on these three mix properties (Table 4.7-A,-B, and -C). High R^2 indicates significant effects of factors included in

Table 4.7 Analysis of variance for triaxial repeated load test results (all data, n = 36)

A. Permanent Strain at 10,000 Cycles of Loading $R^2 = 94.8\%$

Source	DF	Seq SS	Adj SS	Adj MS	F	P
Agg	1	3.18958	1.02943	1.02943	115.24	0.000
Grad	2	0.15953	0.15953	0.07977	8.93	0.001
AC	2	0.36810	0.35770	0.17885	20.02	0.000
Temp	1	1.04510	1.04510	1.04510	117.00	0.000
Error	29	0.25904	0.25904	0.00893		
Total	35	5.02136				

B. Percent Recovery $R^2 = 94.8\%$

Source	DF	Seq SS	Adj SS	Adj MS	F	P
Agg	1	51.628	3.088	3.088	10.04	0.004
Grad	2	18.065	18.065	9.032	29.36	0.000
AC	2	26.544	23.611	11.805	38.37	0.000
Temp	1	65.764	65.764	65.764	213.74	0.000
Error	29	8.923	8.923	0.308		
Total	35	170.922				

C. Rut Rate at 10,000 Cycles of Loading $R^2 = 90.0\%$

Source	DF	Seq SS	Adj SS	Adj MS	F	P
Agg	1	0.069659	0.022062	0.022062	51.48	0.000
Grad	2	0.005404	0.005404	0.002702	6.31	0.005
AC	2	0.013516	0.015105	0.007552	17.62	0.000
Temp	1	0.021183	0.021183	0.021183	49.43	0.000
Error	29	0.012428	0.012428	0.000429		
Total	35	0.122190				

D. Log of Resilient Modulus $R^2 = 92.3\%$

Source	DF	Seq SS	Adj SS	Adj MS	F	P
Agg	1	0.33393	0.02503	0.02503	5.58	0.025
Grad	2	0.00625	0.00625	0.00312	0.70	0.507
AC	2	0.28996	0.05817	0.02908	6.49	0.005
Temp	1	0.93353	0.93353	0.93353	208.18	0.000
Error	29	0.13004	0.13004	0.00448		
Total	35	1.69370				

the statistical models and high repeatability of the triaxial repeated load test. Average permanent strains measured at 40°C and 60°C are shown in Figure 4.2.

The effect of aggregate type and gradation is shown in Figures A.1 through A.5, Appendix A. for each asphalt binder. The triaxial repeated load test is a highly reproducible test method. The results of duplicate test specimens were very similar and able to detect the effect of aggregate type and gradation. For all binder types and test temperatures, mixes with the rounded gravel showed much higher permanent strain than mixes with angular limestone. Also, mixes with coarse gradation showed the highest permanent strain followed by mixes with intermediate gradation. Mixes with fine gradation showed the least permanent strain. As discussed at the previous section, this order of gradations for permanent strain also follows the order for asphalt film thickness.

The effect of asphalt binders on the permanent strain is shown on Figure 4.2 and creep curves are rearranged in Figures A.6 through A.12, Appendix A. For all gradations and test temperatures, without exception, mixes with unmodified binder showed the largest permanent strain. Of two polymer modified binders, SBS resulted in less permanent strain than SBR. The superior performance of mixes with polymer may be due to two facts. First, polymers used in this study have molecular weights over 100,000 and are elastic. The large size of these polymers improved the temperature dependency of the asphalt, provided adequate stiffness, and improved strain recovery characteristics at high temperatures. Second, the differences in binder stiffness had some contribution to the results. At high temperatures (70-76°C), the unmodified binder showed the lowest $G^*/\sin\delta$, whereas the SBS binder showed the highest $G^*/\sin\delta$ (Table 3.2).

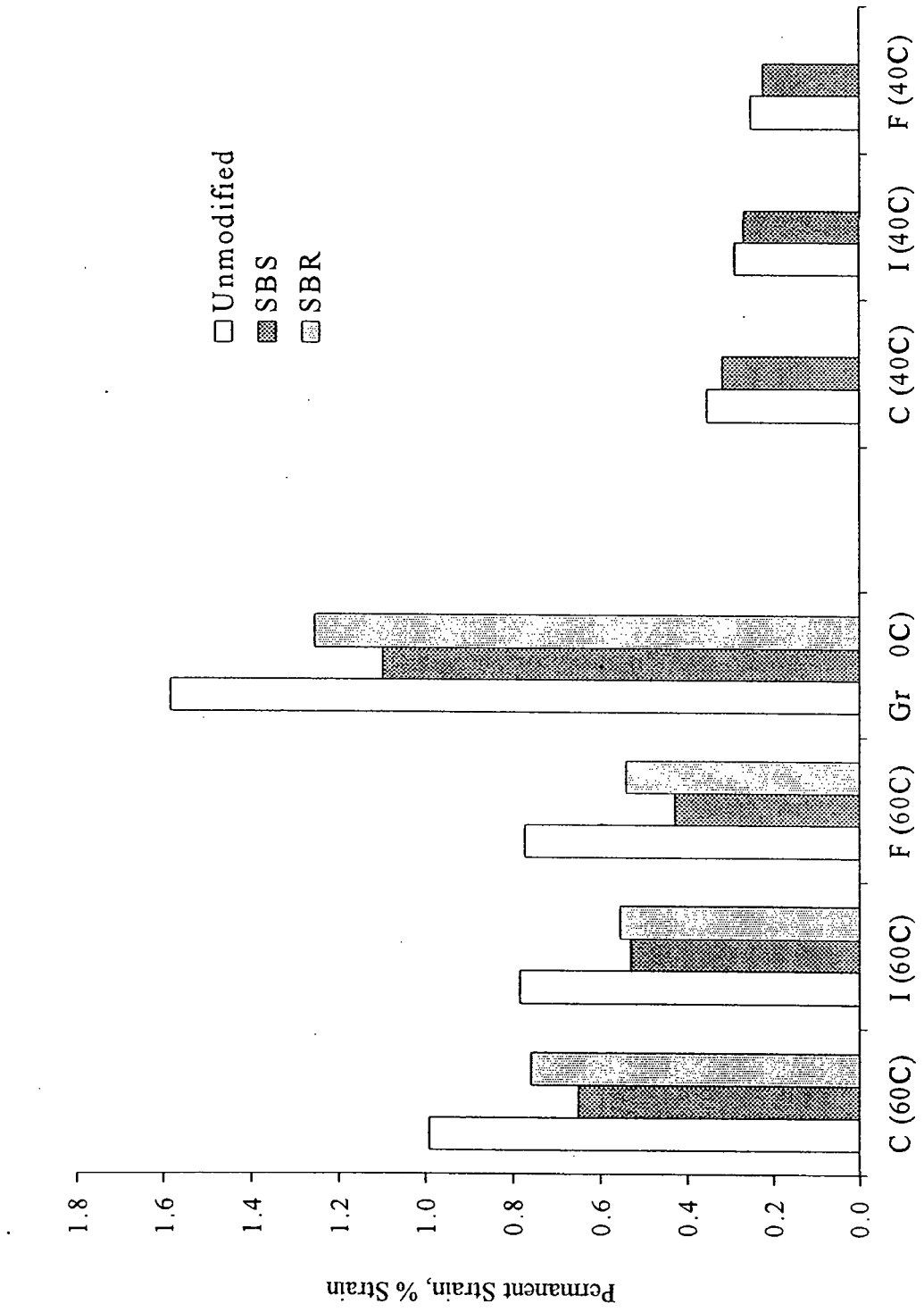

Figure 4.2 Permanent strain after 10,000 cycles of triaxial repeated load test

Temperature change significantly affects rheological and physical properties of viscoelastic materials such as asphalt mixtures. From Figure 4.2, the effect of temperature on permanent strain can be observed. For both modified and unmodified mixes, permanent strains at the higher temperature were much larger than permanent strains at the lower temperature. To show the effect of polymer modification on temperature dependency, creep curves for unmodified and SBS mixes for each gradation are presented at Figures A.13 through A.15, Appendix A. Mixes with the SBS binder showed much lower temperature dependency than mixes with the unmodified binder. At 40°C, permanent strains of unmodified and SBS mixes with three gradations of limestone were similar, whereas permanent strains of the same SBS mixes at 60°C were significantly lower than permanent strains of unmodified mixes. Table 4.8 includes two ANOVAs showing the significantly different temperature dependency of unmodified and SBS binders (asphalt-temperature interaction, Temp*AC). When the interaction term, Temp*AC, is considered in a statistical model, R^2 significantly increased from 89.6% to 98.1%.

The effect of aggregate type, gradation, and binder type on recovery and rate of permanent strain should be very similar to the results for permanent strain due to very strong correlations among them. Percent recovery and rut rates after 1000 and 10,000 cycles of all tested specimens are shown in Figures 4.3, 4.4, and 4.5, respectively. For all asphalt binders, mixes with rounded gravel showed significantly lower recovery and higher rut rates than mixes with limestone. For all binders and test temperatures, mixes with coarse gradation showed the lowest recovery and the highest rut rates, and mixes with fine gradation showed the highest recovery and the lowest rut rates. Again as discussed in APA results, this is likely due to the

Table 4.8 ANOVA for permanent strain to determine temperature dependency of binder (for limestone, unmodified and SBS mixes, n = 24)

Without Considering Asphalt-Temperature Interaction $R^2 = 89.6\%$

Analysis of Variance for Permanent Strain

Source	DF	Seq SS	Adj SS	Adj MS	F	P
Grad	2	0.10721	0.10721	0.05360	6.87	0.006
Asphalt	1	0.17471	0.17471	0.17471	22.39	0.000
Temp	1	0.99727	0.99727	0.99727	127.82	0.000
Error	19	0.14824	0.14824	0.00780		
Total	23	1.42743				

With Considering Asphalt-Temperature Interaction $R^2 = 98.1\%$

Analysis of Variance for Permanent Strain

Source	DF	Seq SS	Adj SS	Adj MS	F	P
Grad	2	0.10721	0.10721	0.05360	35.91	0.000
Asphalt	1	0.17471	0.16858	0.16858	112.93	0.000
Temp*AC	**2**	**1.11864**	**1.11864**	**0.55932**	**374.70**	**0.000**
Error	18	0.02687	0.02687	0.00149		
Total	23	1.42743				

asphalt binder film thickness within the mixes. Film thickness decreased from coarse to intermediate to fine gradation. According to Haung, et al. [63], when asphalt binder is sandwiched between aggregate surfaces forming a film with a thickness of about 10-20μm, apparent viscosity of the asphalt binders may drastically increase as film thickness decreases. An increase in apparent viscosity usually accompanied by increase in elasticity (decrease in phase angle, δ) and increase in stiffness (G*). In other words, mixes with fine gradation that had the least film thickness, would be more elastic and stiffer and could exhibit the highest strain

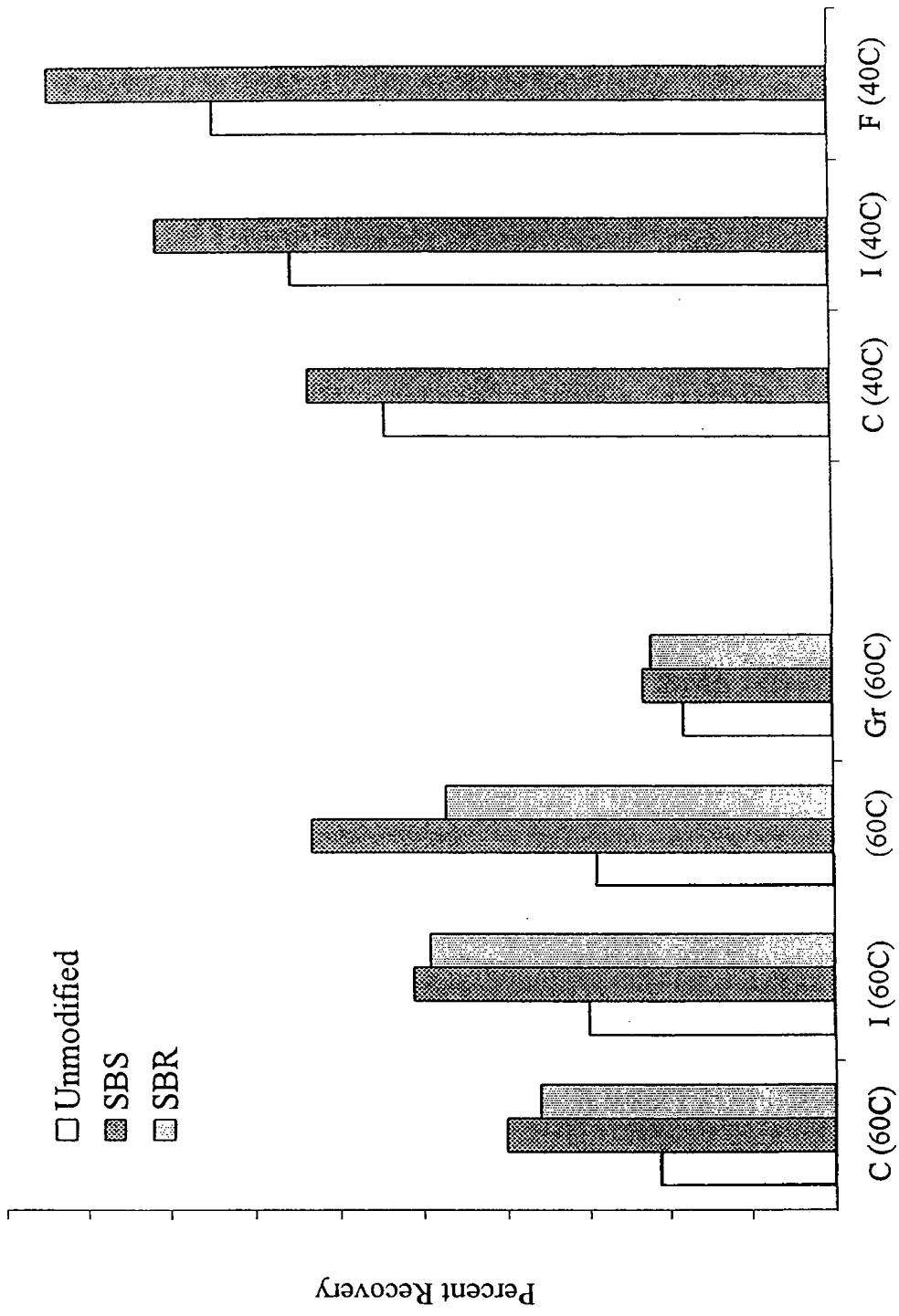

Figure 4.3 Pe recovery of accumu strain for 10,000 load cycles

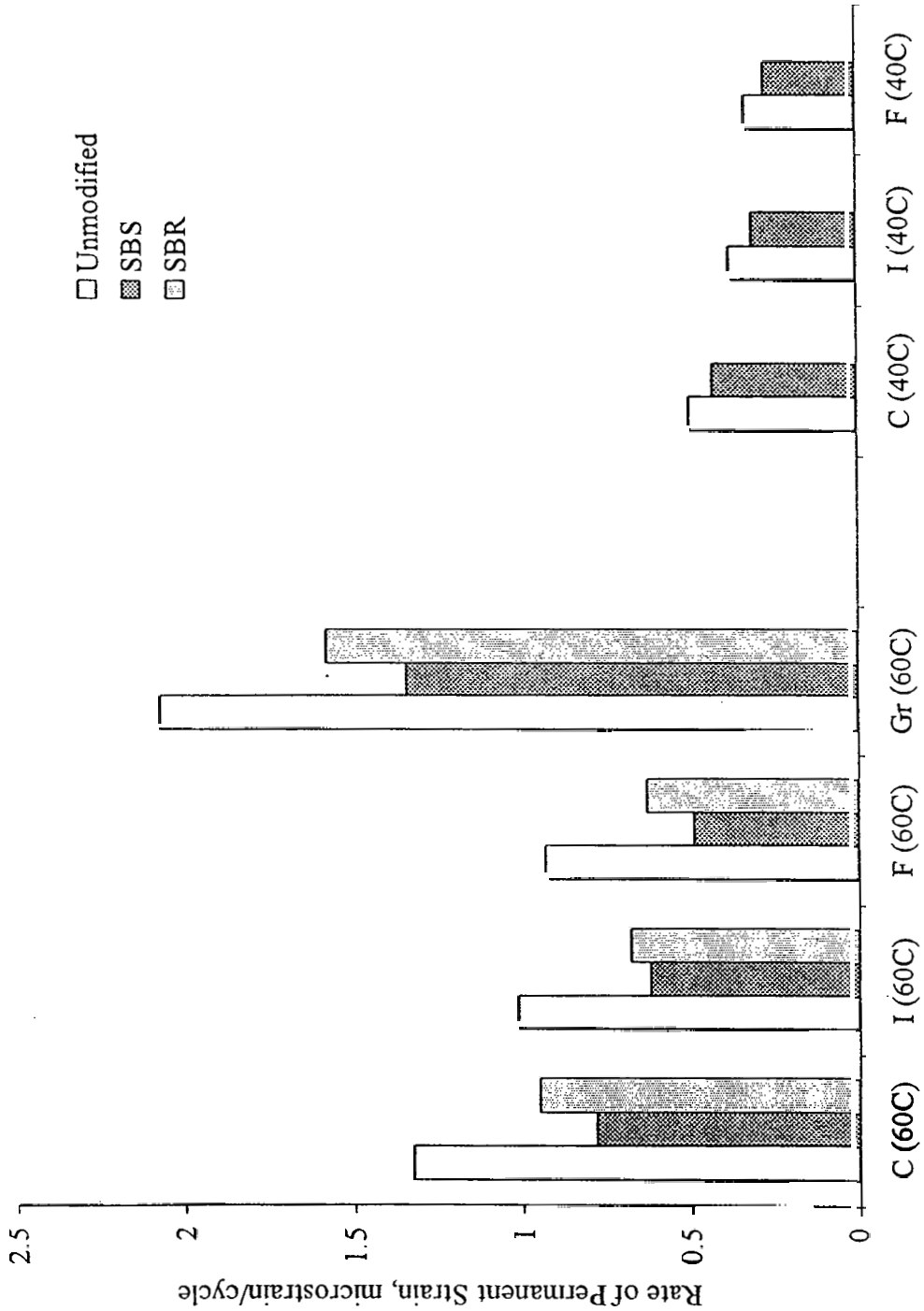

Figure 4.4 Rate of permanent strain at 1,000 load cycles

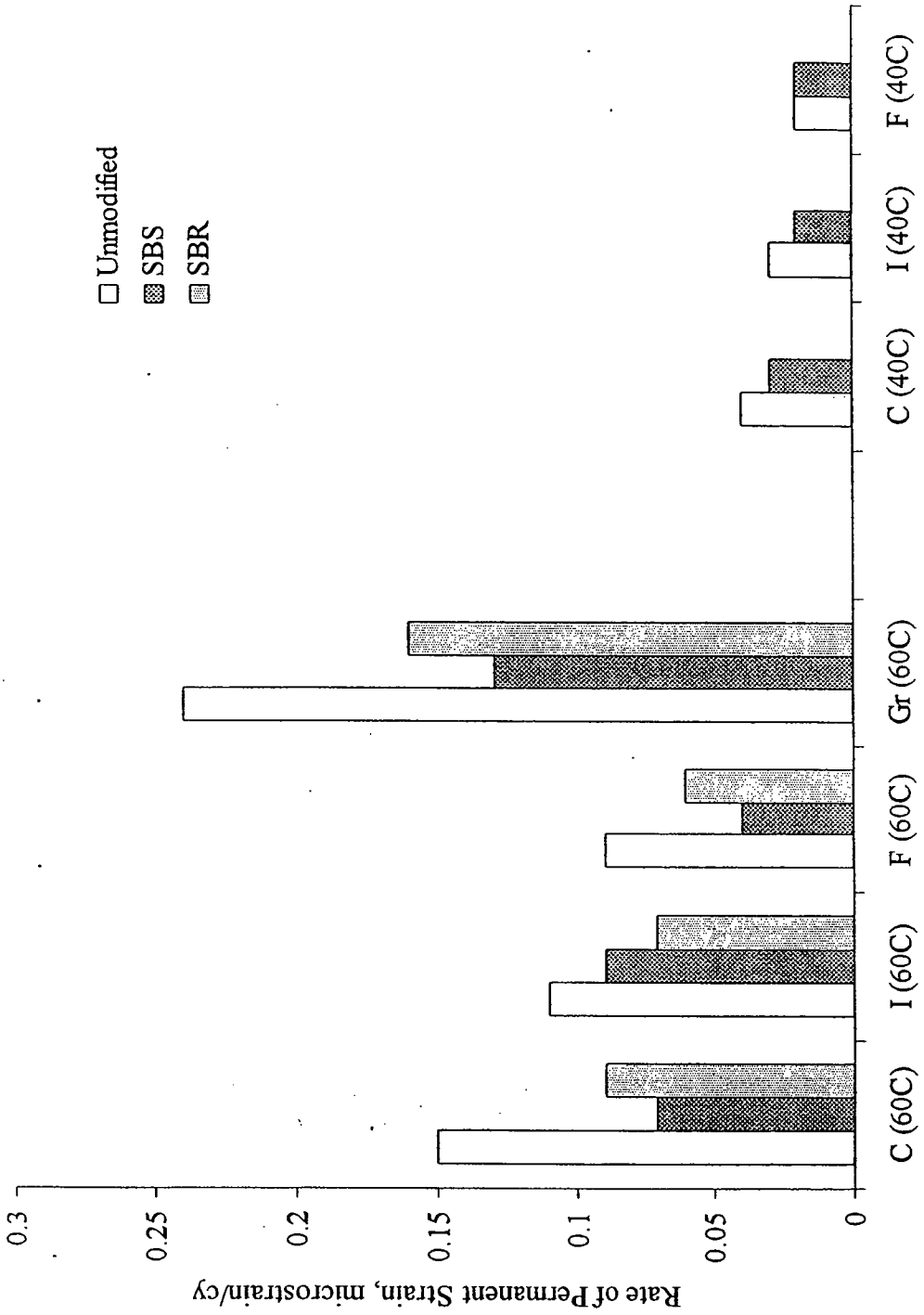

Figure 4.5 Rate of permanent strain at 10,000 load cycles

recovery and smallest rut rate. Effects of asphalt binder on recovery and rut rate for all aggregate types and gradations were significant and consistent. Mixes with coarse gradation showed the least recovery and the highest rut rate, whereas SBS mixes showed the highest recovery and lowest rut rate for each aggregate type and gradation. These trends are more obvious at 60°C.

Resilient modulus is not directly related to performance characteristics of asphalt mixes. However, it is one of the most important mix properties in analysis and design of asphalt pavements, describing pavement responses under traffic loading. As shown in Figure 4.6 and Table 4.7-D, temperature had the biggest effect on resilient modulus whereas gradation is not a factor. For each gradation, effects of binders were significant. At 60°C, mixes with unmodified and SBS binders had similar moduli, and mixes with SBR had slightly, but consistently, lower moduli. This is due to the fact that, at high temperatures, mix properties are predominantly influence by aggregate properties. For the limestone aggregate studied in this project, differences in aggregate gradation do not affect the resilient modulus. At lower temperatures, however, contribution of asphalt binder is larger and significantly influences mix properties. At 40°C, unmodified mixes showed significantly higher resilient moduli than SBS mixes, i.e., unmodified mixes showed poorer temperature dependency than SBS mixes. For each 120 psi deviator stress application at 40°C, mixes with polymer deformed more but recover more, leaving less permanent strain than mixes with unmodified binder. At 60°C, for each axial load application, mixes with polymers deformed similarly to mixes with unmodified binder. However, the polymer mixes recover more and leaving much less permanent strain.

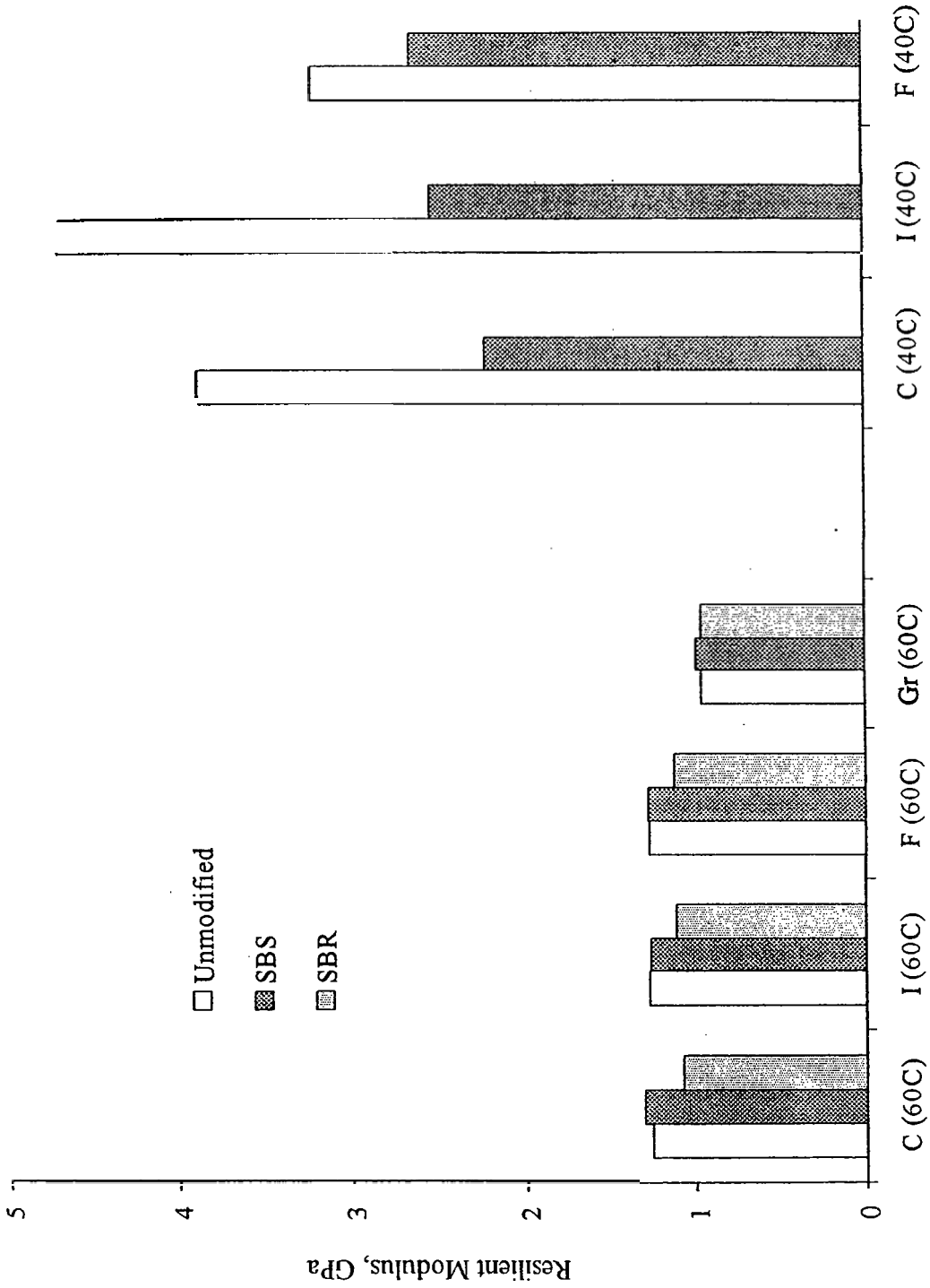

Figure 4.6 Resilient moduli of mixes determined by triaxial repeated load test

The percent air voids for all the samples decreased an average of 0.2% after the test (Table 4.3), consistent with Mallick et al. [10]. They found that the initial air voids were greater than 3%, original voids decreased (consolidation) after a triaxial repeated load test. When the initial air voids were below 3%, the voids increase (dilation) with triaxial repeated loads. The test specimens used in this ODOT project had a 4% average air void and nicely fit with their initial air void and void change relationship. There was no statistically significant difference in air void reduction between limestone and gravel mixes at 60°C. The air void reduction at 40°C was less than at 60°C.

In summary, the triaxial repeated load test is very sensitive to aggregate type, aggregate gradation, asphalt binder type, and polymer modified binder, consistent with previous studies [52, 55]. Mixes with crushed limestone aggregate showed much less rutting potential than mixes with rounded gravel aggregate. The restricted zone did not significantly affect the rutting performance of asphalt mixes. The highest rutting potential was observed from mixes with coarse aggregate (below the restricted zone) followed by mixes with intermediate gradation (through the restricted zone). Mixes with fine gradation (above the restricted zone) showed the lowest rutting potential. It is plausible that the effects of aggregate gradation in this study resulted from difference in asphalt binder film thickness for each mix. Polymer modified mixes showed significantly reduced temperature dependency, improved strain recovery, and reduced rutting potential.

4.3 Uniaxial Static Creep Test

Uniaxial static creep tests were performed on mixes prepared with three gradations of limestone and two binders (unmodified and SBS binders) at 40°C and 60°C. Creep strain after 1 hour of loading, permanent strain after 1 hour of recovery, percent recovery, slope of the steady state portion of creep curve, and creep stiffness at 1 hour were determined from the static creep data. The results are given in Table 4.9 and plotted on Figures 4.7 through 4.11. ANOVA was also performed to determine the effects of aggregate gradation and binder type. Table 4.10 summarizes statistical analyses of mix properties determined from the static creep test.

Total creep strain at 1 hour was significantly affected by test temperature, asphalt type, and aggregate gradation as shown in Table 4.10-A and Figure 4.7. For all binder types and test temperatures, mixes with the coarse gradation passing below the restricted zone showed the highest total creep strain, followed by mixes with the intermediate gradation passing through the restricted zone, as observed in APA and the triaxial repeated load test results. Mixes with the fine gradation passing above the restricted zone showed the least creep strain. This trend is also shown in creep curves presented at Appendix B, Figures B.1 through B.4. The creep curve includes the axial strain of test specimens during 3,600 seconds of 414 kPa (60 psi) loading and 3,600 seconds of recovery. The SBS modified mixes showed significantly lower total strain at 1 hour creep than the unmodified mixes for all gradations and test temperatures except for the mixes with intermediate gradation tested at 60°C. Comparisons of creep curves for binder effects are provided at Appendix B, Figures B.5 through B.10. Compared to the significant difference observed in the triaxial repeated load test, the effects of polymer modified binder on 1 hour total

Table 4.9 Results of uniaxial static creep test

Test Temp	Agg. Type	Asphalt Type	Void* Change (%)	Strain @ 1 hr. (%)	Permanent Strain (%)	Recovery %	Steady State Slope	Stiffness @ 1 hr (MPa)
60°C	Coarse	Unm	0.3	0.553	0.372	32.7	0.096	75.2
		Unm	0.2	0.595	0.413	30.6	0.086	69.3
		SBS	0.2	0.500	0.354	29.2	0.080	82.6
		SBS	0.1	0.453	0.216	52.3	0.082	90.2
	Inter	Unm	0.2	0.446	0.267	40.2	0.054	92.7
		Unm	0.4	0.422	0.244	42.2	0.056	97.9
		SBS	0.2	0.429	0.254	40.9	0.110	96.1
		SBS	-0.1	0.464	0.240	48.2	0.063	88.5
	Fine	Unm	0.2	0.439	0.219	50.0	0.045	94.6
		Unm	0.2	0.420	0.280	33.3	0.046	98.1
		SBS	0.2	0.390	0.235	39.8	0.067	105.8
		SBS	0.2	0.414	0.294	29.0	0.052	100.4
40C	Coarse	Unm	0.0	0.525	0.350	33.3	0.121	78.8
		Unm	0.1	0.485	0.341	29.6	0.120	85.3
		SBS	0.1	0.428	0.281	34.3	0.114	96.7
		SBS	0.0	0.418	0.224	46.5	0.133	99.1
	Inter	Unm	0.0	0.425	0.203	52.2	0.123	97.6
		Unm	0.1	0.413	0.336	18.6	0.134	99.9
		SBS	0.0	0.370	0.223	39.7	0.100	112.1
	Fine	Unm	0.1	0.356	0.215	39.5	0.118	116.5
		Unm	0.1	0.338	0.187	44.7	0.109	122.5
		SBS	0.1	0.343	0.217	36.7	0.086	119.2
		SBS	0.0	0.309	0.131	57.6	0.081	134.0

* Positive value means volume increase

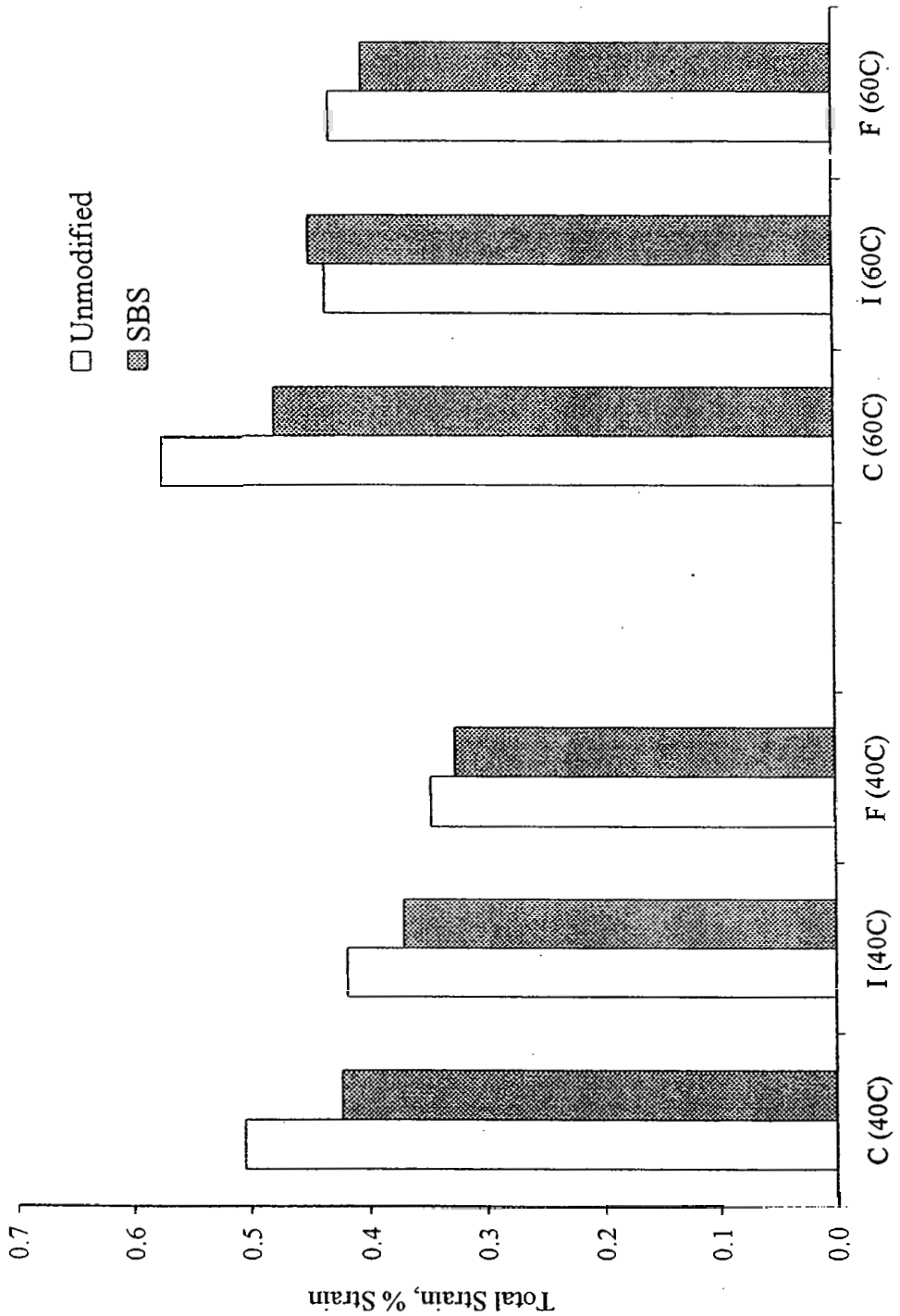

Figure 4.7 Total Strain after 1 hour in uniaxial static creep test

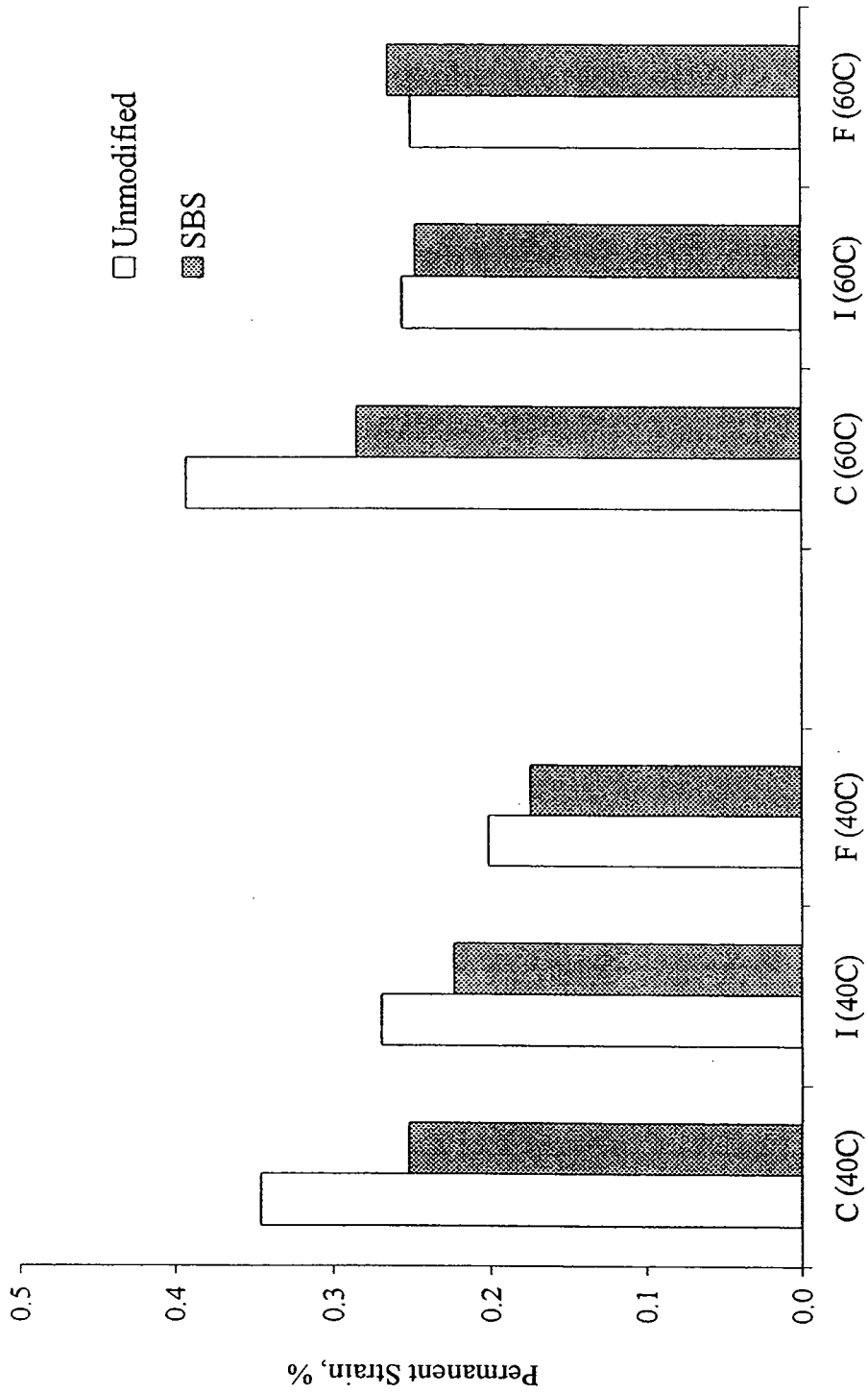

Figure 4.8 Permanent strain in uniaxial static creep test

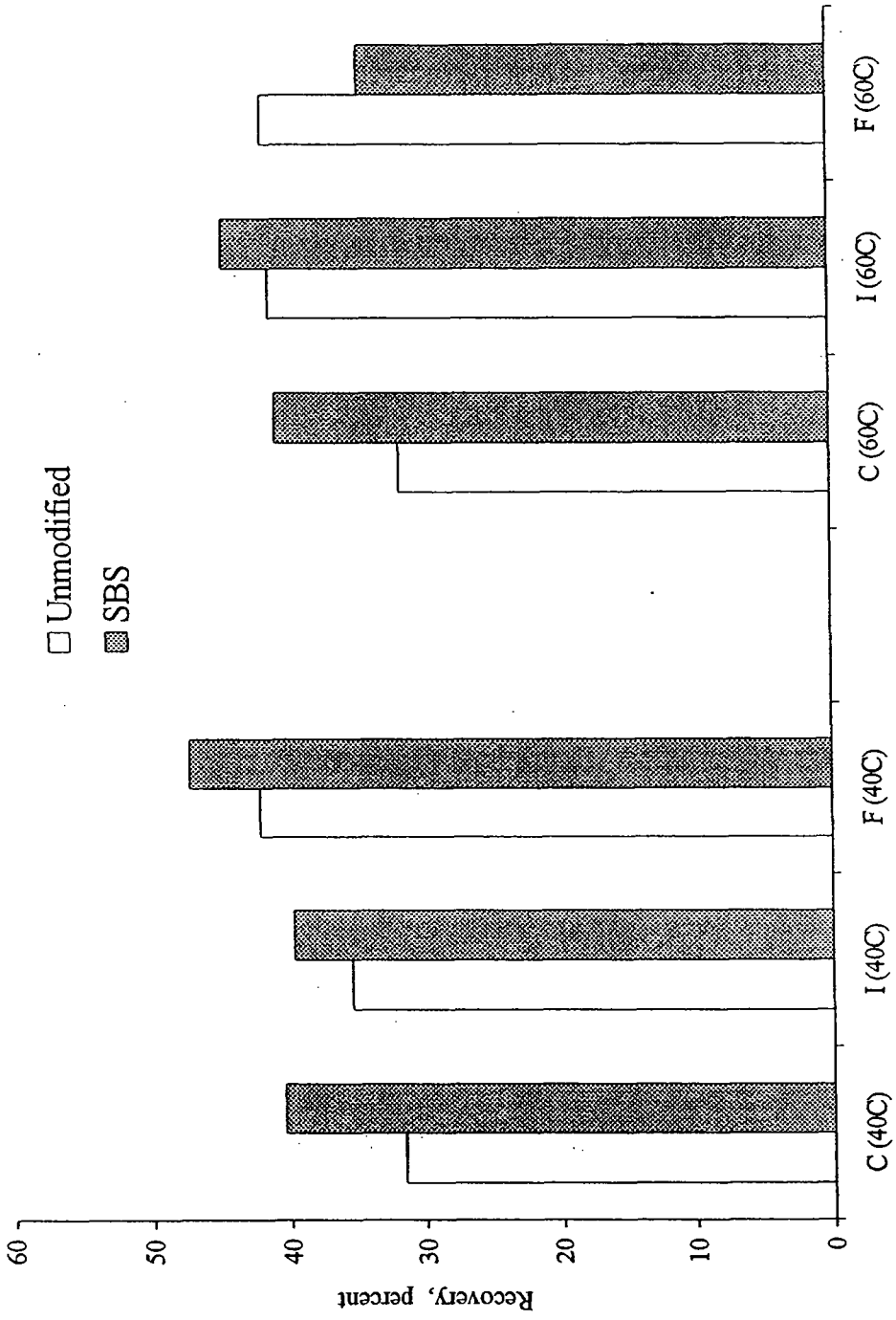

Figure 4.9 Recovery after 1 hour of unloading in uniaxial static creep test

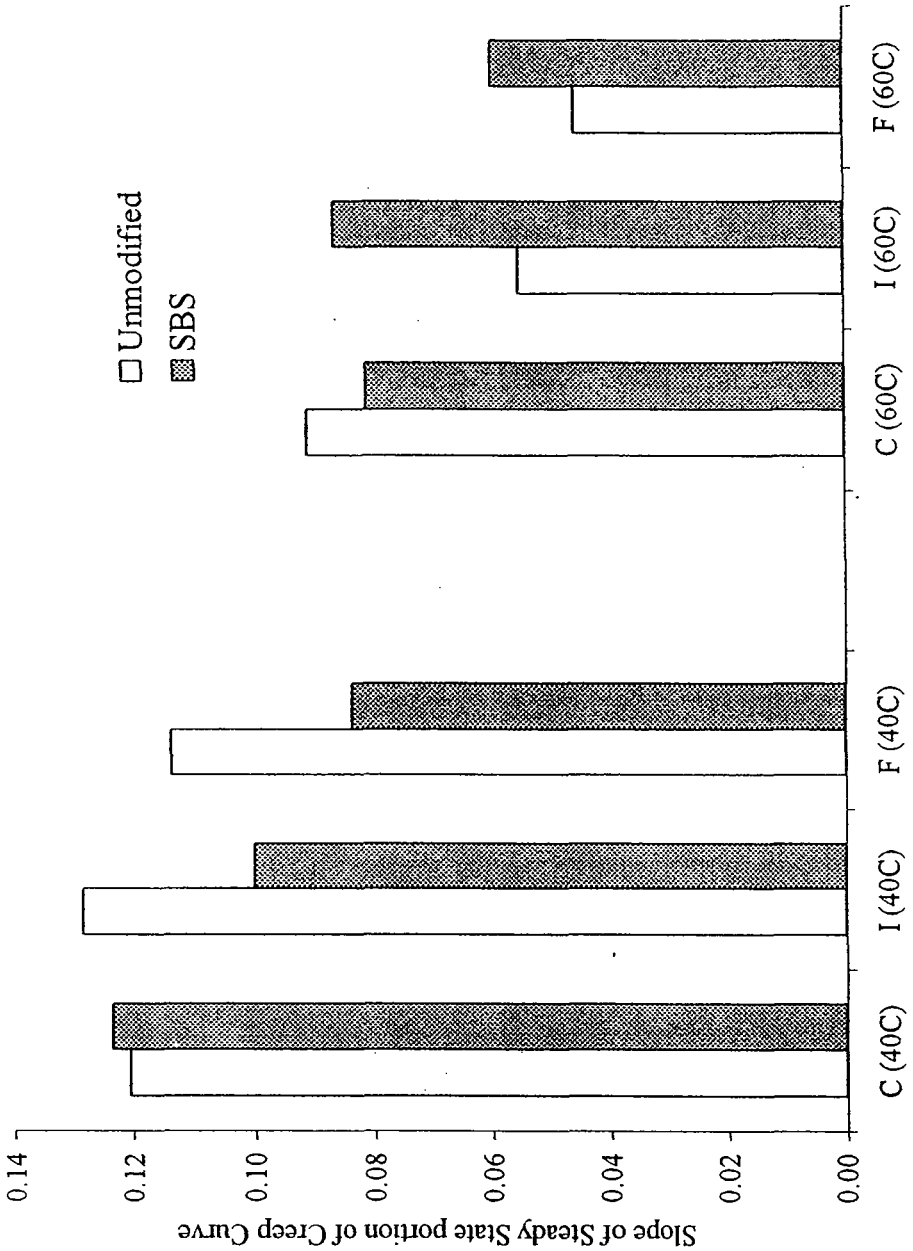

Figure 4.10 Slope of steady state portion of uniaxial static creep curve

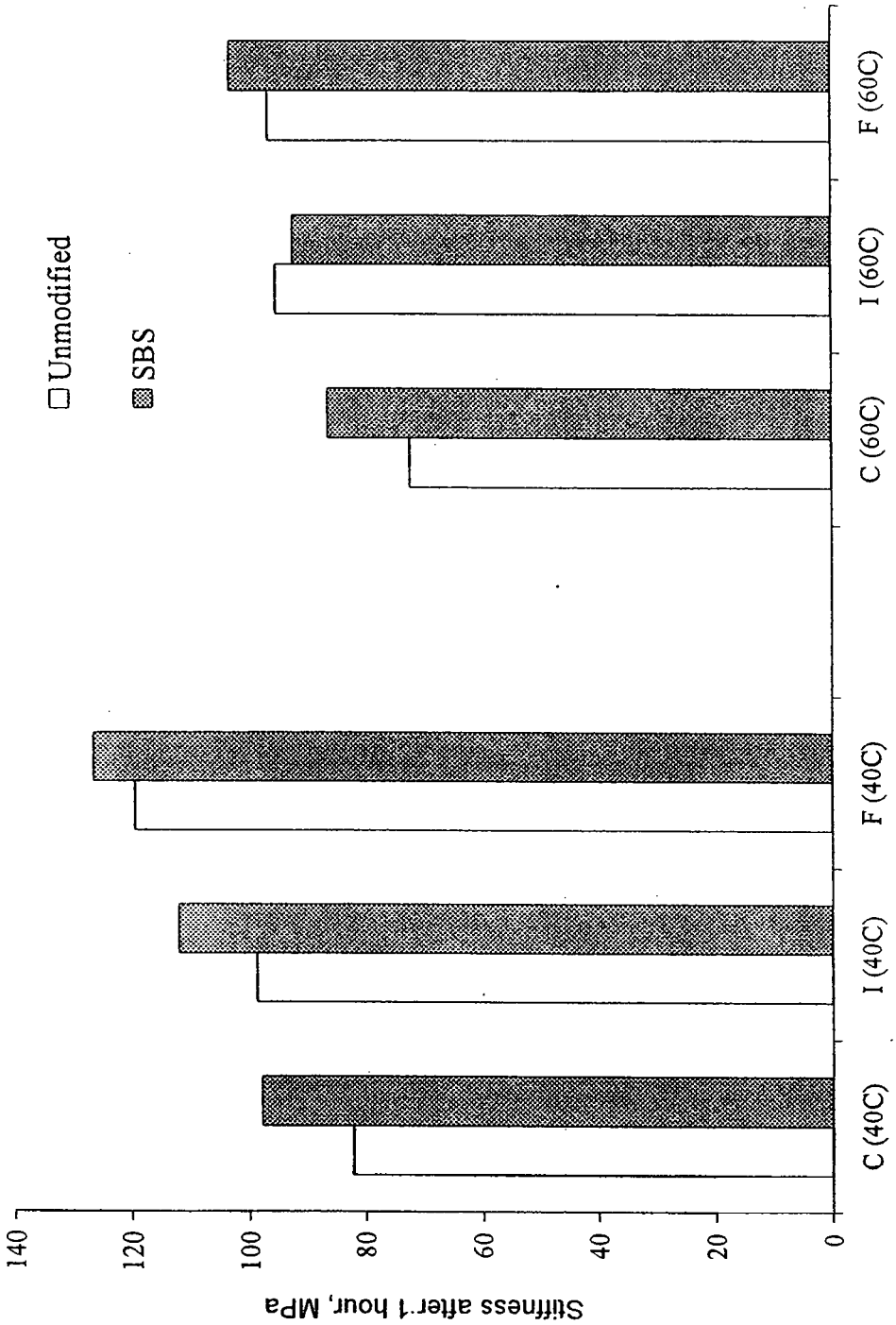

Figure 4.11 Stiffness after 1 hour in uniaxial static creep test

Table 4.10 Analysis of variance for uniaxial static creep test results (n = 24)

A. Total Strain at 1 Hour Loading $R^2 = 86.1$

Source	DF	Seq SS	Adj SS	Adj MS	F	P
Temp	1	0.020323	0.022397	0.022397	27.95	0.000
Asphalt	1	0.010830	0.011381	0.011381	14.20	0.001
Gradation	2	0.057893	0.057893	0.028946	36.12	0.000
Error	18	0.014425	0.014425	0.000801		
Total	22	0.103471				

B. Permanent Strain After 1 Hour Recovery $R^2 = 57.2$

Source	DF	Seq SS	Adj SS	Adj MS	F	P
Temp	1	0.007501	0.008994	0.008994	3.66	0.072
Asphalt	1	0.011435	0.012179	0.012179	4.95	0.039
Gradation	2	0.040189	0.040189	0.020094	8.17	0.003
Error	18	0.044255	0.044255	0.002459		
Total	22	0.103379				

C. Percent Recovery $R^2 = 11.7$

Source	DF	Seq SS	Adj SS	Adj MS	F	P
Temp	1	0.53	2.13	2.13	0.02	0.882
Asphalt	1	94.94	100.28	100.28	1.07	0.315
Gradation	2	128.85	128.85	64.42	0.69	0.515
Error	18	1686.27	1686.27	93.68		
Total	22	1910.58				

D. Slope of Steady State Portion of Creep Curve $R^2 = 75.8$

Source	DF	Seq SS	Adj SS	Adj MS	F	P
Temp	1	0.0105556	0.0105737	0.0105737	42.84	0.000
Asphalt	1	0.0000327	0.0000251	0.0000251	0.10	0.754
Gradation	2	0.0033513	0.0033513	0.0016757	6.79	0.006
Error	18	0.0044428	0.0044428	0.0002468		
Total	22	0.0183824				

creep strain measured in the uniaxial static creep test were relatively small. Raising test temperature from 40°C to 60°C increased the total creep strain for mixes of all gradations and binders. Comparisons of creep curves for temperature effects are provided at Appendix B, Figures B.11 through B.16. Unlike other properties of viscoelastic materials showing very large temperature dependence, total creep strain varied little at 20°C test temperature change. This can be seen from an ANOVA for total creep strain in Table 4.10-A. The sequential sum of square (seq SS) provides variability contributed by each variable, i.e., between-sample variation. Seq SS of error is the variability unexplainable with variables considered, i.e,within-sample variation [64]. Inspection of Table 4.10-A suggests that the largest influence on the total strain came from three aggregate gradations, followed by two test temperatures and two asphalt types. In this study of limited scope, the relative contributions to total creep strain response were about 56% from gradations, 20% from test temperatures, and 10% from asphalt binders. Variables with significant impact on creep strain and the slope of the steady state creep curve, have been identified, in order of influence: air void content of mixture, aggregate type, stress level, temperature, asphalt cement grade, and asphalt cement content [58]. These are in good agreement with the ranking of relative contribution determined from the ANOVA for total strain in this study.

Rutting of asphalt pavement results from accumulation of irreversible deformation. However, total creep strain includes both irreversible strain and some reversible strain since recovery is not allowed during test. It makes logical sense to investigate permanent strain for evaluation of rutting potential of asphalt mixtures. For permanent strain after 1 hour recovery test, immediately following 1 hour creep test, gradation and binder type showed a statistically

significant effect, while temperature was not a significant factor, $\alpha = 0.05$. Aggregate gradation showed the largest influence among the three variables considered. At 40°C, mixes with coarse gradation exhibited the largest rutting potential (the largest permanent strain), followed by mixes with gradations passing through or above the restricted zone. The SBS mixes showed less permanent strain than the unmodified mixes, and the differences (the beneficial effect of polymer modification) were largest for mixes with gradation passing below the restricted zone. The effects of gradation and binder type were more pronounced at 40°C (Figure 4.8).

As shown in Table 4.10-C, effects of aggregate gradation, binder type, and test temperature on percent recovery were not statistically significant because of, in part, large test variability (a large sequential sum of square of error). No statistically significant difference was found from an ANOVA for the absolute value of recovered strain. Rebound of asphalt mixes during a recovery test can be attributed to the resilient property of the aggregate matrix [58]. Therefore, aggregate type and gradation likely influence recovery. Figure 4.9 shows a general trend that SBS mixes and mixes with fine gradation show more recovery. There were no difference between average recovery at 40°C and 60°C.

The ANOVA given in Table 4.10-D indicated a significant effect of temperature and gradation on the slope of the steady state portion of creep curve. In general, as shown in Figure 4.10, the slope was high for mixes with gradation passing below the restricted zone (higher rutting potential) and low for mixes with gradation passing above the restricted zone (lower rutting potential). At high temperature, the slope was lower. This does not imply that the rutting potential of the mix is low at high temperatures but it represents a slope of the later stage of a stable creep process; higher temperature being equivalent to a longer loading time. Although, an

unstable creep process involves tertiary creep leading to a catastrophic shear failure, a stable creep process involves monotonic decrease in the rate of creep (slope). Following the viscoelaticity time-temperature superposition principle, the slope of steady state portion of 1 hour creep curve at 60°C is equivalent to the slope of the steady state portion of a longer than 1 hour creep curve at 40°C. As shown in Figures B.11 through B.16, creep in the 60°C test reached steady state faster than creep in 40°C tests.

Creep stiffness at 1 hour for limestone mixes were shown in Figures 4.11. Creep stiffness is inversely proportional to the total creep strain at a constant creep stress. Specimens subjected to this unconfined static creep test under 60 psi load for 3,600 seconds exhibited increases in air void contents (dilation). The magnitude of increase was higher at the higher test temperature. This behavior is opposite to that observed in the triaxial repeated load test (consolidation). Field rutting results from two processes; (1) consolidation causing a reduction in air voids and better particle-to-particle contact and (2) plastic shear flow involving dilation at very low air voids where asphalt may act as a lubricant. Sousa [13] reported that rutting failure at the laboratory uniaxial creep test did not show densification but dilation caused by crack development. This suggests uniaxial static or uniaxial repeated load creep tests is not adequately simulate pavement field loading conditions and the rutting mechanism. Consolidation observed during the triaxial repeated load test is a better representation of field rutting process.

Aggregate gradation plays a more important role than the asphalt binder type in the uniaxial creep test. For all creep test responses, sequential sum of square (Seq SS) for three gradations were much larger than those for two binder types (Table 4.10).

The permanent strain at 10,000 load cycles of triaxial repeated load test and the total strain at 1 hour of the uniaxial static creep test are compared in Figure 4.12. At 40°C, the creep strains measured by the two test methods exhibited very strong correlation ($R^2 = 0.95$), and both tests ranked the mixtures by aggregate gradation; the fine gradation mixes showed the least creep strain followed by the intermediate and coarse mixes as discussed earlier. Within the same gradation, the polymer modified mixes showed less creep strain for both tests. However, at 60°C, tests were poorly correlated ($R^2 = 0.57$). Further, the uniaxial static creep test ranked the mixes by aggregate gradation and then by binder type (except intermediate gradation), while the triaxial repeated load test ranked the mixes by asphalt type then by gradation. This is likely due to time and temperature dependency of the asphalt binder or the asphalt mixes. Fig 4.13 shows a typical master curve for the shear modulus of an asphalt binder and illustrates the effects of temperature and loading time. For this example, the master curve for SHRP AAB-1 asphalt was used because master curves for asphalt binders used in this project were not available. Loading rates for the triaxial repeated load test (0.1 second) and for the uniaxial static creep test (3,600 seconds) were converted into frequency. Using time-temperature shifting relationship applicable to asphalt binder, 40°C and 60°C were shifted to a 25°C reference temperature to determine shear moduli at each test condition. Christensen and Anderson [65] showed that a 15°C temperature change is equivalent to approximately 1 decade (a ten-fold) of frequency shift at high temperature (40-60°C). As shown in the Figure 4.13, for one hour static creep tests at 40 and 60°C, binder stiffness was approximately10 Pa and the responses of mixes at this test condition were predominantly affected by aggregate. This is supported by the fact that an

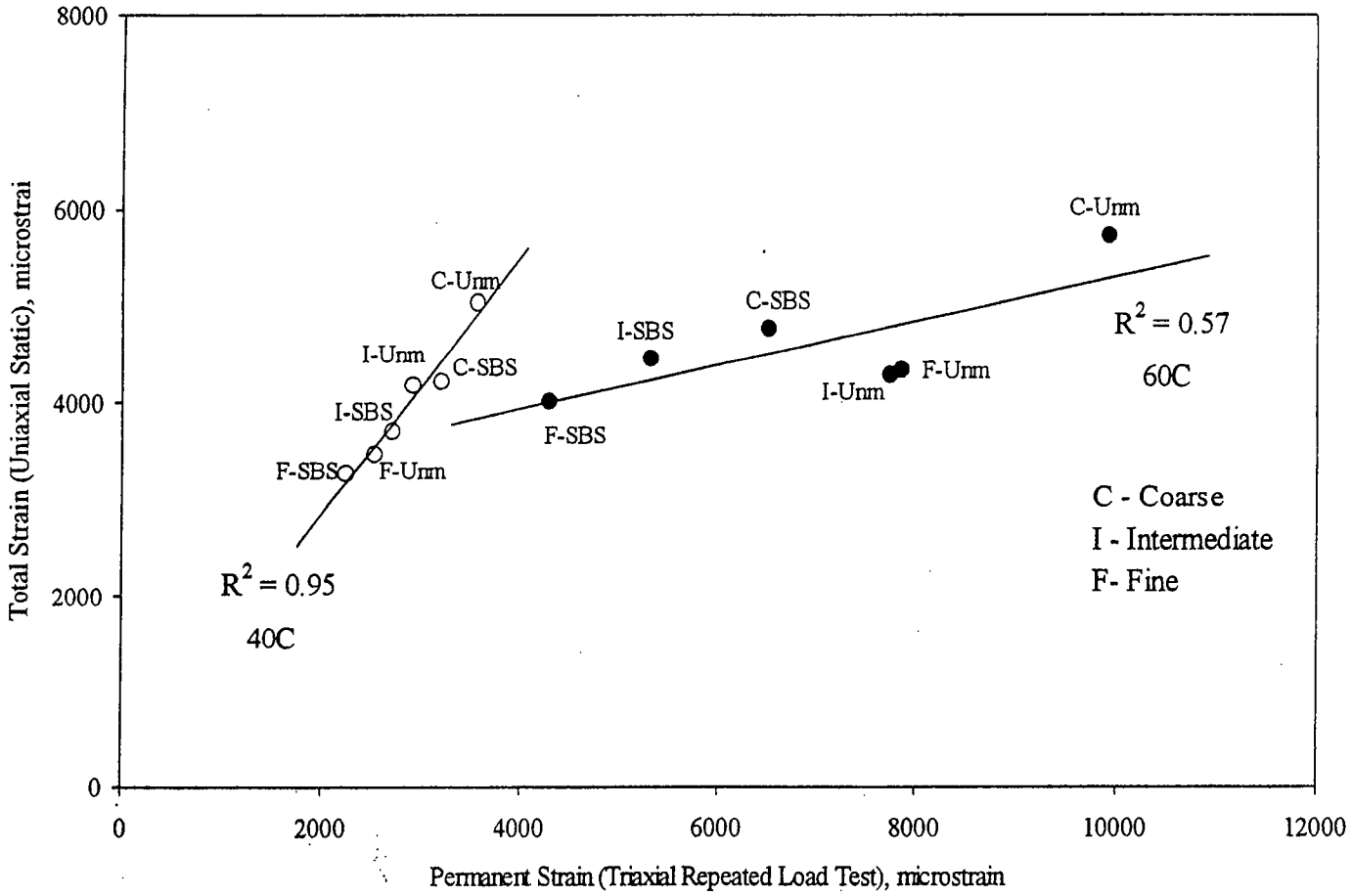

Figure 4.12 Comparison of creep strains determined by triaxial repeated load test and uniaxial static creep test

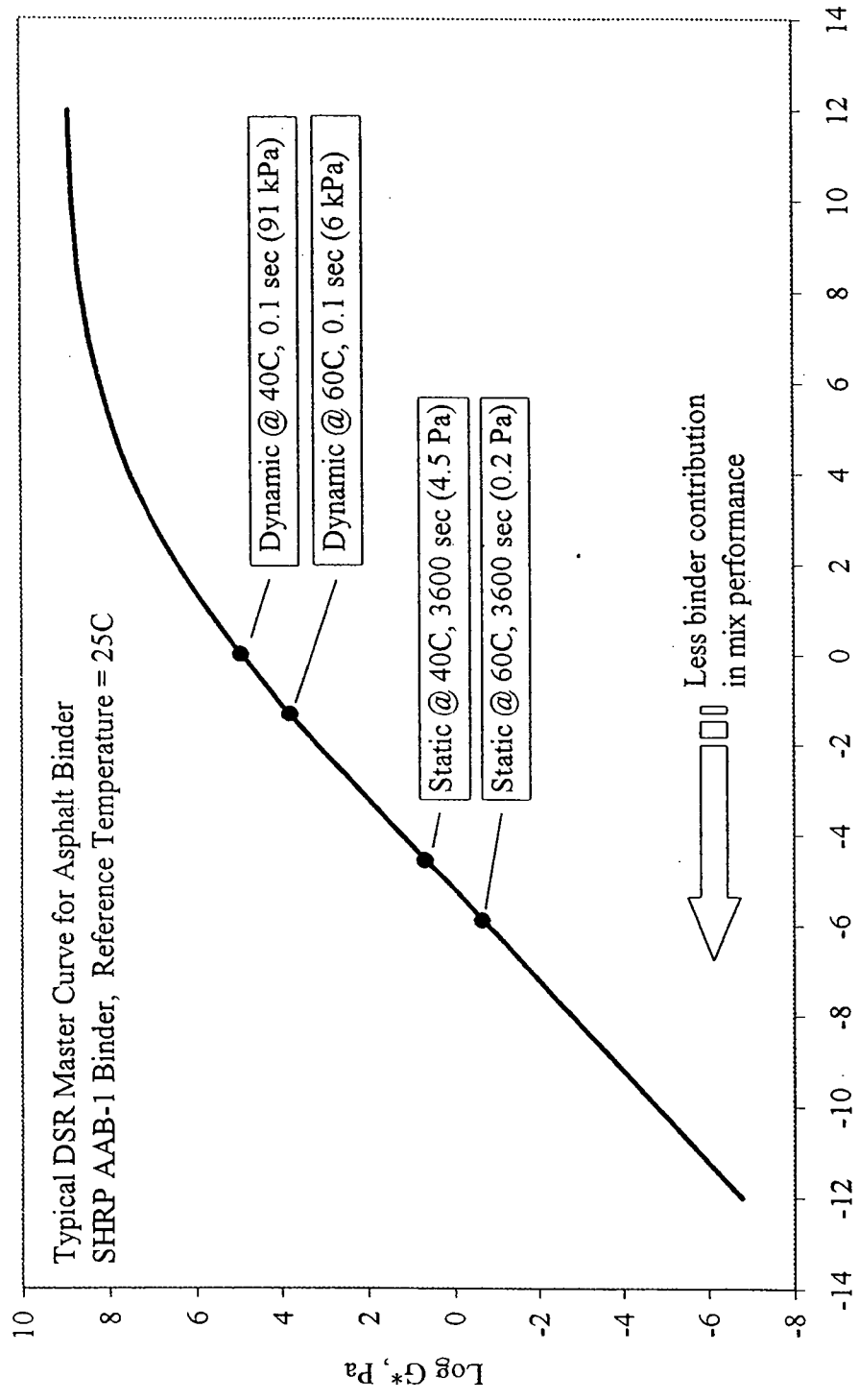

Figure 4.13 Shear moduli of asphalt binder estimated for test temperatures and loading times

ANOVA for the uniaxial static creep test data (Table 4.10) showed that aggregate effects were greater than binder effects (larger seq SS for gradations). For the triaxial repeated load tests, shear moduli indicated both aggregate and asphalt binder played significant roles. This is evident by that gradation, aggregate type, and binder type are statistically significant in ANOVAs for the triaxial repeated load test data (Table 4.7). Dynamic testing was more appropriate to evaluate the beneficial effects of polymer. The polymer property that reduces rutting potential by increased ability to recover upon unloading, is more significant at higher temperature where the unmodified binder becomes less elastic.

In summary, statistically significant effects of binder types and gradation were observed. Analyses of total creep strain, creep stiffness, and permanent strain indicate that mixes with SBS binder resisted rutting better than unmodified mixes. It also indicated that mixes with gradation passing above the restricted zone shows the best rutting resistance. Mixes with gradation passing below the restricted zone showed the least rutting resistance. After the uniaxial creep test, tested specimens increased in volume. It is believed that rutting mechanisms in the uniaxial creep test and at field are different.

4.4 Flexural Beam Fatigue Test

Mixes prepared with three limestone gradations and two asphalt binders (unmodified and SBS) were used for a flexural beam fatigue test. During the fatigue test, flexural stiffness of specimen under constant strain loading was continuously recorded (see Figure 4.14). Failure was defined as the number of load repetition (N_f) where the flexural stiffness became 50% of the initial flexural stiffness. In addition to the number of cycles to failure (N_f), the initial flexural stiffness, the cumulative dissipated energy, phase angles, and the steady state slope were determined. Fatigue curves for mixes with each gradation are given at Figures C.1 through C.3, Appendix C. The results of the flexural beam fatigue test are given in Table 4.11 and ANOVAs for the fatigue test results are given in Table 4.12. All of the analyses were performed using

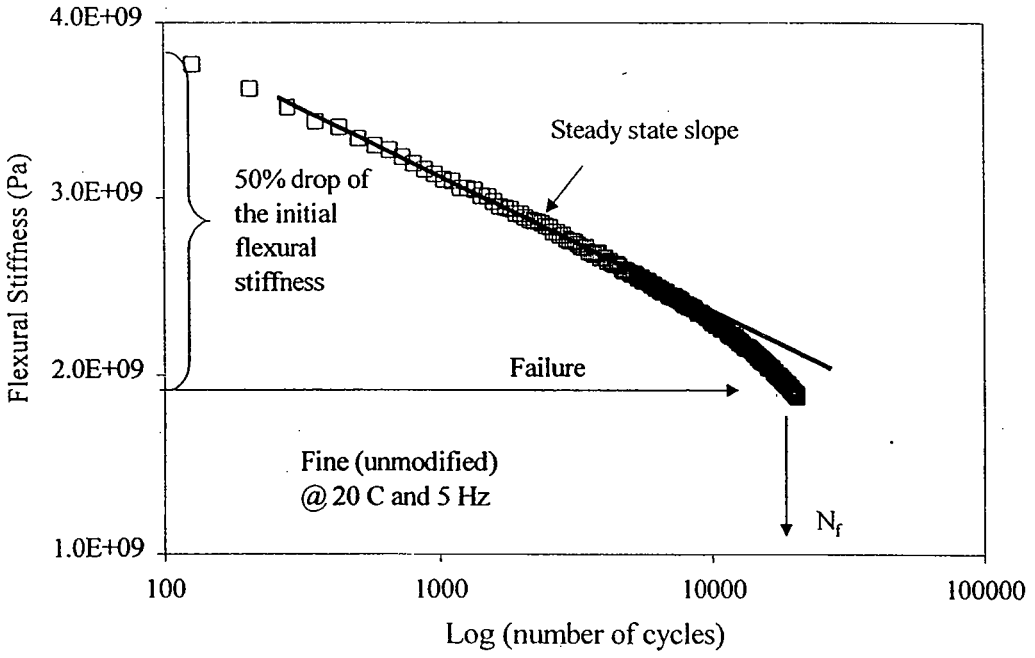

Figure 4.14 Typical graph of stiffness versus log (number of load cycles)

Table 4.11 Results of flexural beam fatigue tests on limestone mixes at 20°C, 5 Hz

Gradation	AC Type	Applied Strain (μm/m)	Number of cycles to failure	Initial Flexural Stiffness (GPa)	Cumulative Dissip Energy (J/m^3)	Initial Phase Angle (degree)	Phase Angle @ fail (degree)	Steady State Slope GPa/Log cy
C	Unm	275	35,090	3.85	3.13E+07	24.6	33.3	0.712
	Unm	250	121,310	4.33	9.21E+07	21.9	32.1	0.686
	Unm	250	41,110	4.24	2.86E+07	23.3	31.5	0.682
	SBS	275	170,000*	1.69	1.17E+08	27.8	36.0	0.214
	SBS	275	283,022	2.64	1.50E+08	26.9	35.3	0.350
I	Unm	275	33,112	3.81	1.93E+07	23.9	31.4	0.715
	Unm	275	10,636	3.62	9.21E+06	25.1	32.3	0.719
	SBS	275	223,047*	2.83	4.37E+08	26.5	34.7	0.355
	SBS	275	442,329	2.14	2.36E+08	29.2	37.0	0.288
F	Unm	300	8,644	3.82	8.25E+06	26.0	31.7	0.985
	Unm	275	20,533	3.76	9.48E+06	25.5	33.1	0.789
	SBS	275	357,000	2.71	2.20E+08	28.1	36.4	0.288
	SBS	275	1,275,865*	2.48	1.79E+09	29.2	37.3	0.288

*estimated value due to interrupted test

only 275 με data. Asphalt binder type had a significant impact on the fatigue performance of asphalt mixes, whole aggregate gradation did not. Figures 4.15 through 4.18 illustrate the effects of asphal binder and aggregate gradation on the fatigue life, initial stiffness, slope of the steady state fatigue curve, and cumulative dissipated energy. Mixes with SBS binder achieved much longer fatigue life, lower initial stiffness, larger cumulative dissipated energy, higher phase angles, and milder fatigue slope than mixes with unmodified binder. Different gradations (passing above, through, and below the restricted zone) did not affect the fatigue life. Fatigue

Table 4.12 Analysis of variance for flexural beam fatigue test results (n=10)

Log Number of Cycles to Failure $R^2 = 87.4\%$

Source	DF	Seq SS	Adj SS	Adj MS	F	P
Gradation	2	0.3295	0.1240	0.0620	0.72	0.526
Asphalt	1	3.2777	3.2777	3.2777	37.89	0.001
Error	6	0.5191	0.5191	0.0865		
Total	9	4.1264				

Initial Stiffness $R^2 = 84.0\%$

Source	DF	Seq SS	Adj SS	Adj MS	F	P
Gradation	2	0.2429	0.0999	0.0499	0.35	0.715
Asphalt	1	4.1987	4.1987	4.1987	29.79	0.002
Error	6	0.8457	0.8457	0.1409		
Total	9	5.2872				

Log Cumulative Dissipated Energy $R^2 = 80.6\%$

Source	DF	Seq SS	Adj SS	Adj MS	F	P
Gradation	2	0.2493	0.1165	0.0582	0.35	0.718
Asphalt	1	3.8917	3.8917	3.8917	23.41	0.003
Error	6	0.9974	0.9974	0.1662		
Total	9	5.1384				

Initial Phase Angle $R^2 = 82.7\%$

Source	DF	Seq SS	Adj SS	Adj MS	F	P
Gradation	2	3.7418	2.2827	1.1414	1.24	0.354
Asphalt	1	22.7344	22.7344	22.7344	24.71	0.003
Error	6	5.5198	5.5198	0.9200		
Total	9	31.9960				

Phase Angle at Failure $R^2 = 87.2\%$

Source	DF	Seq SS	Adj SS	Adj MS	F	P
Gradation	2	5.399	2.327	1.163	1.43	0.310
Asphalt	1	27.888	27.888	27.888	34.37	0.001
Error	6	4.869	4.869	0.812		
Total	9	38.156				

Steady State Slope of Stiffness vs Log (N_f) $R^2 = 96.6\%$

Source	DF	Seq SS	Adj SS	Adj MS	F	P
Gradation	2	1.6330E+16	1.4188E+15	7.0938E+14	0.27	0.775
Asphalt	1	4.4254E+17	4.4254E+17	4.4254E+17	166.15	0.000
Error	6	1.5981E+16	1.5981E+16	2.6635E+15		
Total	9	4.7485E+17				

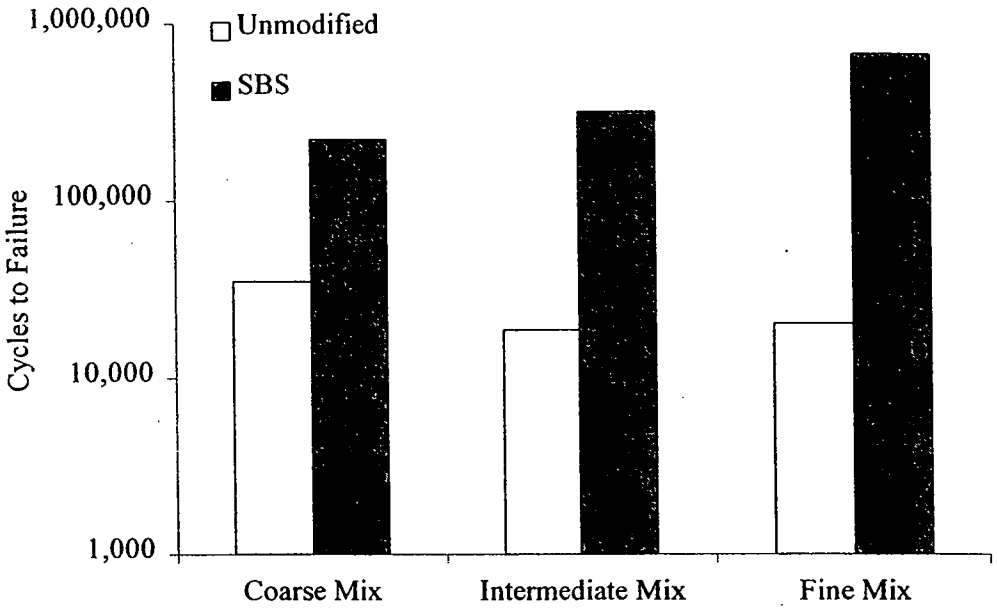

Figure 4.15 Number of cycles to failure for limestone mixes

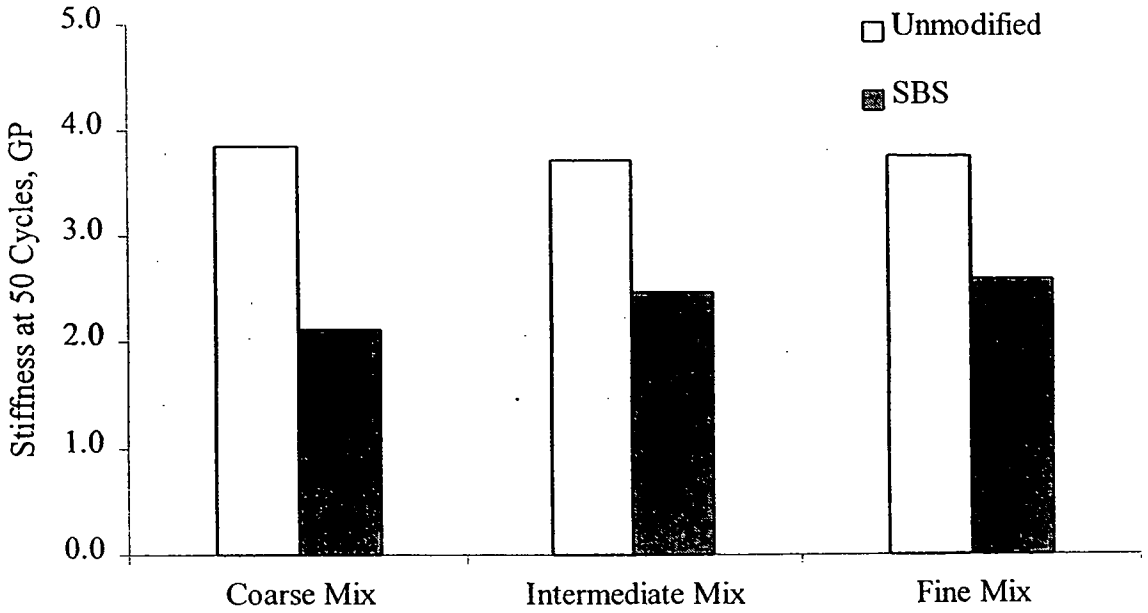

Figure 4.16 Initial flexural stiffness of limestone mixes

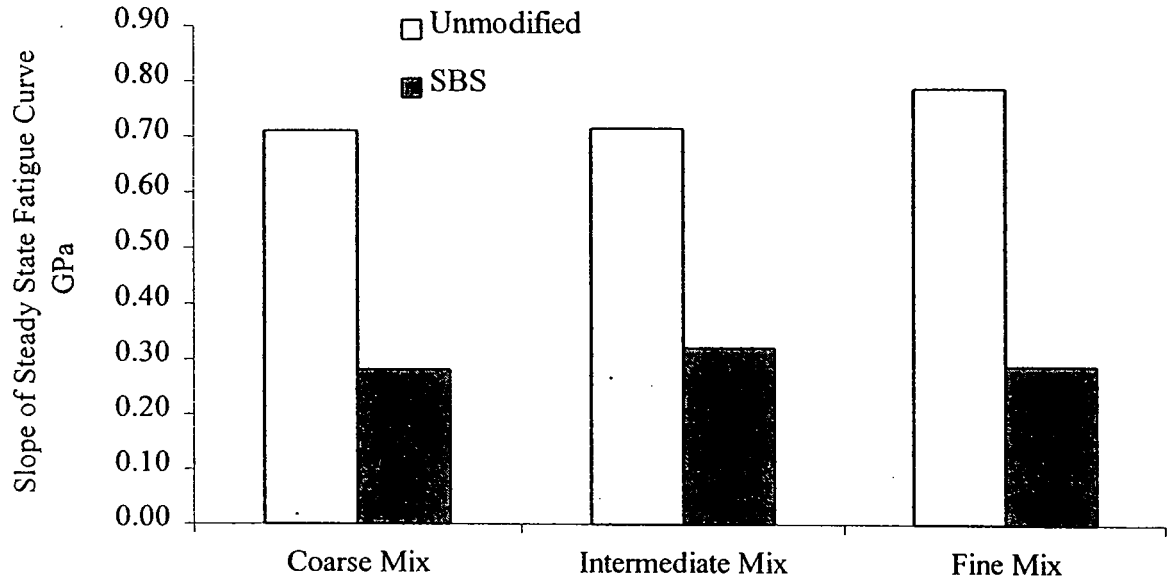

Figure 4.17 Steady state slope of fatigue curve for limestone mixes

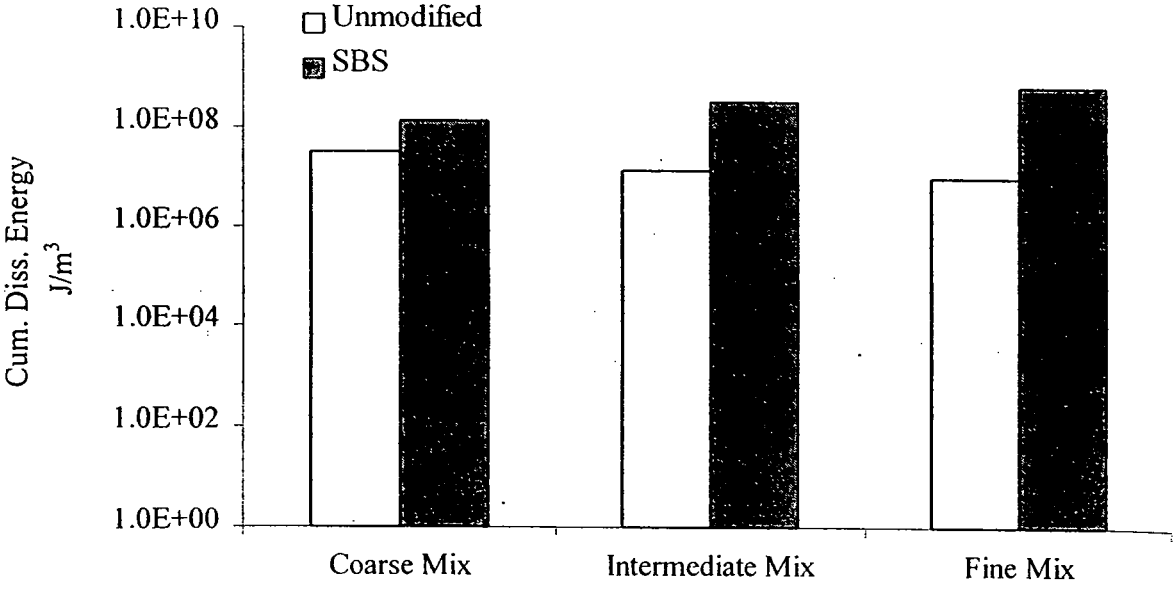

Figure 4.18 Cumulative dissipated energy for limestone mixes

failure proceeds by the formation and propagation of cracks under tensile load. In tensile response of asphalt mixes such as fatatigue cracking, asphalt binder would plays an important role, while aggregate has little influence. Among fatigue related mix properties, very strong correlations exist as shown in Table 4.13. These correlations should be viewed with caution because of the small number of samples (n=10) and limited mix variables.

The better fatigue performance characteristics of SBS modified mixes are rendered by the added elasticity from polymer addition. Elastomeric polymers, such as SBS and SBR, stretch under load and recover easily after the load is removed [46]. For a given load, this can be translated into larger strain or lower stiffness. In the strain controlled fatigue test used for this study, the significantly lower flexural stiffness allowed the SBS mixes to bend with ease. Therefore, for SBS mixes, damage caused by each load application was smaller, and the rate of stiffness reduction indicated by the steady state slope of the fatigue curve was smaller, resulting in longer fatigue life. The relationship between initial flexural stiffness and fatigue life are given in Figure 4.19. All mixes are divided into two clusters, mixes with unmodified binder and mixes with SBS binder. Lower flexural stiffness influences the fatigue life favorably in a controlled-strain mode laboratory fatigue test. However, at field, lower stiffness of mixes also causes higher tensile strain at the bottom of the pavement layer for a given load, and influences the fatigue life adversely as well.

In summary, mixes with SBS binder showed much longer fatigue life than mixes with unmodified binsers in a strain controlled laboratory fatigue test. Mixes with gradations passing below, through, and above the restricted zone did not show differences in performance.

Table 4.13 Pearson Correlations for fatigue properties of limestone mixes with unmodified and SBS modified binders (n=10)

	Log N_f	Initial Stiffness	Log Cum. Diss. Energy	Initial Phase Angle	Final Phase Angle
Initial Stiffness	-0.788				
Log Cum. Diss. Energy	0.966	-0.725			
Initial Phase Angle	0.881	-0.869	0.816		
Final Phase Angle	0.920	-0.867	0.862	0.976	
Steady State Slope	0.902	-0.949	0.865	0.878	0.907

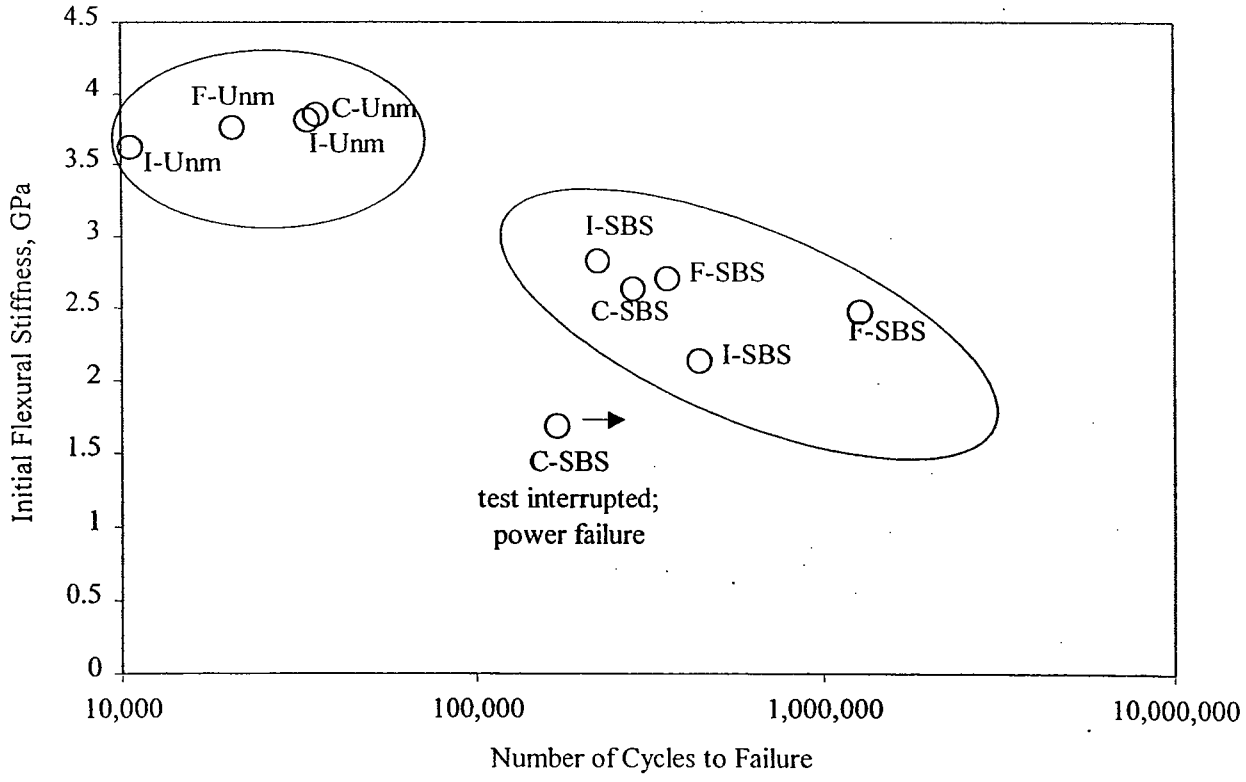

Figure 4.19 Relationship between initial flexural stiffness and fatigue life

4.5 Indirect Tensile Resilient Modulus Test and Indirect Tensile Strength Test

The results of the indirect tensile (IDT) resilient modulus test and the indirect tensile strength tests (ITS) are given in Table 4.14. The indirect tensile resilient modulus data are presented in graphic form for each gradation in Figures 4.20 through 4.22. Results of ITS are shown in Figure 4.23.

Results of analysis of variance (ANOVA) for the IDT resilient modulus are summarized in Table 4.15. Analysis of data for all three test temperatures indicates that asphalt binder type (unmodified and SBS) showed significant effect whereas aggregate gradations passing below, through, and above the restricted zone showed only moderately significant effect. This finding is similar to the results of resilient modulus determined by the triaxial repeated load test. ANOVA was performed for each test temperature. The effect of difference in gradation on the resilient modulus is moderately significant only at 25°C and not significant at 5 and 40°C. Asphalt mixes with different binder type did not show significantly different resilient modulus at 5°C. But the difference in binder type showed a significant effect at 25 and 40°C. When subjected to low temperature (5°C) and fast loading (0.1 second IDT load duration), mixes with both unmodified and SBS modified become very stiff and behaves as similar elastic materials. The increased elasticity rendered by polymer is relatively small when compared with the resiliency of asphalt mixes at this temperature and loading rate used in the resilient modulus test. As temperature increases, modulus of asphalt mix decreases rapidly and the added elasticity by polymer would become significant.

Table 4.14 Results of indirect tensile resilient modulus and indirect tensile strength test

Gradation	Asphalt Type	Resilient Modulus, GPa					Indirect Tensile Strength (kPa)
		Indirect Tensile Test			Triaxial Test*		
		5 °C	25 °C	40 °C	40 °C	60 °C	
Coarse	Unm	19.2	8.4	3.5	4.6	1.25	1748
	Unm	17.9	9.7	4.1	3.1	1.26	2053
	SBS	16.6	6.4	2.4	2.2	1.26	1556
	SBS	18.9	6.4	2.2	2.2	1.34	1562
Intermediate	Unm	22.5	11.9	4.6	4.5	1.28	2191
	Unm	19.5	11.2	3.2	5.0	1.26	1924
	SBS	19.2	9.1	3.1	2.6	1.24	2007
	SBS	15.6	7.7	2.8	2.4	1.29	1825
Fine	Unm	17.1	10.5	3.9	2.9	1.21	2171
	Unm	17.9	8.8	3.7	3.5	1.34	1973
	SBS	21.1	8.5	3.5	2.8	1.23	2060
	SBS	16.4	9.3	3.2	2.5	1.33	2209

* Resilient moduli measured by triaxial test (Table 4.3) were provided for comparison purpose.

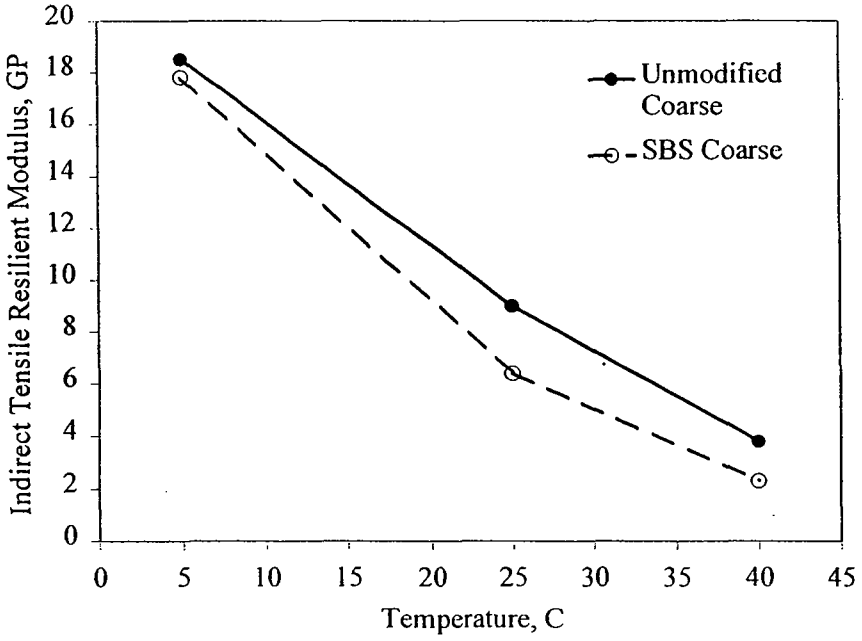

Figure 4.20 Indirect tensile resilient moduli of coarse mixes

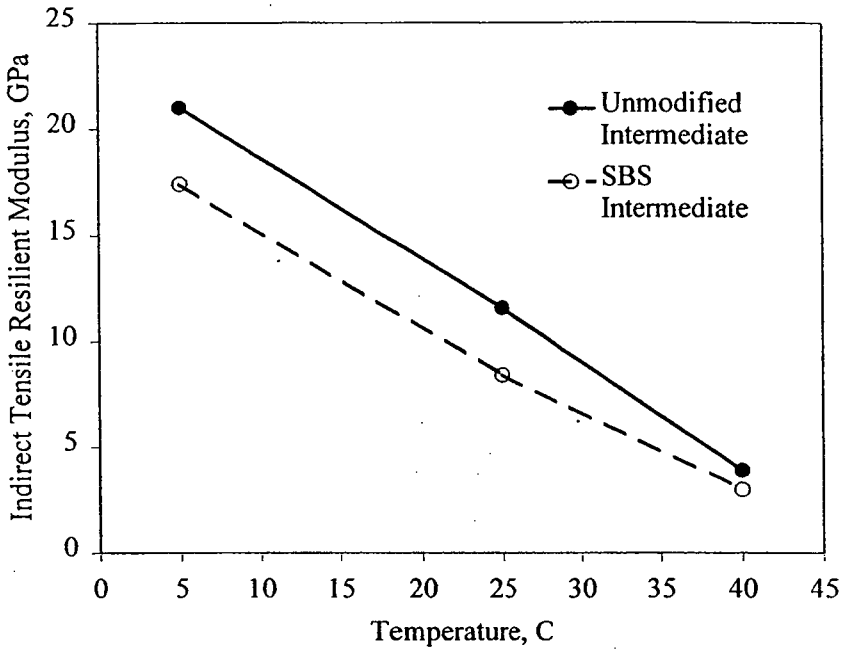

Figure 4.21 Indirect tensile resilient moduli of intermediate mixes

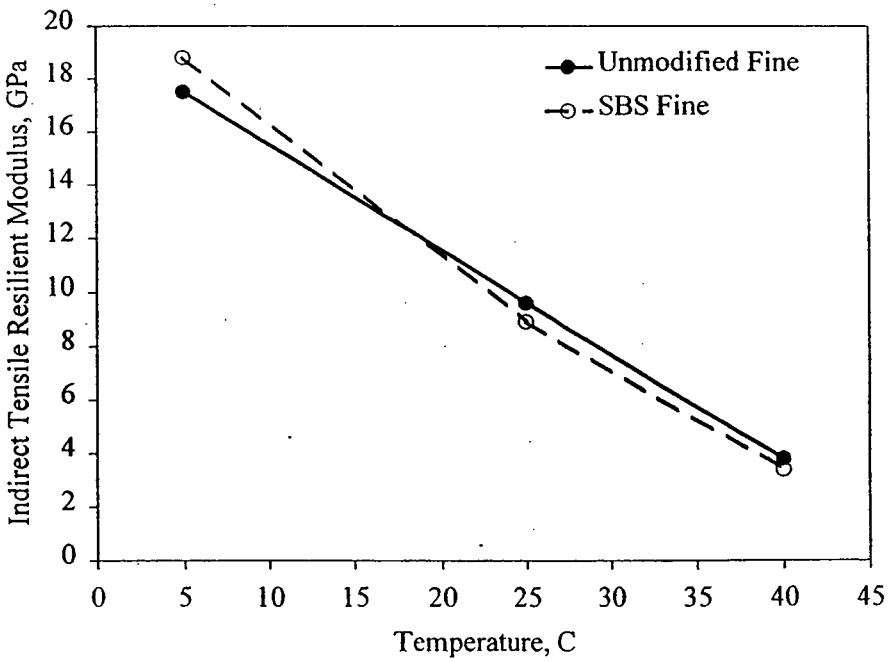

Figure 4.22 Indirect tensile resilient moduli of fine mixes

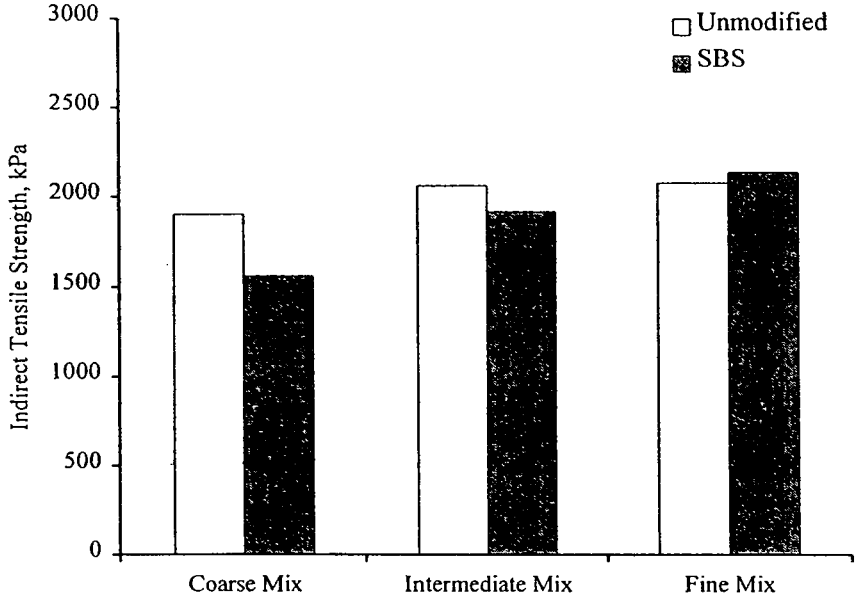

Figure 4.23 Indirect tensile strength of limestone mixes

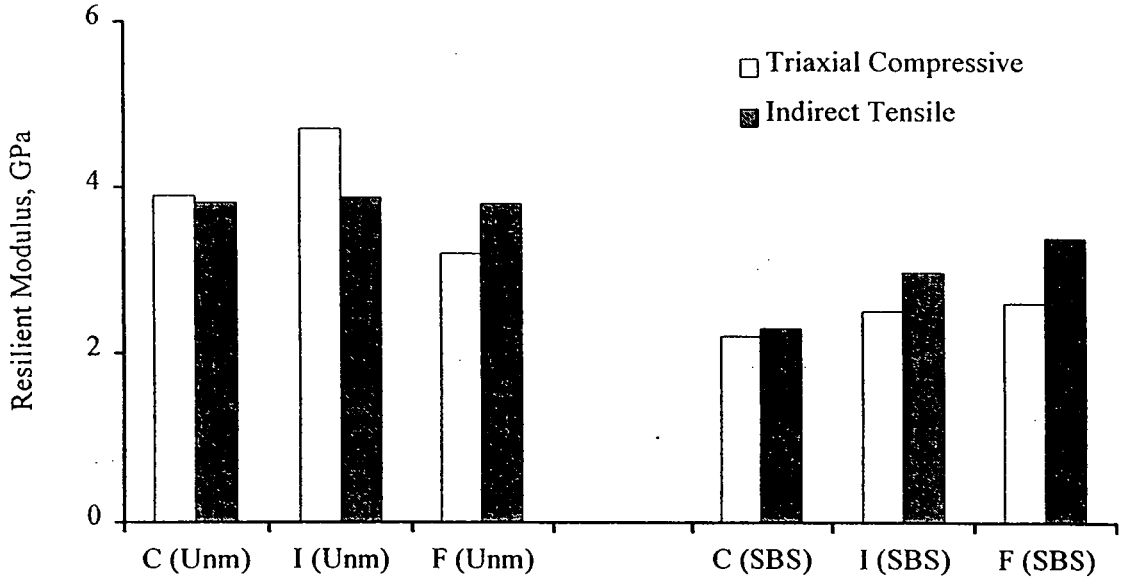

Figure 4.24 Comparison of resilient moduli determined by triaxial repeated load test and indirect tensile test at 40°C

Table 4.15 Analysis of variance for indirect tensile resilient modulus and indirect tensile strength of mixes

A. Log Resilient Modulus at 3 Temperatures $R^2 = 97.2\%$

Source	DF	Seq SS	Adj SS	Adj MS	F	P
Temp	2	3.38655	3.38655	1.69328	506.40	0.000
Grad	2	0.02845	0.02845	0.01423	4.25	0.024
AC	1	0.06860	0.06860	0.06860	20.51	0.000
Error	30	0.10031	0.10031	0.00334		
Total	35	3.58392				

B. Log Resilent Modulus at 5°C $R^2 = 14.2\%$

Source	DF	Seq SS	Adj SS	Adj MS	F	P
Grad	2	0.001351	0.001351	0.000676	0.27	0.773
AC	1	0.001928	0.001928	0.001928	0.76	0.409
Error	8	0.020279	0.020279	0.002535		
Total	11	0.023558				

C. Log Resilent Modulus at 25°C $R^2 = 78.6\%$

Source	DF	Seq SS	Adj SS	Adj MS	F	P
Grad	2	0.027234	0.027234	0.013617	6.47	0.021
AC	1	0.034743	0.034743	0.034743	16.51	0.004
Error	8	0.016838	0.016838	0.002105		
Total	11	0.078815				

D. Log Resilent Modulus at 40°C $R^2 = 67.5\%$

Source	DF	Seq SS	Adj SS	Adj MS	F	P
Grad	2	0.014180	0.014180	0.007090	1.83	0.221
AC	1	0.049878	0.049878	0.049878	12.90	0.007
Error	8	0.030931	0.030931	0.003866		
Total	11	0.094989				

E. Indirect Tensile Strength $R^2 = 62.5\%$

Source	DF	Seq SS	Adj SS	Adj MS	F	P
Grad	2	292165	292165	146082	5.54	0.031
AC	1	58940	58940	58940	2.23	0.173
Error	8	211050	211050	26381		
Total	11	562155				

In spite of the fact that the SBS binder is stiffer than the unmodified binder is, SBS mixes show lower resilient moduli than unmodified mixes for each gradation and test temperature as shown in Figures 4.20 through 4.22. Between 25 and 40°C, SBS mixes showed lower temperature susceptibility than unmodified mixes, indicated by the milder slope of modulus versus temperature curve.

Figure 4.24 compares resilient moduli of mixes at 40°C determined by triaxial repeated load test (compressive mode) and indirect tensile test. Considering variability of each test, the values are in very good agreement for the mixes used in this study.

The indirect tensile strength value can be used as a relative indicator of the resistance of the asphalt mix to fracture related phenomena, such as fatigue cracking or low temperature thermal cracking. ANOVA for the indirect tensile strength shows moderately significant effect of gradation and no effect of binder type (Table 4.15-E). As shown in Figure 4.38, mixes with fine gradation and intermediate gradation tend to have little higher ITS. It also showed that ITS of the SBS mixes and the unmodified mixes are not significantly different. The average ITS of SBS mixes (1,870 kPa) were lower than the average ITS of unmodified mixes (2,020 kPa). This supports that higher fatigue life for SBS mixes comes from added flexibility rather than higher tensile strength.

4.6 Moisture Susceptibility Test

The gravel aggregate and the absorptive limestone aggregate used in this study were not known for moisture susceptibility problem. It was expected that the standard AASHTO T 283 procedure with one cycle of freeze/thaw conditioning would not cause enough damage to the

mixes and meaningful comparison of binder type for moisture damage would be difficult. For this reason, specimens were subjected to three cycles of freeze/thaw conditioning. For limestone mixes, tensile strength ratios (TSR) after one and two freeze/thaw conditions were also determined. Table 4.16 shows the results of the moisture susceptibility test.

Indirect tensile strength (ITS) of control specimens are lower than ITS of specimens discussed at the previous section because of their higher air void content (7% instead of 4%). For both gravel and coarse graded limestone aggregate, SBS mixes showed consistently lower ITS values than unmodified mixes.

Table 4.16 Results of moisture susceptibility test

Agg Type	Asphalt Type	Test Number	Indirect Tensile Strength (ITS) (kPa)				Tensile Strength Ratio (TSR)		
			Control	Cycle 1	Cycle 2	Cycle 3	Cycle 1	Cycle 2	Cycle 3
LS Coarse	Unm	1	1459.1	1393.8	1137.3	1098.9			
		2	1444.5	1546.3	1199.7	1094.8			
		3	1475.6	1501.7	1063.1	1125.2			
		Avg.	*1459.7*	*1480.6*	*1133.4*	*1106.3*	*1.01*	*0.78*	*0.76*
	SBS	1	1334.5	1266.4	1133.4	967.4			
		2	1339.5	1277.7	1216.0	1117.2			
		3	1341.5	1292.8	1202.5	1037.9			
		Avg.	*1338.5*	*1279.0*	*1184.0*	*1040.8*	*0.96*	*0.88*	*0.78*
Gravel	Unm	1	1093.0	--	--	699.0			
		2	1102.6	--	--	713.0			
		3	1052.2	--	--	733.3			
		Avg.	*1082.6*	--	--	*715.1*	--	--	*0.66*
	SBS	1	1029.9	--	--	756.3			
		2	936.7	--	--	753.2			
		3	999.9	--	--	806.5			
		Avg.	*988.8*	--	--	*772.0*	--	--	*0.78*

Statistical analysis of a ratio variable such as TSR requires extra attention because of its unique characteristics. One of the major differences between ratio variables and ordinary non-ratio variables is that most of ratio variables are not normally distributed, an important assumption that must be made to use many statistical analysis procedures [66]. To test statistical significance of the binder type on TSR, 95% confidence interval was obtained for each TSR by bootstrapping, one of non-parametric procedures applicable to nay form of sample distributions. If confidence intervals of two TSR did not overlap, the difference between the two TSR was said to be statistically significant at $\alpha \approx 0.05$. Mean and 95% confidence interval of TSR determined by bootstrapping are given in Table 4.17. As number of freeze/thaw conditioning increased, TSR for both mixes decreased as shown in Figure 4.25. The first freeze/thaw cycle did not caused much damage to both the SBS and the unmodified limestone mixes as evidenced by high TSR; 1.01 and 0.96 for the unmodified limestone mix and the SBS limestone mix, respectively. The TSR difference was not significant. After the second conditioning, however, there was a large drop in TSR of unmodified limestone mix, while the SBS mixes performed well. The TSR difference was significant. While TSR of SBS mix decreased gradually, most of TSR reduction for unmodified mix happened during the second freeze/thaw conditioning. After three freeze/thaw cycles, TSR of limestone mixes did not exhibit significantly difference; 0.76 and 0.78 for unmodified binders and SBS binder, respectively. For gravel, three cycles of freeze/thaw conditioning brought a significant difference between TSRs for unmodified and SBS mixes. TSR for unmodified gravel was significantly lower than TSR for unmodified limestone mix. Smooth surface texture of the rounded gravel provided lower stripping resistance than rough surface texture of crushed limestone aggregate. The use of SBS binder significantly improved the

Table 4.17 Confidence interval and mean of TSR determined by non-parametric procedure

Aggregate Type	Number of Freeze Cycle	Asphalt Binder	Mean TSR Ratio	95% Confidence Interval		Are TSRs different?
				Low	High	
Lomestone Coarse Gradation	1	Unm	1.014	0.955	1.070	NO
		SBS	0.956	0.949	0.964	
	2	Unm	0.762	0.720	0.787	YES
		SBS	0.885	0.849	0.908	
	3	Unm	0.758	0.753	0.763	NO
		SBS	0.740	0.722	0.774	
Gravel	3	Unm	0.661	0.640	0.697	YES
		SBS	0.781	0.734	0.807	

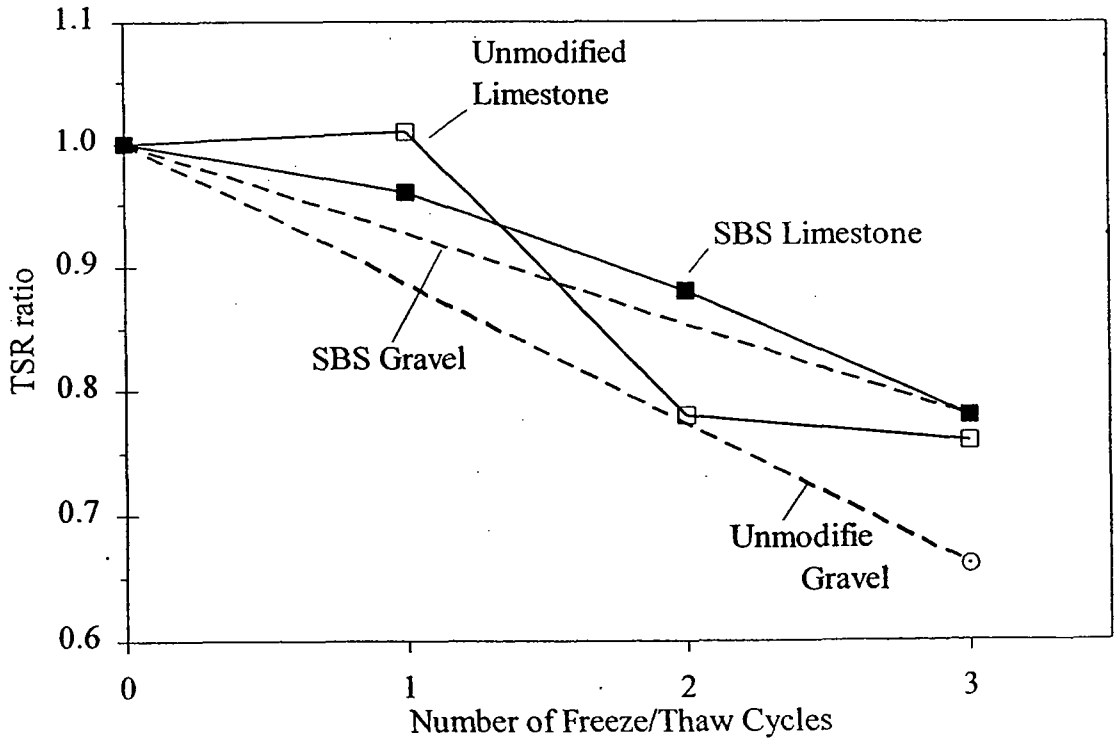

Figure 4.25 Tensile strength ratio (TSR) of coarse limestone and gravel mixes

adhesion property between smooth gravel surface and asphalt binder. TSR for the SBS gravel mix was similar to TSR for the SBS and unmodified limestone mixes.

CHAPTER 5

TESTING IN THE ACCELERATED PAVEMENT LOADING FACILITY

One task in this research project was to construct a large pad in the Ohio Accelerated Pavement Loading Facility (APLF) at Lancaster and evaluate the rut resistance of three Type I asphalt concrete mixes as they were subjected to repeated wheel loads. The APLF contains a test pit 13.7 m (45 ft) long by 11.6 m (38 ft) wide by 2.4 m (8 ft) deep. Approximately seven feet of A-6 subgrade was placed in the pit at the time the APLF was constructed and compacted to a density commonly observed in A-6 material in Ohio. Base materials and either asphalt cement concrete (ACC) or portland cement concrete (PCC) pavements are added to accommodate the specific objectives of individual projects. Loads of up to 133 kN (30,000 lb). can be applied with either super single or dual tires, and air temperature in the test chamber can be controlled between -12.2°C (10°F) and 54.4°C (130°F).

Three Type I ACC mixes were to be constructed in the APLF for this project after laboratory tests had been completed and three candidate materials had been selected for evaluation. Unfortunately, the contractor had a difficult time adapting the laboratory mixes to a full-scale installation. The three mixes accepted for the APLF were similar to the laboratory mixes, but not identical. They consisted of: Pad 1, a coarse aggregate gradation with PG 70-22 asphalt binder modified with 3% SBS, Pad 2, the same gradation with PG 70-22 unmodified asphalt binder, and Pad 3, a fine aggregate gradation with PG 70-22 unmodified asphalt binder.

Aggregates and asphalt binders were from the same source and prepared in the same manner by the same suppliers as they did for the materials used in the laboratory phase study. Mix designs for APLF test pads were done by a contractor with the same N_{desgin}. Actual binder contents were also determined by the contractor after construction. Core density and air void contents were determined at Ohio University. This information is shown in Table 5.1. Aggregates gradations used for construction of APLF test pads are presented in Figure 5.1 together with gradations used for the laboratory study.

Table 5.1 Mix designs for Type I asphalt concrete tested in the APLF

Test Pad	Mix Design					Construction				
	% of Agg. Size in Mix				Opt. AC %	Actual AC %	G_{mm}	Core G_{mb}	In Situ. Air (%)	Air (%) @ N_{design}
	#7	#8	#9	LS Sand						
1	10	45	10	35	5.0	5.22	2.469	2.167	12.3	4.0
2	10	45	10	35	5.0	4.63	2.490	2.140	14.1	6.6
3	10	25	0	65	6.0	6.42	2.427	2.073	14.6	1.0

5.1 Construction

PCC slabs from a previous test were sawed into manageable sections and removed from the APLF. The six inches of 304 dense grade aggregate base remaining from that test was scarified, graded and compacted for the ACC pad to be constructed for this project. To provide a stable base for the Type I ACC materials being tested, 178 mm (7 in.) of ODOT 301 asphalt treated base was placed in two equal layers on the 304 base. Three, 2.4-m (8-ft) wide pads were laid out side-by-side for the Type I mixes, which were placed in two 38 mm (1.5-in.) thick compacted layers on the 301. The screed on the paving machine was reduced to an 2.4-m (8-ft)

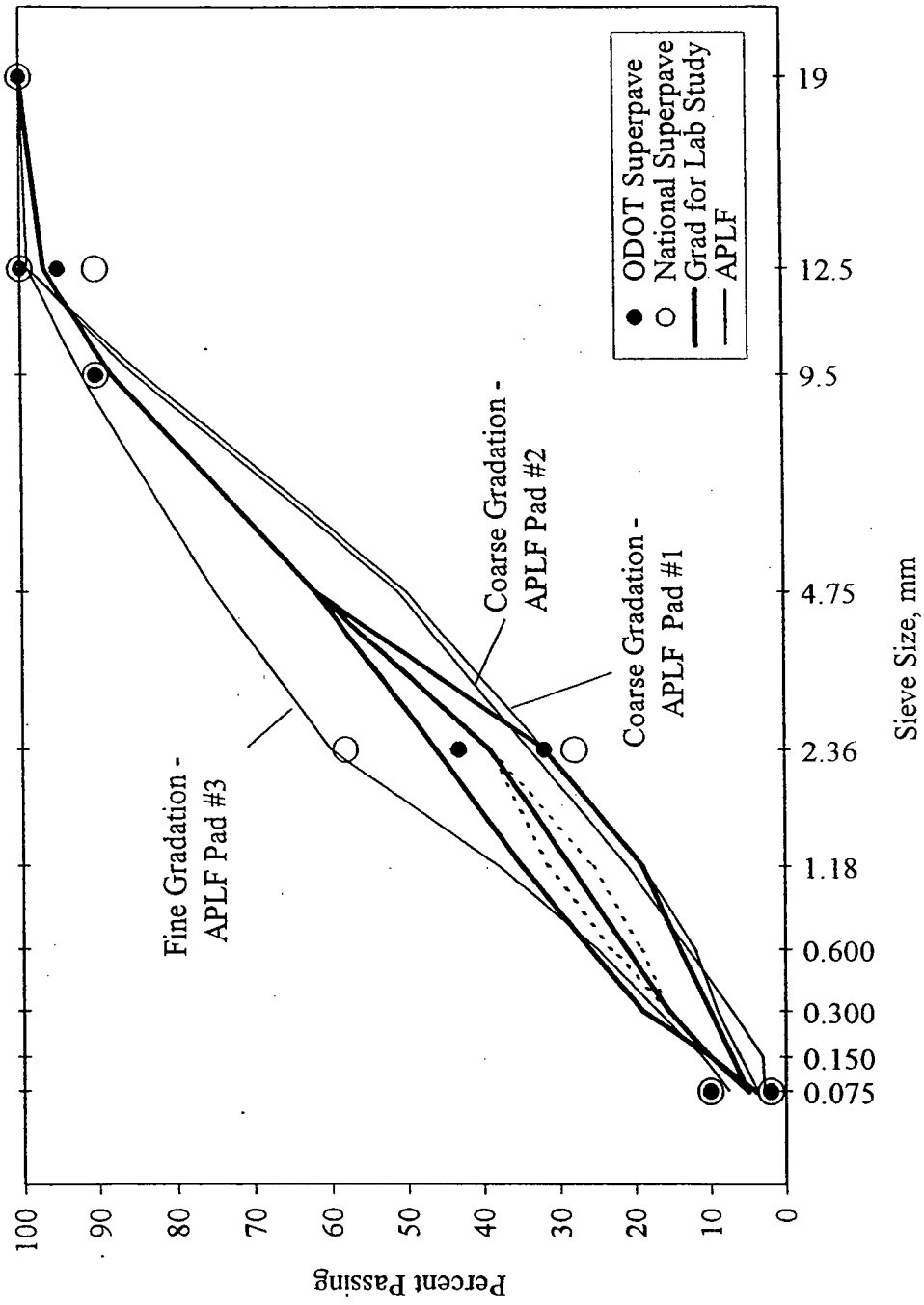

Figure 5.1 Aggregate gradation used in APLF test pads

width for this job and a vibrating roller was used to compact the mix. Actual layer thickness was monitored by taking level readings along the center of the pads after the 304, 301 and Type I materials had been placed. One point along the top edge of the test pit was taken as the benchmark and assumed to be at elevation 3.0480 m (10.000 ft) for these measurements. Table 5.2 shows these elevations.

The pads were constructed in mid-December when the outside temperature was around -5°C (20s°F) and the only plant available to prepare the asphalt concrete was a large capacity drum mixer approximately 32-40 km (20-25 miles) from the APLF. Since the batch sizes needed

Table 5.2 Elevation of material layers

Surface Elevation of Layers North to South (m)									
Test Pad	1			2			3		
Material	304	301	Type I	304	301	Type I	304	301	Type I
	2.7597	2.9480	3.0459	2.7847	2.9450	3.0434	2.7136	2.9566	3.0422
	2.7737	2.9483	3.0392	2.7761	2.9495	3.0181	2.7715	2.9517	3.0413
	2.7673	2.9489	3.0364	2.7578	2.9462	3.0282	2.7749	2.9316	3.0428
	2.7581	2.9401	3.0343	2.7615	2.9291	3.0276	2.7703	2.9322	3.0395
	2.7581	2.9316	3.0306	2.7706	2.9224	3.0227	2.7624	2.9221	3.0373
	2.7676	2.9322	3.0309	2.7731	2.9215	3.0218	2.7685	2.9273	3.0386
	2.7679	2.9322	3.0340		2.9227	3.0248	2.7584	2.9300	3.0379
		2.9361	3.0373		2.9215	3.0312		2.9355	3.0376
		2.9566	3.0386		2.9413	3.0392		2.9459	3.0331
			3.0413		2.9593	3.0370		2.9556	3.0297
Avg. Elev.	2.7645	2.9416	3.0367	2.7706	2.9358	3.0294	2.7600	2.9389	3.0379
Avg Thick, m		0.1771	0.0951		0.1652	0.0936		0.1789	0.0991
Avg Thick. in.		6.972	3.744		6.504	3.684		7.044	3.900

for this project were only 178-222 kN (20-25 tons), it was difficult with this equipment to maintain a close tolerance on the mix components. There also was concern that this haul distance might lower the mix temperature too much. Air temperature was maintained at a reasonable level in the APLF during construction by closing the large door on one end of the building and keeping the heaters on. Because the mix temperature averaged about 160°C (320°F) upon arrival from the plant, low placement temperature did not appear to be a major issue. Compaction was monitored with a nuclear density gauge until the target density of 91-92% was met. However, density measured later with cores was less, ranging 85-88% for all mixes. Cold temperature and use of smaller vibrating roller might have contributed to the low mix density. At the end of Pad 3 (fine mix) rolling, surface crack started to appear. Such problem did not happen for Pads 1 and 2, coarse SBS and coarse unmodified mixes, respectively.

One phase of the APLF testing was to install strain gauges to monitor longitudinal and transverse strain at various depths in the pads, and linear variable differential transformers (LVDT) to monitor deflection of the pad surfaces under a matrix of temperature and loading conditions. To perform the required tests, each of the three pads was divided into three 4.57 m (15-ft) long sections. The southern and middle sections were used for the mix rutting tests and the northern section was used to measure dynamic response. Strain gauges and LVDTs were installed in the northern section of each of the three pads, as follows:

1) After completion of the 304 base, one hole was drilled to the top of the subgrade and one hole was drilled to a depth of about seven feet in the subgrade. A 50-mm (2-in.) diameter PVC pipe was placed in each hole to prevent the sides from collapsing and a steel reference rod for each LVDT was inserted in each pipe and

anchored to the bottom of hole with grout. The tops of the reference rods and the pipes were brought even with the top of the 304 base and the pipes were plugged to prevent the intrusion of unwanted material during paving.

2) As the first course of 301 mix was about to be placed, Dynatest PAST-II AC strain gauges were set longitudinally and transversely on the 304 base along the pad centerline, and covered with hot 301 mix to hold them in place as the paver passed over the section. Large aggregate particles were removed from the asphalt mix covering the gauges to minimize the possibility of damage during compaction. Additional gauges were placed similarly on top of the 301, and on the first course of the Type I mix. See Table 5.3 for sensor locations and identification tags.

3) ACC temperature was monitored with thermocouples placed on the 304 and on each lift of 301 and Type I.

4) After completion of the test pads, cores were drilled through the Type I and 301 ACC layers to the top of the reference rods and PVC pipes. Fixtures were epoxied to the Type I layers inside the core hole and LVDTs were fastened to the fixtures at an elevation that allowed the spring-loaded LVDT cores to maintain contact with the top of the reference rods throughout the deflection cycle. Deflections

Table 5.3 Sensor identification tags

Pad	Top of Layer	Nominal Depth, mm (in.)	Strain Gauge ID Tag		LVDT ID Tag		Thermo-couple
			Long. Strain	Trans. Strain	Top of Subgrade	2.1 m below Subgrade	
1	304	254 (10)	SG 12	SG 11	5	4	TC 1
	301-1*	165 (6.5)	--	--			TC 2
	301-2	76 (3)	SG 14	SG 13			TC 3
	Type I-1	38 (1.5)	SG 16	SG 15			TC 4
2	304	254 (10)	SG 22	SG 21	3	2	TC 5
	301-1	165 (6.5)	--	--			TC 6
	301-2	76 (3)	SG 24	SG 23			TC 7
	Type I-1	38 (1.5)	SG 26	SG 25			TC 8
3	304	254 (10)	SG 52	SG 51	1	0	TC 9
	301-1	165 (6.5)	--	--			TC 10
	301-2	76 (3)	SG 54	SG 53			TC 11
	Type I-1	38 (1.5)	SG 56	SG 55			TC 12

* First course of 301

measured with the LVDTs were actually changes in length between the Type I ACC layer and the bottom of the reference rods.

5. 2 Pavement Response to Dynamic Loading

Upon completion of the pads, air temperature inside APLF was maintained at about 70°F as the pads cooled, and as the sensors were wired and connected to the data acquisition systems. A Megadac 5108A system was used to monitor the strain gauges and LVDTs during dynamic testing, and a Campbell Scientific CR 7 system was used to monitor the thermocouples at 30-minute intervals during the various test sequences.

A matrix of wheel loads and lateral wheel positions was developed to measure pavement response at various temperatures. The super single test tire had a contact width of about 356 mm

(14 in.) on the pavement surface. As part of the test matrix, the tire was centered over the sensors, moved laterally in both directions so the edges of the tire were over the sensors ±178 mm (±7 in.) and to the maximum wander provided by the equipment ±254 mm (±10 in.). Loads of 26.7, 40.0, and 53.4 kN (6,000, 9,000 and 12,000 lb, respectively) were run at 8.0 km/hr (5 mph) over the full 13.7 m (45-ft) length of the test pit at these lateral offsets and in the order shown in Table 5.4. This matrix was repeated while the air temperature in the facility was maintained at a constant 5, 20, and 40° C, and twice while the air temperature was being changed in the facility. Some additional 50° C tests were run at 22.2, 31.1, and 40 kN (5,000, 7,000 and 9,000 lb, respectively) and lateral offsets of 0 and ±254 mm (±10 in.), as shown in Table 5.5.

Thermocouples recorded the temperature at various depths in the three pads during each set of dynamic response measurements. After 2- 6 days of holding air temperature constant,

Table 5.4 Typical sequence for dynamic response testing

Wheel Load, kN (lb)	Test Numbers				
	Lateral Offset from Sensors, mm (in.)				
	0	+178 (+7)	+254 (+10)	-178 (-7)	-254 (-10)
26.7 (6,000)	1	2	3	4	5
40.0 (9,000)	6	7	8	9	10
53.4 (12,000)	11	12	13	14	15

Table 5.5 Sequence for dynamic response testing at 50°C

Wheel Load, kN (lb)	Test Numbers		
	Lateral Offset from Sensors, mm (in.)		
	0	+254 (+10)	-254 (-10)
22.2 (5,000)	1	2	3
31.1 (7,000)	4	5	6
40.0 (9,000)	7	8	9

pavement temperatures were considered to be equilibrium pavement temperatures. Table 5.6 summarizes air temperatures and corresponding pavement temperatures at various depths within each test pads.

During the five sets of dynamic measurements and a few trial wheel passes made in March, 2001, approximately 80 total wheel passes were carried along the full length of each pad prior to initiation of the rutting tests. Another 10 dynamic wheel passes were added on June 8, 2001, just before the 8.0 km/hr at 50°C rut test. Table 5.7 shows the file names and run numbers assigned to the valid wheel passes recorded on the data acquisition system. Results of these tests

Table 5.6 Pad temperatures during dynamic response measurements

Test Date	Nominal Air Temp., °C	Pad No.	Temperature (°C) @ Nominal Depth, mm (in.)			
			38 (1.5)	76 (3.0)	165 (6.5)	254 (10.0)
3/1/01	20	1	19.8	19.6	19.4	19.3
		2	20.2	20.0	19.7	19.6
		3	20.2	20.0	19.7	19.6
3/6/01	5	1	8.3	9.2	9.8	11.1
		2	8.1	9.0	9.9	11.1
		3	8.1	9.1	10.2	11.3
3/6/01	Transition from 5°C to 40°C	1	17.9	14.0	12.3	11.7
		2	19.5	15.1	12.5	11.9
		3	19.4	14.9	12.4	11.9
3/12/01	40	1	34.5	32.9	31.7	29.6
		2	35.4	33.9	32.2	30.3
		3	34.3	32.7	30.9	29.3
3/12/01	Transition from 40°C to 30°C	1	29.0	30.8	31.0	29.6
		2	28.8	31.3	31.6	30.3
		3	28.9	30.7	30.7	29.4
6/8/01	50	1	45.6	43.4	41.9	39.0
		2	46.8	44.7	42.5	39.9
		3	45.4	43.4	41.1	38.8

Table 5.7 File names and run numbers for dynamic response measurements

Test Date	Air Temp., °C	Time of Day	Test Sequence	Data Acquisition	
				File	Run No.
3/1/01	20	4:30 PM	15 Run Matrix on Pad 1	PPT1	7-15 [1]
		5:11 PM	15 Run Matrix on Pad 1	PPT1a	1-15
			15 Run Matrix on Pad 2	PPT1a	16-32 [2]
			15 Run Matrix on Pad 3	PPT1a	33-47
		10:42 AM	15 Run Matrix on Pad 3	PPT1c	1-15
		12:26 PM	15 Run Matrix on Pad 2	PPT1e	1-15
			15 Run Matrix on Pad 1	PPT1e	16-30
3/6/01	+ Gradient	5:24 PM	15 Run Matrix on Pad 1	PPT1f	1-15
			15 Run Matrix on Pad 2	PPT1f	16-30
			15 Run Matrix on Pad 3	PPT1f	31-45
3/12/01	40	10:43 AM	15 Run Matrix on Pad 3	PPT1g	1-17 [3]
			15 Run Matrix on Pad 2	PPT1g	18-32
			15 Run Matrix on Pad 1	PPT1g	33-49 [4]
3/12/01	30	1:07 PM	15 Run Matrix on Pad 1	PPT1h	1-15
			15 Run Matrix on Pad 2	PPT1h	15-30
			15 Run Matrix on Pad 3	PPT1h	30-45
6/8/01	50	11:11 AM	9 Run Matrix on Pad 3	PPT1i	1-9
			9 Run Matrix on Pad 2	PPT1i	10-18
			9 Run Matrix on Pad 1	PPT1i	19-27

[1] Runs 1-6 did not archive on the computer
[2] Disregard Runs 16-17
[3] Disregard Runs 2 and 3
[4] Disregard Runs 39 and 41

will be analyzed and used for future development of an empirical-mechanistic asphalt pavement design procedure.

5.3 Rut Testing

Unidirectional loads of 40 kN (9,000 lb) with 689.4 kPa (100 psi) tire pressure were repeatedly applied with no lateral wander in all of the southern and middle sections of each pad

until sufficient deformation (rutting) had occurred to determine the rut resistance of the three Type I mixes. Test temperature used in this discussion refers to air temperature measured inside APLF. Corresponding pavement temperatures at various depths within test pads are given in Table 5.6. Three lateral profiles were recorded with a laser profilometer across the longitudinal deformation at each of three locations in each section periodically during the loading. The profiles consisted of surface elevations recorded at one-millimeter intervals over a length of 2,500 millimeters. Large washers were epoxied to the pavement surface for locating the profilometer in the same position each time and, thereby, maintaining a uniform line and reference elevation for each set of profile measurements. Figure 5.2 shows the location and number assigned to each profile location. A three-digit profile number was developed to identify the pad number, section number and position number in that order. For example, Profile 321 was located in Pad 3, Section 2 in that pad, and Position 1 in that section. A letter suffix followed each profile number to indicate the total number of wheel passes traversing the section to that stage in the rut testing. In the initial series of rut testing, 6,000 wheel passes were run at 40°C (35°C at mid-depth of Type-I) in Section 1 of each of the three pads. To leave Sections 2 and 3 intact for other runs and not to overheat the carriage braking system, the wheel was programmed to only run over the 4.57 m (15-ft) length of Section 1 and the wheel speed was reduced to 3.2 km/hr (2 mph). Section 2 in the three pads was tested next at 50°C (46°C at mid-depth of Type-I) by running 1,500 wheel passes at 8.0 km/hr over the entire 13.7 m (45-ft) length of the pads. Profiles were only measured in Section 1 while it was being tested, and in both Sections 1 and 2 during the Section 2 tests since additional loads were being applied to Section 1. By changing two variables (temperature and wheel speed) to test the two sections, rut resistance of mix could

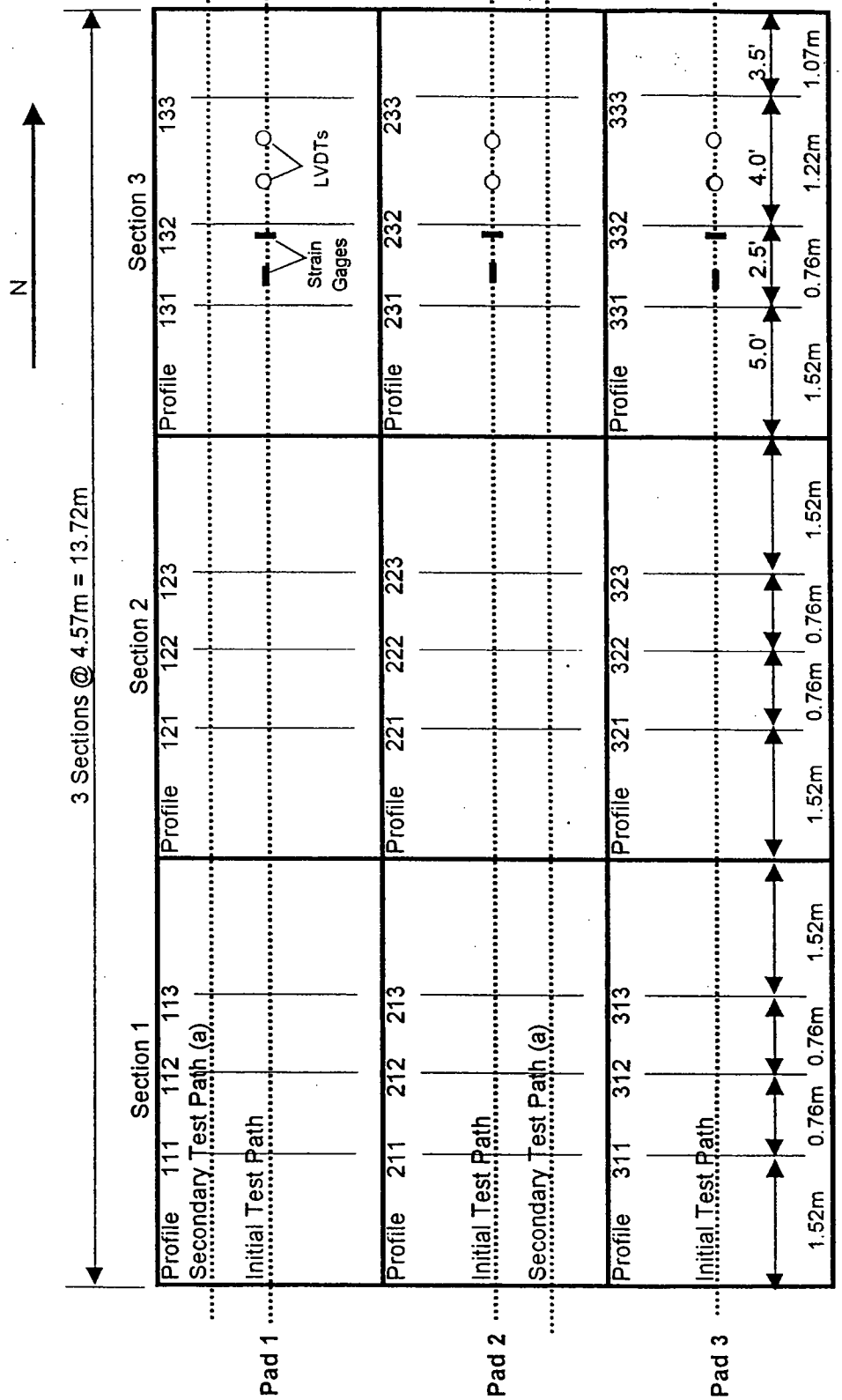

Figure 5.2 Location and identification of test pad profiles

be compared for those conditions, but it was not possible to evaluate the individual effects of these variables on rut resistance. For this reason, another set of 1,500 runs was made on an unused portion of Sections 1 and 2 at 8.0 km/hr and 40° C. These additional runs made it possible to compare the rut resistance of the mixes and to evaluate the effects of temperature and wheel speed on rut depths of each mix.

The specific order of testing was as follows:

1. Surface profiles were recorded at three locations in each of three sections in each pad before any passes of the test wheel. This initial profile was the reference from which elevation changes (rut depths) were measured after completion of the dynamic response tests.

2. Five series of dynamic response measurements, totaling approximately 80 wheel passes along the entire length of each pad, were recorded at 8.0 km/hr and at five different temperature conditions. These passes were equally distributed across five lateral positions of the test wheel.

3. A second complete set of profiles was recorded on the pads. This profile served as the reference for the rut testing in Sections 11, 21 and 31.

4. The initial set of rut testing was conducted along the centerline of Section 1 only in each of the three pads at 40.0 kN (9,000 lb), 3.2 km/hr and 40°C (35°C pavement temperature). Profiles were taken at 1,500, 3,000 and 6,000 passes in Pads 1 and 2, and at 1,000, 2,000, 4,000 and 6,000 passes in Pad 3.

5. An abbreviated set of dynamic response measurements was recorded at 8.0 km/hr and 50°C, which added another 10 passes to the run total on all pavement sections.

6. Another set of profiles was recorded at all nine locations in each pad. These profiles served as the reference for the rutting tests in Sections 12, 22 and 32.

7. A second set of rut testing was conducted along the centerline of Section 2 in each of the three pads at 40.0 kN, 8.0 km/hr and 50°C (46°C pavement temperature). The test wheel was run the full length of the pads during these tests. Profiles were recorded in Sections 11, 12, 21, 22, 31 and 32 at 200, 500 and 1,500 passes of the test wheel.

8. On an unused portion of Pads 1 and 2, profiles were recorded at three locations in Sections 11, 12, 21 and 22.

9. A third set of rut resistance measurements was conducted in these new test paths at 40.0 kN, 8.0 km/hr and 40°C, and profiles were taken at 200, 500 and 1,500 passes.

The profiles consist of a running average of five data points to reduce scatter in the data caused by texture on the pavement surface. Also, Points 1-300 on each line were normalized to the same points on the initial plot of that section to minimize any discrepancy between plots caused by slight differences that might have occurred in the way the profilometer was set up for each set of profiles. Figure 5.3 shows the series of lateral profiles made at Position 311 during the APLF rutting tests at 3.2 km/hr and 40° C. Each trace represents an average of three passes of the profilometer at that location on the pavement and point in time. To measure and compare the rut resistance of the different mixes, average elevations of the middle 254 mm (10 in.) of the 356 mm (14 in.) wide tire were calculated from the profiles and plotted against the number of passes of the wheel. The 254 mm (10 in.) width was selected to avoid the rapidly changing profiles around the tire edges.

5.4 Results of APLF rut tests

As shown in Figure 5.3, rut depth under the tire increased and uplift (swelling) of about 10-inch width outside both tire-edges increased with number of wheel passes. If there had been tire wander, the uplift would have been reduced or eliminated. The eighty wheel passes applied for the dynamic testing did not cause significant rutting as shown in Figure 5., where the initial and the post dynamic test profiles are almost identical to each other.

Final rut depths for the three APLF test conditions are summarized in Table 5.8. Figure 5.4 shows APLF rut depth versus number of wheel passes for all tests. Figures 5.5 through 5.7 show APLF rut depth versus number of wheel passes for each test condition.

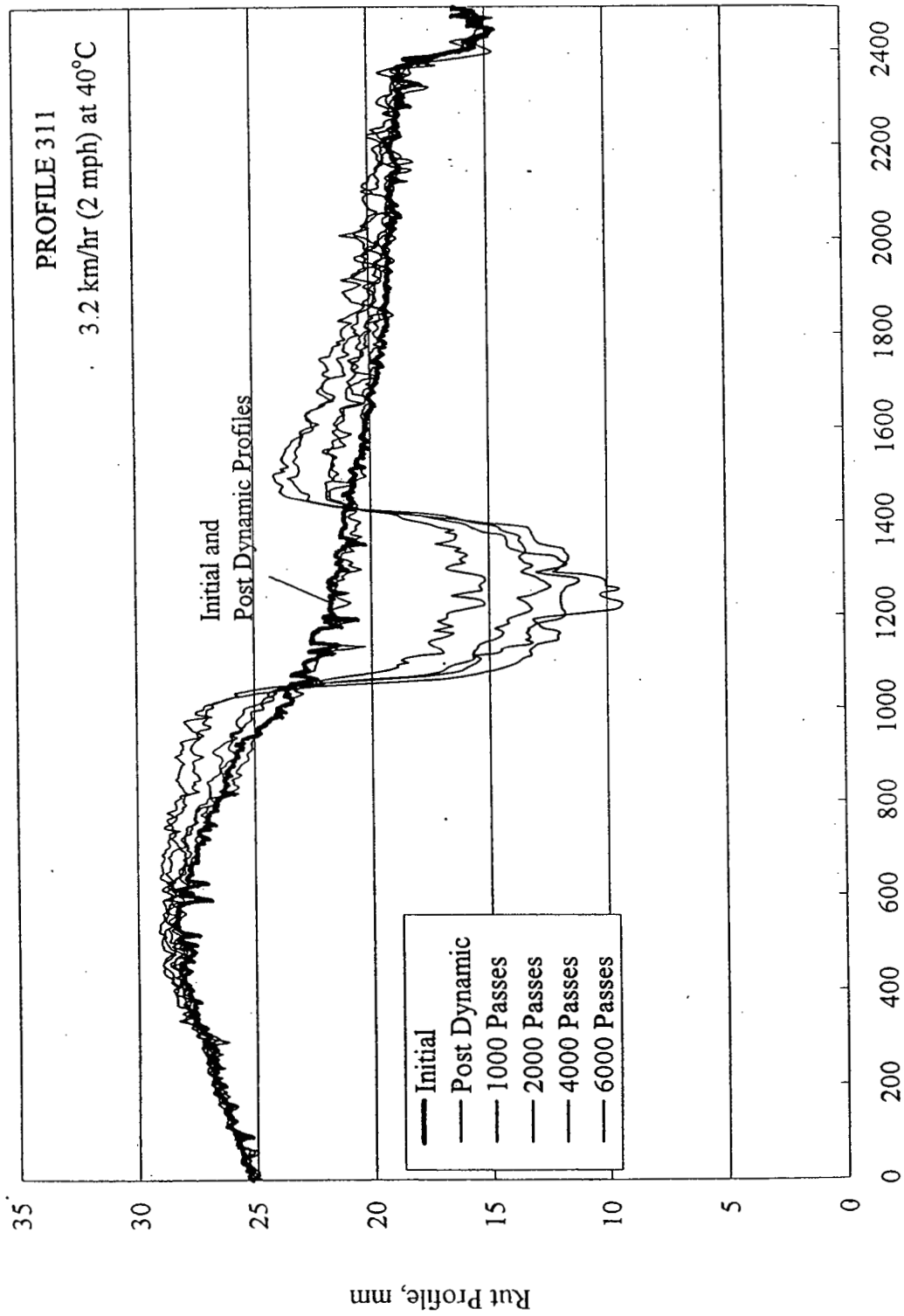

Figure 5.3 Profile of Position 311 during rut testing

Table 5.8 Summary of average APLF rut depths at three testing conditions

Test Condition	Test Pad	Rut Depth, mm @ Number of Wheel Pass						
		0	1,000	1,500	2,000	3,000	4,000	6,000
3.2 km/hr at 40°C	1	0.00		4.07		5.66		6.77
	2	0.00		3.27		4.87		5.54
	3	0.00	4.61	5.89*	6.79		7.85	8.77

Test Condition	Test Pad	Rut Depth, mm @ No. of Wheel Pass			
		0	200	500	1,500
8.0 km/hr at 40°C	1	0	2.17	2.87	4.29
	2	0	2.14	2.88	4.21

Test Condition	Test Pad	Rut Depth, mm @ No. of Wheel Pass			
		0	200	500	1,500
8.0 km/hr at 50°C	1	0.00	1.49	2.43	4.77
	2	0.00	1.82	2.82	4.80
	3	0.00	2.95	3.40	5.34

* Interpolated rut depth from linear relationship between rut depth versus log (number of wheel passes)

As shown in Table 5.1, compaction of the plant mixes with N_{design} = 109 resulted in 4.0, 6.6, and 1.0% air void contents for Pad 1 (coarse SBS), Pad 2 (coarse unmodified) and Pad 3 (fine unmodified), respectively. Asphalt binder content determined for Pad 1 was close to the optimum. The measured binder content for Pad 2 was lower than the optimum, while the binder content in Pad 3 was higher than the optimum binder content. For two test conditions, 3.2 km/hr at 40°C and 8.0 km/hr at 50°C, Pad 3 exhibited significantly higher rut depth than the two other

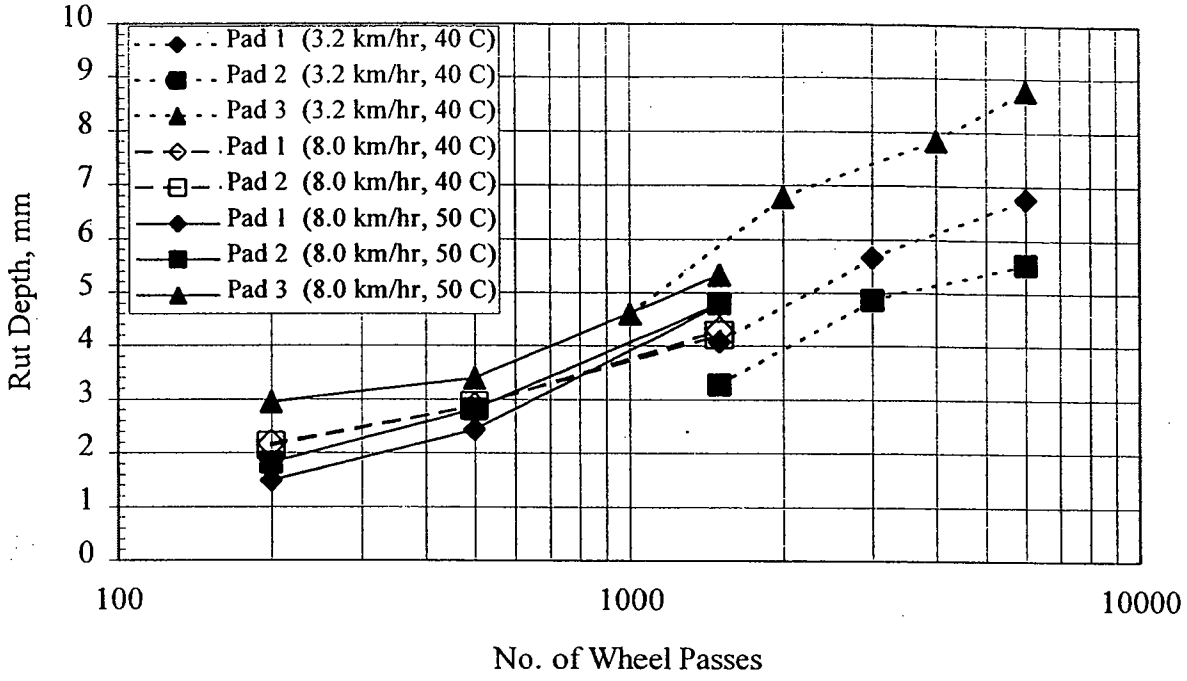

Figure 5.4 APLF rut depth versus number of wheel passes; all tests

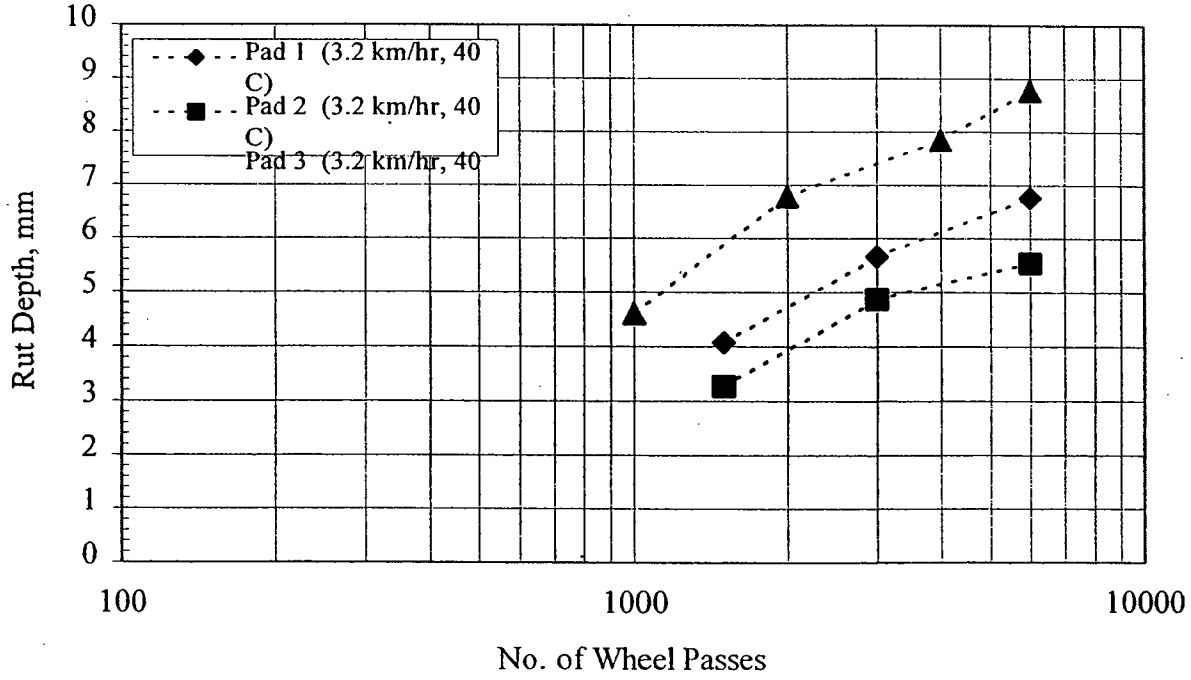

Figure 5.5 APLF rut depth versus number of wheel passes; 3.2 km/hr at 40°C

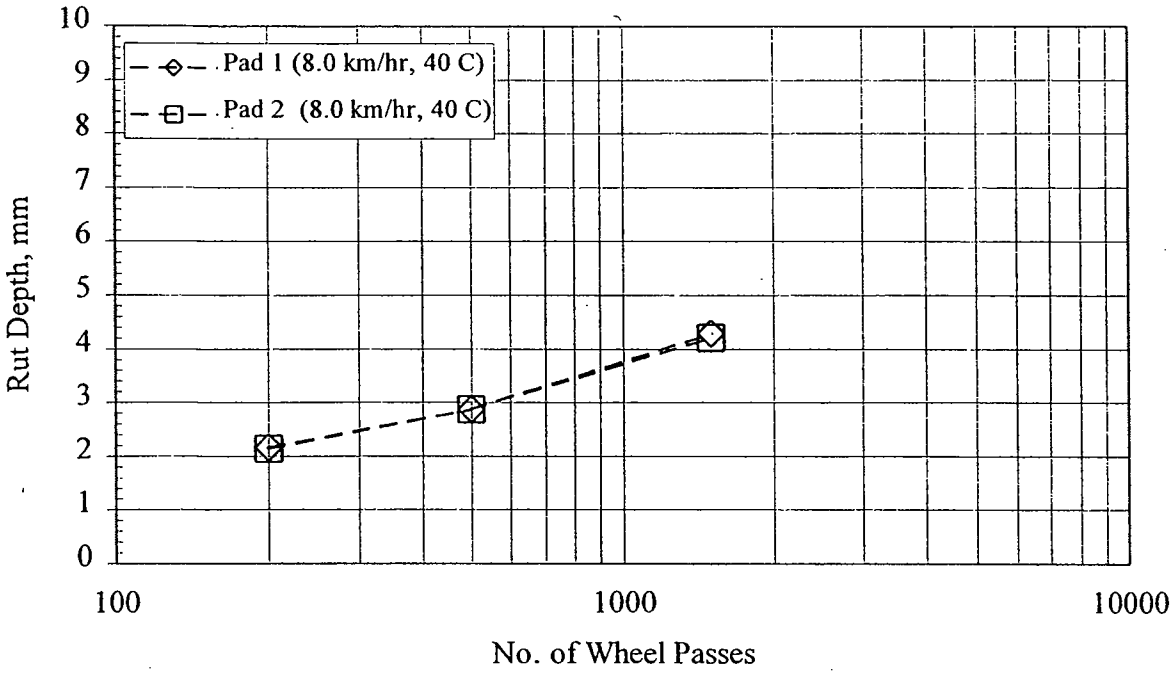

Figure 5.6 APLF rut depth versus number of wheel passes; 8.0 km/hr at 40°C

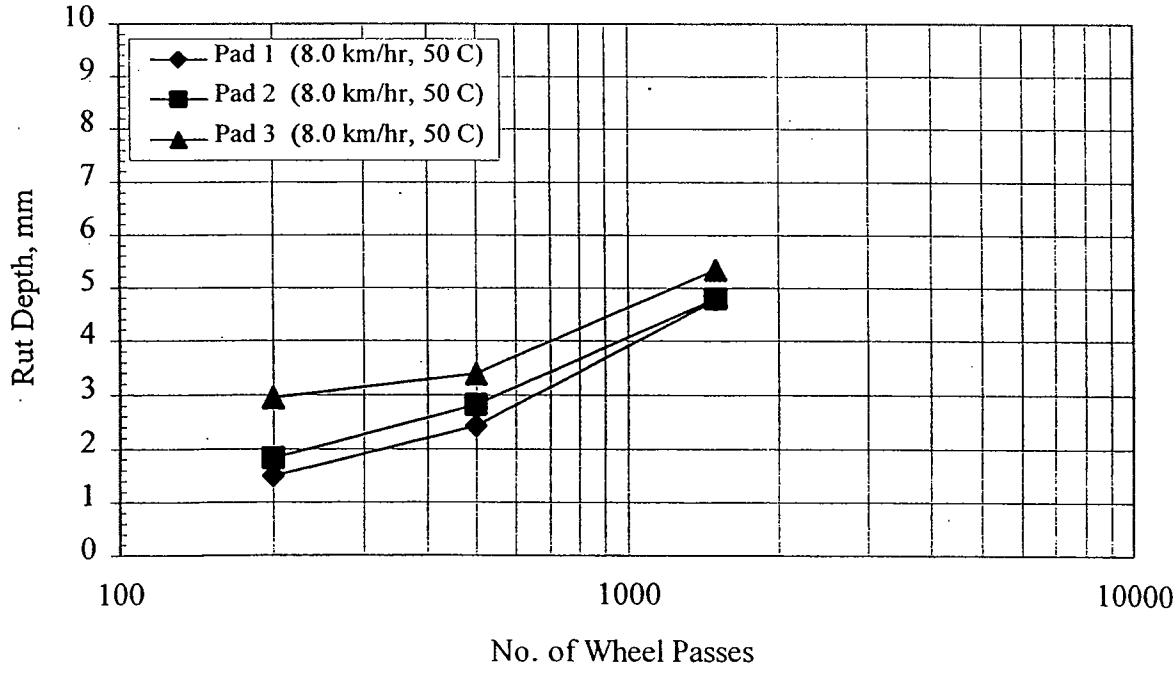

Figure 5.7 APLF rut depth versus number of wheel passes; 8.0 km/hr at 50°C

test pads. This is believed to be due to the higher than optimum asphalt binder content in Pad 3 and the sensitivity of the fine mix to variation of binder content.

For 3.2 km/hr at 40°C rut test, Pad 2 (coarse mix with unmodified binder) exhibited consistently lower rut depth than Pad 1 (coarse mix with SBS binder), partly due to a lower asphalt binder content. When wheel speed increased to 8.0 km/hr at 40°C, relative performance of the SBS modified mix (Pad 1) was improved and rut depths for Pads 1 and 2 were almost identical. This seems to be in agreement with the results of the triaxial repeated load test and the static creep test, i.e., in comparison with unmodified mixes, SBS modified mixes showed better rut resistance for dynamic loading (or fast moving traffic) than for static loading (or slow moving traffic).

The effect of temperature can be seen from results of 8.0 km/hr at 40°C rut test and 8.0 km/hr at 50°C rut test. As discussed, at 8.0 km/hr at 40°C test, Pads 1 and 2 exhibited almost identical rut resistance. When the temperature increased to 50°C, there were small but consistent differences between the rut depths on Pads 1 and 2. Rut depths on Pad 1 (SBS) were slightly less than on Pad 2 (unmodified) showing the SBS modified mix with less temperature dependency than the unmodified mix, as shown in laboratory test results.

Dry Asphalt Pavement Analyzer (APA) tests were performed on the plant mixes at 60°C with 689 kPa (100 psi) hose pressure and 511.5 N (115 lb) wheel load. Six specimens were prepared for each mix using SGC to have 7±1% air void contents. The results of the dry APA tests are shown in Figure 5.8 together with APLF rut depths measured for three test conditions. The APA results exhibited the best correlation with the 3.2 km/hr at 40°C APLF test.

Coincidentally, the speed of the APA wheel is closer to 3.2 km/hr than 8.0 km/hr. In APA, the motion of a 138 mm (5.5-in.) long arm rotating at 60 rpm is transformed into a translational motion through a mechanical device and rut depth of a SGC specimen is measured at 63.5 mm (2.5 in.) and 114.3 mm (4.5 in.) from the center of APA wheel stroke. When constant angular velocity (2π rad/sec or 60 rpm) of the rotating arm is assumed, wheel speeds of 2.9 km/hr and 1.8 km/hr are calculated at distances 2.5 and 4.5 inches from the center of the wheel stroke, respectively. Even though, wheel speeds at APA and APLF tests are similar, loading rates would not be similar because of different time of load duration. Implication of wheel speeds in APA test and APLF test on rut depths and their correlation needs further investigation.

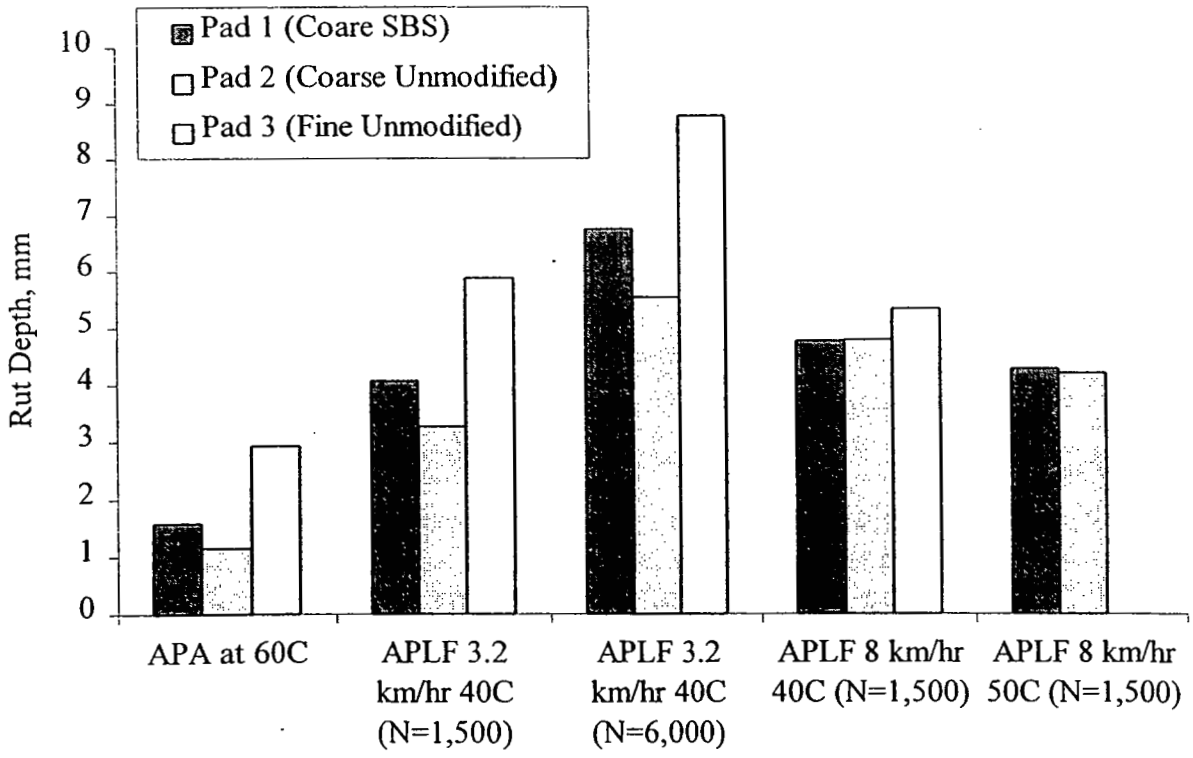

Figure 5.8 Results of APA test on plant mixes and comparison with APLF test results

CHAPTER 6

SUMMARY AND CONCLUSION

The effects of aggregate type, aggregate gradation, and asphalt binder type on hot mix asphalt performance were investigated using several laboratory test methods, including asphalt pavement analyzer (APA), triaxial repeated load test, uniaxial static creep test, flexural beam fatigue test, indirect tensile strength test, indirect tensile resilient modulus test, and moisture susceptibility. Specific conclusions drawn from these tests are as follows:

- Aggregate angularity was the most significant factor influencing rutting. Mixes with crushed limestone exhibited much less rutting than mixes with rounded gravel.
- APA, triaxial repeated load, and uniaxial static creep tests indicated that aggregate type, gradation, and binder type were all statistically significant factors in rut development.
- An intermediate aggregate gradation passing through the restricted zone performed as well as other gradations. A coarse gradation passing below the restricted zone showed the most rutting potential, while a fine gradation passing above the restricted zone exhibited the least rutting potential.
- It is plausible that conclusions stated above regarding the effect of aggregate gradation on rutting were influenced by the different asphalt binder film thickness associated with each mix with similar air void content.

- Polymer modified mixes showed significantly reduced temperature dependency, improved strain recovery, and reduced rutting potential when compared with unmodified mixes. These differences between modified and unmodified binders were most noticeable in dynamic testing and in gravel mixes with less aggregate interlock.
- For many mixes, rut depths measured by the wet APA test were less than rut depths measured by the dry APA test. This was believed to be due to excess pore water pressure developed in the mixes under APA wheel load. An improved test procedure, including suitable moisture conditioning, should be developed for the wet APA test to accurately measure the moisture susceptibility of asphalt mixes.
- The triaxial repeated load test was very sensitive to aggregate type, aggregate gradation, and asphalt binder type, which is consistent with previous studies [52, 55]. The uniaxial static creep test was less sensitive to mix variables than the triaxial repeated load test.
- Due to the long loading times involved, the static creep test was affected primarily by aggregate properties and, to a lesser degree, by asphalt binder properties and test temperature.
- Test specimens decreased in volume during the triaxial repeated load test, indicating a consolidation similar to that occurring in pavements ruts. However, test specimens increased in volume during the uniaxial creep test, indicating a different response mechanism.
- The resilient moduli of polymer (SBS) modified mixes were significantly lower than those of unmodified mixes at 40°C while they were about the same at 60°C.

- Aggregate gradation did not affect the resilient moduli of the test mixes.
- Resilient moduli determined from the indirect tensile and compressive modes in the triaxial repeated load test were in good agreement.
- In the flexural beam fatigue test, the fatigue behavior of asphalt mixes was predominently controlled by asphalt binder type. Mixes with SBS binder showed longer fatigue life, lower initial stiffness, lower fatigue rates, and higher phase angles than mixes with unmodified binders in strain-controlled tests.
- Mixes with gradations passing below, through, and above the restricted zone did not show differences in fatigue performance.
- Statistically, the indirect tensile strength (ITS) of mixes prepared with three aggregate gradations and two binder types were not significantly different. On average, SBS mixes exhibited slightly lower ITS than unmodified mixes, and mixes with coarse gradation tended to have slightly lower ITS than mixes with the other two gradations.
- For gravel with rounded surfaces, SBS mixes exhibited a significantly higher tensile strength ratio (TSR) than mixes with unmodified binder after three freeze/thaw cycles. For limestone with rough fractured surfaces, TSRs after 3 cycles of freeze/thaw for mixes with modified and unmodified binders were about the same. However, mixes with SBS binder showed a gradual reduction of TSR with freeze/thaw cycles while mixes with unmodified binder exhibited a major reduction in TSR during the second freeze/thaw cycle.

Based on the laboratory test results, three mixes were chosen for further evaluation at the Ohio Accelerated Pavement Loading Facility (APLF). The three mixes were placed in the APLF using materials from the same sources as was used in the laboratory tests. Specific conclusions are drawn, as follows:

- When the nominal air temperature was increased from 40°C to 50°C, rutting increased more in the mix with an unmodified binder (Pad 2) than in a similar mix with SBS modified binder (Pad 1). This observation supports the laboratory results where mixes with polymer modified binders had lower temperature susceptibility than unmodified binders.
- When wheel speed was increased from 3.2 to 8.0 km/hr (2 to 5 mph), rut resistance of the SBS modified mix (Pad 1) was significantly improved in comparison with rut resistance of the unmodified mix (Pad 2). This observation supports laboratory results where mixes with polymer modified binders performed better than mixes with unmodified binders under dynamic loading.
- For the three mixes tested, APA results at 60°C correlated well with APLF test results at 3.2 km/hr (2 mph) and 40°C. The speed of the APA wheel is closer to 3.2 km/hr (2 mph) than 8.0 km/hr (5 mph).
- The asphalt concrete mix in APLF Pad 3 (fine mix with unmodified binder) exhibited significantly more rutting than either the modified or unmodified mixes with coarser aggregate. This was believed to be caused, at least partially, by the binder content being above optimum.

- The use of a small capacity batch mixer and better density controls are recommended for improved quality control on test pads in the APLF.

In summary, aggregate shape (crushed vs. rounded) exhibited the most significant effect on the rutting resistance of asphalt concrete mixes. When angular crushed limestone aggregate was used, mixes with all gradations and asphalt binder types were highly rut resistant. Mixes with gradations passing through the restricted zone performed as well as mixes with gradations passing above or below the restricted zone. Even though there were statistically significant differences in the rut resistance of three gradations, the magnitude of the differences seemed to be too small to be practically significant. Asphalt concrete mixes with polymer modified binder exhibited significantly lower temperature dependency, better rut resistance, and improved fatigue resistance than mixes with unmodified binders. The effects of the polymer modified binder were more pronounced in dynamic tests than in static tests. Polymer modified binders also exhibited significantly more resistance to stripping on round gravel aggregate particles under severe moisture conditions.

Some findings from the laboratory study were validated by tests at APLF on three selected mixes. Mixes with SBS and unmodified binders exhibited the about the same rut depth development when tested at 40°C and with a 3.2 km/hr (2 mph) wheel speed. However, at higher test temperatures or at a faster wheel speed, mixes with polymer modified binder performed better than mixes with an unmodified binder. The effect of aggregate gradation on rut resistance could not be validated at APLF due to an above optimum binder content.

REFERENCES

(1) Cominsky, R., R. B. Leahy, and E. T. Harrigan. "Level One Mix Design: Materials Selection, Compaction, and Conditioning." SHRP-A-408. Strategic Highway Research Program. National Research Council, Washington, D. C., 1994.

(2) Watson, D.E., A. Johnson, and D. Jared. "The Superpave Gradation Restricted Zone and Performance Testing with the Georgia Loaded Wheel Tester." Transportation Research Board Record 1583, Transportation Research Board, Washington, D.C., 1997. pp. 106-111.

(3) Blankenship, P.B., A.H. Myers, A.S. Clifford, T.W. Thomas, H.W. King, and G.N. King. "Are All PG 70-22s the Same? Lab Tests on KY I-64 Field Samples." Journal of Association of Asphalt Paving Technologist, vol. 67, AAPT, St. Paul, MN, 1998. pp. 493-552.

(4) Oliver, J.W. and P. Tredrea. "Relationship between Asphalt Rut Resistance and Binder Rheological Properties." Journal of Association of Asphalt Paving Technologist, vol. 67, AAPT, St. Paul, MN, 1998. pp. 623-643.

(5) "Superpave Mix Design", Asphalt Institute, Superpave Series No. 2 (SP-2), 1996.

(6) Choubane, B., James A. Musselman, and G. C. Page, " Investigation of the Suitability of the Asphalt Pavement Analyzer for Predicting Pavement Rutting", paper submitted for presentation at the 79th Transportation Research Board meeting and publication in the Transportation Research Record, Washington DC, 2000.

(7) Decker, D. S., and J. L. Goodrich, " Asphalt Cement Related Pavement Performance", *Proceedings of the Association of Asphalt Paving Technologists*, Vol. 58, 1989, pp.503-518.

(8) Anderson, D. A., and T. W. Kennedy, " Development of SHRP Binder Specification", *Journal of the Association of Asphalt Paving Technologists*, Vol. 62, 1993, pp.481-507.

(9) Lai, J. S., and T.-M. Lee, "Use of a Loaded-Wheel Testing Machine to Evaluate Rutting of Asphalt Mixes", Transportation Research Record 1269, TRB, National Research Council, Washington, DC, 1990, pp.116-124.

(10) Mallick, R. B., R. Ahlrich, and E.R. Brown, " Potential of Dynamic Creep to predict rutting", Engineering Properties of Asphalt Mixtures and the Relationship to their Performance, ASTM STP 1265, Gerald A. Huber and Dale S. Decker, Eds., American society for Testing and Materials, Philadelphia, 1995.

(11) Brown, E. R., and S. A. Cross, " A study of In-Place Rutting of Asphalt Pavement", *Proceedings of the Association of Asphalt Paving Technologists*, Vol. 58, 1989, pp.1-39.

(12) "Permanent Deformation Response of Asphalt Aggregate Mixes", SHRP-A-415, Strategic Highway Research Program, National Research Council, Washington DC, 1994.

(13) Sousa, J. B., "Asphalt-Aggregate Mix Design Using Simple Shear Test (Constant Height)", *Proceedings of the Association of Asphalt Paving Technologists*, Vol. 63, 1994, pp.298-345.

(14) Mohamed, E. H. H., and Yue, Z., "Criteria for Evaluation of Rutting Potential Based on Repetitive Uniaxial Compression Test", Transportation Research Record 1454, TRB, National Research Council, Washington, DC, 1994, pp. 74-81.

(15) Kamel, N. I., and L. J. Miller, "Comparative Performance of Pavement Mixes Containing Conventional and Engineered Asphalts", Transportation Research Record 1454, TRB, National Research Council, Washington, DC, 1994, pp. 172-180.

(16) McGennis, B. R, R. M. Anderson, T. W. Kennedy, and M. Solaimanian, "Background of Superpave Asphalt Mixture Design and Analysis", National Asphalt Training Center Demonstration Project 101, Publication No. FHWA-SA-95-003, February 1995.

(17) Roberts, F. L., P.S. Kandhal, R. E. Brown,, T. W. Kennedy, D.Y. Lee, "Hot Mix Asphalt Materials, Mixture Design, and Construction", Second Edition, NAPA Educational Foundation, Lanham, Maryland, 1996.

(18) Kim, R. Y., H.J. Lee, and D. Little, " Fatigue Characterization of Asphalt Concrete Using Viscoelasticity and Continuum Damage Theory", *Journal of the Association of Asphalt Paving Technologists*, Vol. 66, 1997, pp.520-569.

(19) Tayebali, A., J. A. Deacon, J. Coplantz, J. T. Harvey, C. L. Monismith, and "Mixture and Mode-of-Loading Effects on Fatigue Response of Asphalt-Aggregate Mixtures", *Journal of the Association of Asphalt Paving Technologists*, Vol. 63, 1994, pp.118-151.

(20) "Fatigue Response of Asphalt-Aggregate Mixes", SHRP-A-404, Strategic Highway Research Program, National Research Council, Washington DC, 1994.

(21) Olson, Gary K., and Byron E. Ruth, "Creep Effects on Fatigue Testing of Asphalt Concrete", *Proceedings of the Association of Asphalt Paving Technologists*, Vol. 46, 1977, pp.176-195.

(22) Kalcheff, I. V., and D. G. Tunnicliff, "Effects of Crushed Stone Aggregate Size and Shape on Properties of Asphalt Concrete", *Proceedings of the Association of Asphalt Paving Technologists*, Vol. 51, 1982, pp.453-483.

(23) Ruth, B. E., H. E. Schweyer, A. S. Davis,, and J. D. Maxfield, "Asphalt Viscosity: An Indicator of Low Temperature Fracture Strain in Asphalt Mixtures", *Proceedings of the Association of Asphalt Paving Technologists*, Vol. 48, 1979, pp.221-237.

(24) Epps, A., "A Comparison of Measured and Predicted Low Temperature Cracking Conditions", *Journal of the Association of Asphalt Paving Technologists*, Vol. 67, 1998, pp.277-310.

(25) Oliver, J., and P. Tredrea, "Relationship Between Asphalt Rut Resistance and Binder Rheological Properties", *Journal of the Association of Asphalt Paving Technologists*, Vol. 67, 1998, pp.623-643.

(26) Kandhal, P., R. Dongre, and M. Malone, " Prediction of Low-Temperature Cracking of Pennsylvania Project Using Superpave Binder Specifications", *Journal of the Association of Asphalt Paving Technologists*, Vol. 65, 1996, pp.491-531.

(27) Roque, R., and B. E. Ruth, " Mechanisms and Modeling of Surface Cracking in Asphalt Pavements", *Journal of the Association of Asphalt Paving Technologists*, Vol. 59, 1990, pp.396-421.

(28) Von Quintus, H.L., J.A. Scherocman, C.S. Hughes, and T.W. Kennedy, " Asphalt-Aggregate Mixture Analysis System AAMAS", National Cooperative Highway Research Program Report 338, TRB, National Research Council, Washington DC, 1991.

(29) Terrel, R. L., T. V. Scholz, A. Al-Joaib, and S. Al-Swailmi, " Validation of Binder Properties Used to Predict Water Sensitivity of Asphalt Mixtures", *Proceedings of the Association of Asphalt Paving Technologists*, Vol. 62, 1993, pp.172-222.

(30) Fromm, H. J., "The Mechanisms of Asphalt Stripping From Aggregate Surfaces", *Journal of the Association of Asphalt Paving Technologists*, Vol. 43, 1974, pp.191-223.

(31) Amirkhanian, S., and K. W. Kim, "Evaluation of Effectiveness of Antistrip Additives Using Fuzzy Set Procedures", Transportation Research Record 1323, TRB, National Research Council, Washington, DC, 1991, pp. 112-122.

(32) Brown, E. R., R. E. Graves, and D. I. Hanson, " Laboratory Evaluation of the Addition of Lime Treated Sand to Hot-Mix Asphalt", Transportation Research Record 1469, TRB, National Research Council, Washington, DC, 1994, pp. 34-42.

(33) Kandhal, P. S., and R.B. Mallick, " Evaluation of Rut Testers for HMA Mix Design", Final Report prepared for Alabama DOT, NCAT, January 1999.

(34) Anderson, R. M., and Hussain U. Bahia, "Evaluation and Selection of Aggregate Gradations for Asphalt Mixtures Using Superpave", Transportation Research Record 1583, TRB, National Research Council, Washington, DC, 1997, pp. 91-97.

(35) Aschenbrener, T., and C. MacKean, "Factors that Affect the Voids in the Mineral Aggregate of Hot-Mix Asphalt", Transportation Research Record 1469, TRB, National Research Council, Washington, DC, 1994, pp. 1-8.

(36) Adu-Osei, A., Stephen A. Cross, R. K. Fredrichs, and Mohd Rosli Hainin, "Effects of Gradation on Performance of Asphalt Mixtures", Presented at 78th Annual Transportation Board Meeting, Washington, DC, 1999.

(37) Chowdhury, A., J.D.C. Grau, J.W. Button, and D.N. Little, "Effect of Aggregate Gradation on Permanent Deformation of Superpave HMA", Presented at 80th Annual Transportation Board Meeting, Washington,D.C., 2001.

(38) Lenoble, C., and N.C. Nahas, " Dynamic Rheology and Hot-Mix Performance of Polymer Modified Asphalts", *Journal of the Association of Asphalt Paving Technologists*, Vol. 63, 1994, pp.450-480.

(39) Airey, G., and S. Brown, " Rheological Performance of Aged Polymer Modified Binders", *Proceedings of the Association of Asphalt Paving Technologists*, Vol. 67, 1998, pp.66-100.

(40) Gilbert, B. Y., and M. J. Khattak, "Engineering Properties of Polymer Modified Asphalt Mixtures", prepared for 77th Transportation Research Board Annual Meeting, Washington DC, Jan. 11-15, 1998.

(41) "Bituminous Binders and Mixes, State of the Art and Interlaboratory Tests on Mechanical Behavior and Mix Design", Report of RILEM Technical committee 152-PBM performance of Bituminous Materials, Report 17, Edited by Francken, L., 1998.

(42) Gunderson, B., L. Planque, and A. F. Stock, "Field and Laboratory Evaluation of Specialist High Performance Binders", Volume two, 7th International Conference on Asphalt Pavements, The International Society of Asphalt Pavements, Austin, Texas, 1992.

(43) David, R., C. Ifft, and L. G. Scholl, "Relating Hot-Mix properties to Properties of Conventional or Polymer-Modified Binders", Transportation Research Record 1269, TRB, National Research Council, Washington, DC, 1990, pp. 158-167.

(44) Zhou, J., S. E. Nodes, and J. Nichols, "Evaluation of Three Polymer Modified Asphalt Concretes", Transportation Research Record 1454, TRB, National Research Council, Washington, DC, 1994, pp. 181-192.

(45) Khosla, N. P., "Effect of the Use of Modifiers on Performance of Asphaltic Pavements", Transportation Research Record 1317, TRB, National Research Council, Washington, DC, 1991, pp. 10-22.

(46) King,G., H. King, R.D. Pavlovich, A. Epps, and P. Kandhal, "Additives in Asphalt", 75th Anniversary Historical Review and Index of Journals, *Proceedings of the Association of Asphalt Paving Technologists*, Vol. 68A, 1999, pp.32-69.

(47) Campbell, B., R. Collins, and D. Watson, "Development and Use of Georgia Loaded wheel Tester", Transportation Research Record 1492, TRB, National Research Council, Washington, DC, 1995, pp. 202-207.

(48) Collins, R., J. S. Lai, and H. Shami, "Use of Georgia Loaded Wheel Tester to Evaluate Rutting of Asphalt Samples Prepared by Superpave Gyratory Compactor", Transportation Research Record 1545, TRB, National Research Council, Washington, DC, 1996, pp. 161-168.

(49) Daly, William H., Z. Qui, and I. Negulescu, "Preparation and Characterization of Asphalt-Modified Polyethylene Blends", Transportation Research Record 1391, TRB, National Research Council, Washington, DC, 1993, pp. 56-64.

(50) Von Quintus, H. L., J. B. Rauhut, and T. W. Kennedy, "Comparisons of Asphalt Concrete Stiffness as Measured by Various Testing Techniques", *Proceedings of the Association of Asphalt Paving Technologists*, Vol. 51, 1982, pp.35-52.

(51) Mamlouk, M. S., and R. T. Sarofim, "Modulus of Asphalt Mixtures-An Unresolved Dilemma", Transportation Research Record 1171, TRB, National Research Council, Washington, DC, 1988, pp. 193-198.

(52) Valkering, C.P., D. J. L. Lancon, E. deHilster, and D.A. Stocker, and. "Rutting Resistance of Asphalt Mixes Containing Non-Conventional and Polymer-Modified Binders", *Journal of the Association of Asphalt Paving Technologists*, Vol. 59, 1990, pp.590-609.

(53) Sousa, J. B., and S. L. Weissman, "Modeling Permanent Deformation of Asphalt-Aggregate Mixes", Proceedings of the Association of Asphalt Paving Technologists, Vol. 63, 1994, pp.224-257.

(54) Brown, S., and J. M. Gibb, "Validation of Experiments for Permanent Deformation Testing of Bituminous Mixtures", *Journal of the Association of Asphalt Paving Technologists*, Vol. 65, 1996, pp.255-299.

(55) Tayebali, A.A., J.L. Goodrich, J. B. Sousa, and C.L. Monismith, "Relationship Between Modified Asphalt Binders Rheology and Binder-Aggregate Mixture Permanent Deformation Response", *Journal of the Association of Asphalt Paving Technologists*, Vol. 60, 1991, pp.121-159.

(56) Leahy, R.B. and M.W. Witczak, "The influence of Test Conditions and Asphalt Concrete Mix Parameters on Permanent Deformation Coefficients Alpha and Mu", Jornal of *Proceedings of the Association of Asphalt Paving Technologists*, Vol. 60, 1991, pp.333-363.

(57) Kenis, W.J. "Predictive Design Procedures, VESYS Users Manual", Report Number FHWA-RD-77-154, FHWA, Washington, D.C., January 1978

(58) Button, Joe W., Dallas N. Little, and H. Youssef, " Development of Criteria to Evaluate Uniaxial Creep Data and Asphalt Concrete Permanent Deformation Potential", Transportation Research Record 1417, TRB, National Research Council, Washington, DC, 1993, pp. 49-57.

(59) Harrigan, E.T., R.B. Leahy, and J.S. Youtcheff, " The SUPERPAVE Mix Design System Manual of Specifications, Test Methods, and Practices", SHRP-A-379, Strategic Highway Research Program, National Research Council, Washington, DC 1994.

(60) Little, D. N., "Performance Assessment of Binder-Rich Polyethylene-Modified Asphalt Concrete Mixtures (Novophalt)", Transportation Research Record 1317, TRB, National Research Council, Washington, DC, 1991, pp. 1-9.

(61) Kandhal, P. S., "Field and Laboratory Investigation of Stripping in Asphalt Pavements: State of the Art Report", Transportation Research Record 1454, TRB, National Research Council, Washington, DC, 1994, pp. 36-47.

(62) Cross, S.A., M.D. Voth, "Effects of Sample Preconditioning on Asphalt Pavement Analyzer (APA) Wet Rut Depths," Presented at 80th Annual Transportation Board Meeting, Washington,D.C., 2001.

(63) S-C Huang, J. F. Branthaver, R. E. Robertson, and S. S. Kim. "Effect of Film Thickness on the Rheological Properties of Asphalts in Contact with Aggregate Surface," Transportation Research Record 1638, 31-39 1998.

(64) Mendenhall, W. and T. Sincich, Statistics for Engineering and the Sciences. 4th ed. Prentic-Hall, UpperSaddle River, New York. 1995.

(65) Christensen, D.W., and D.A. Anderson, "Interpretation of Dynamic Mechanical Test Data for Paving Grade Asphalt Cements,' *Journal of the Association of Asphalt Paving Technologists*, Vol. 61, 1992, pp.67-116.

(66) Kim, H.S., "Evaluation of the Distributions of Cost-Effectiveness Ratios and Comparison of Methods to Constructing Confidence Intervals for Such Ratios," Ph.D. Dissertation. The Ohio State University, 2000.

APPENDIX A

CREEP CURVES (TRIAXIAL REPEATED LOAD TEST)

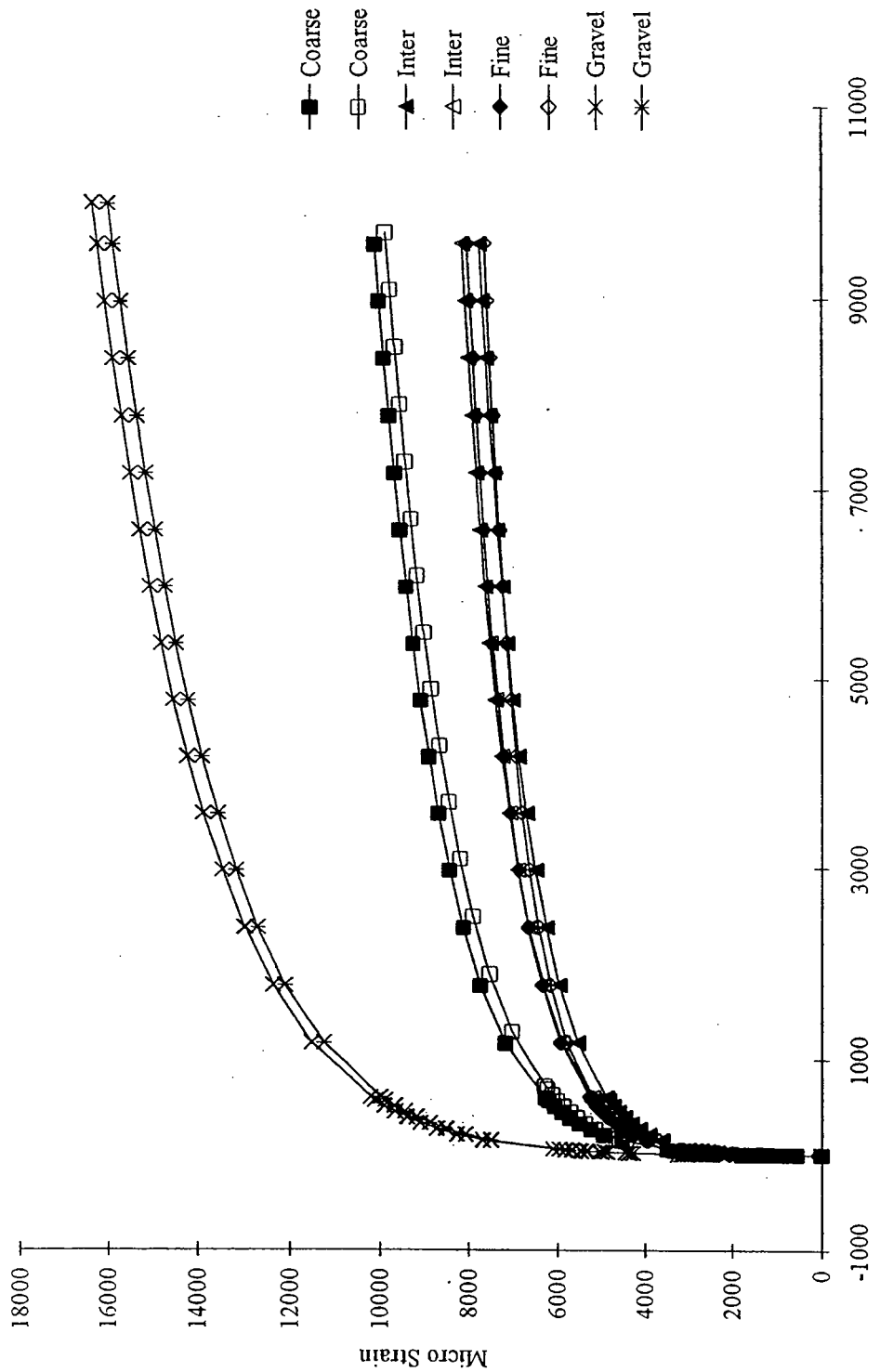

Figure A.1 Creep curves of unmodified mixes at 60 ^{O}C; effects of aggregate gradation and type

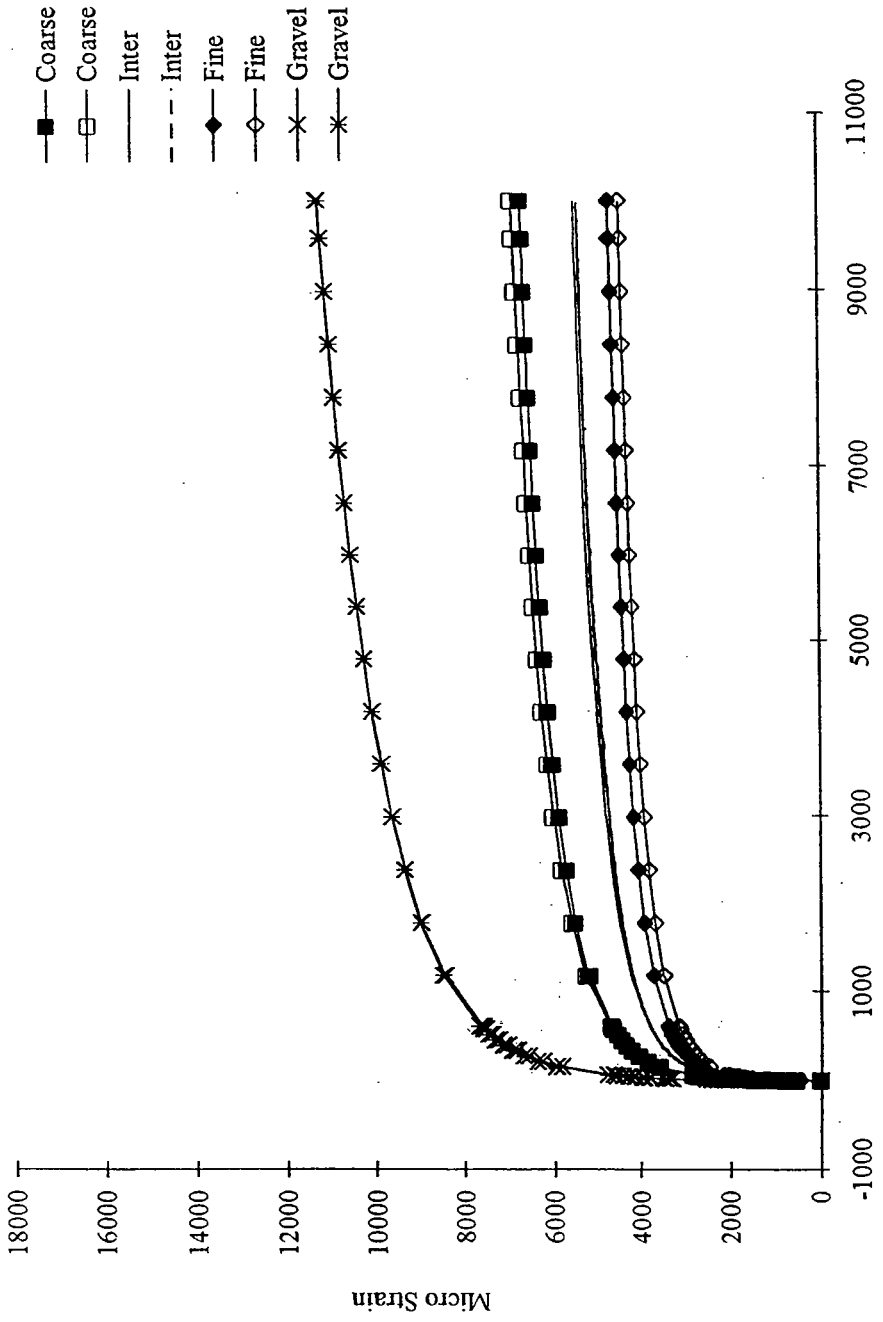

Figure A.2 Creep curves of SBS mixes at 60 ^{O}C; effects of aggregate gradation and type

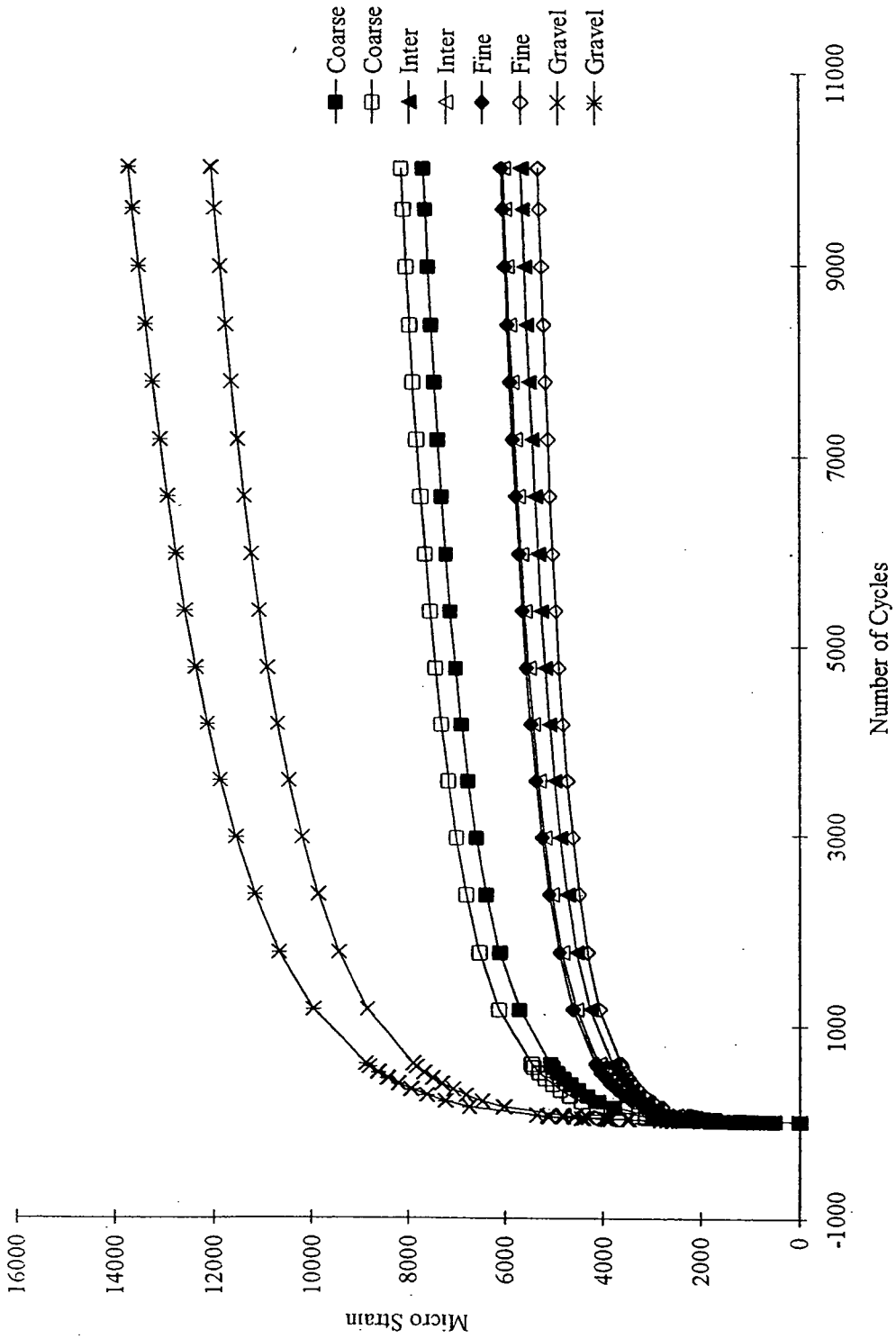

Figure A.3 Creep curves of SBR mixes at 60 ^{O}C; effects of aggregate gradation and type

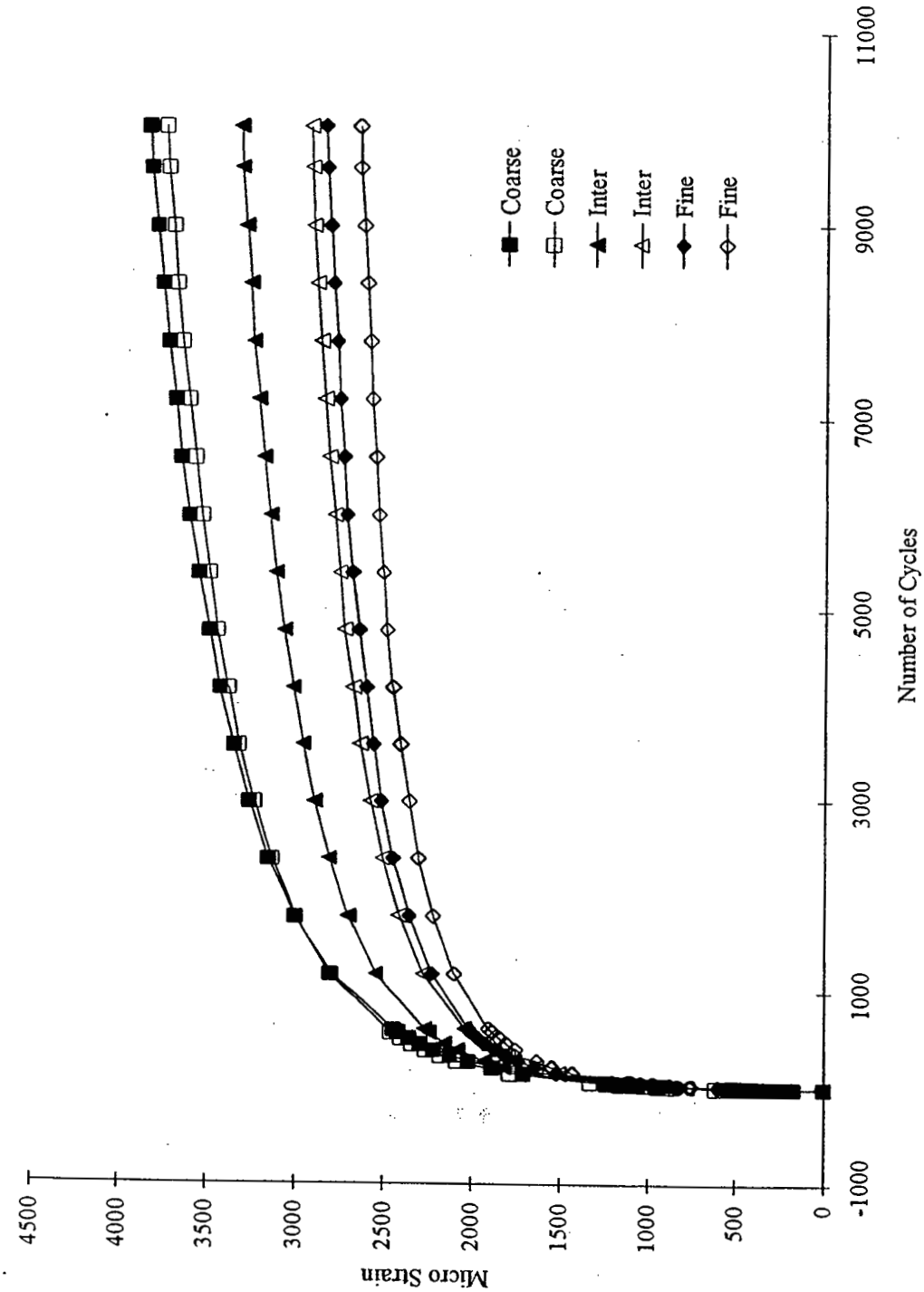

Figure A.4 Creep curves of unmodified mixes at 40 ^{O}C; effects of aggregate gradation

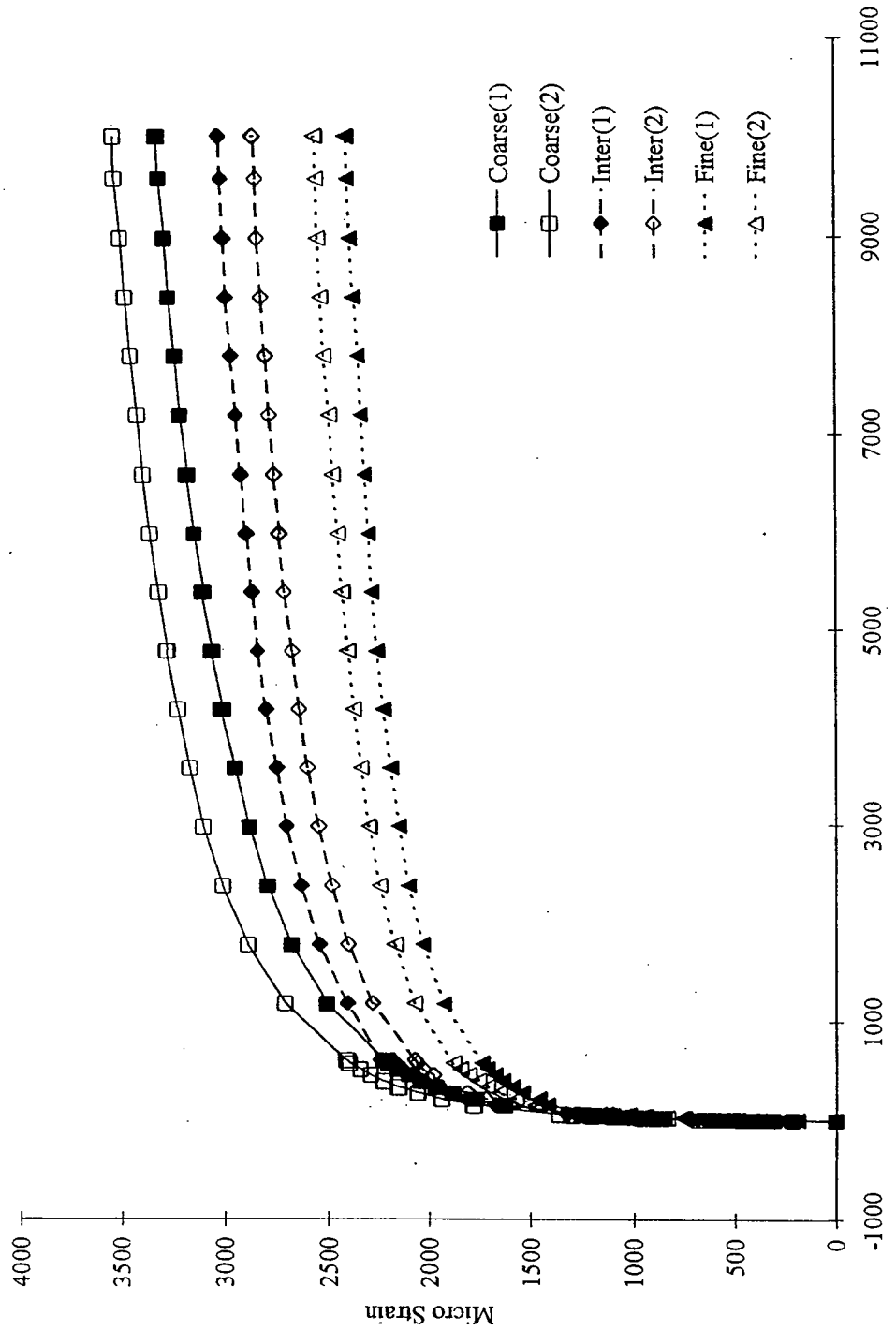

Figure A.5 Creep curves of SBS mixes at 40 ^{o}C; effects of aggregate gradation

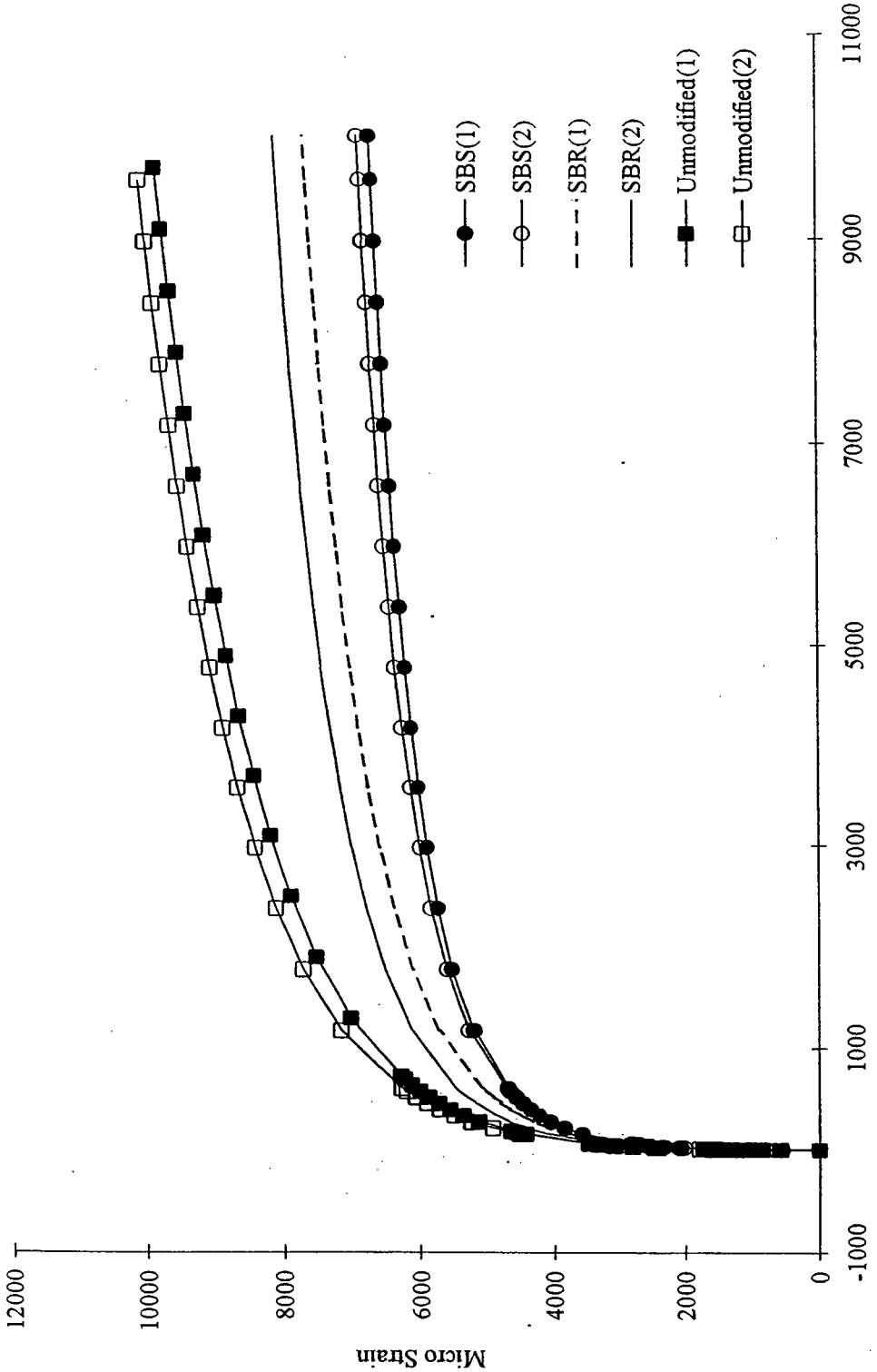

Figure A.6 Creep curves of coarse mixes at 60 ^{O}C; effects of asphalt type

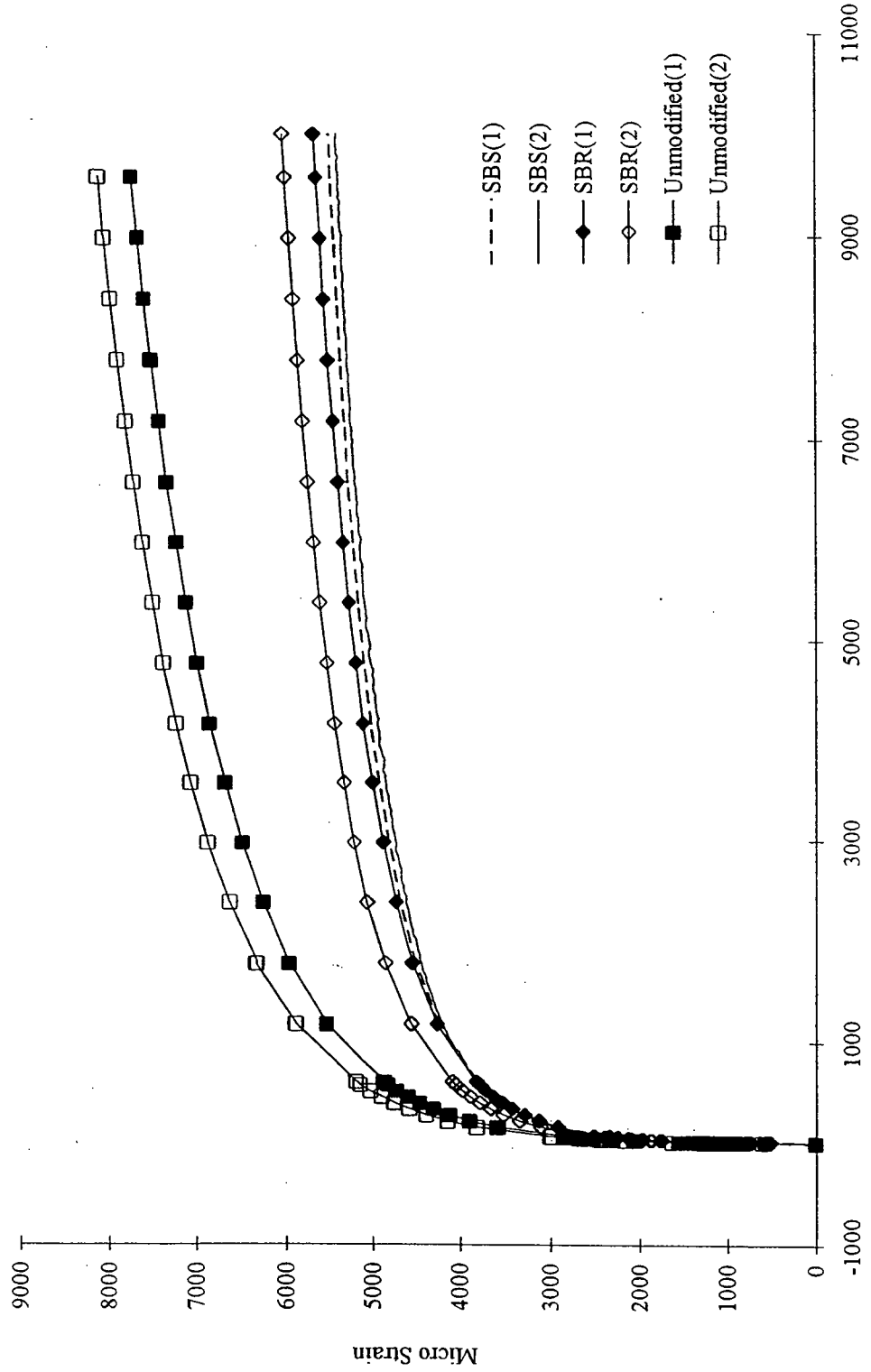

Figure A.7 Creep curves of intermediate mixes at 60 ^{O}C; effects of asphalt type

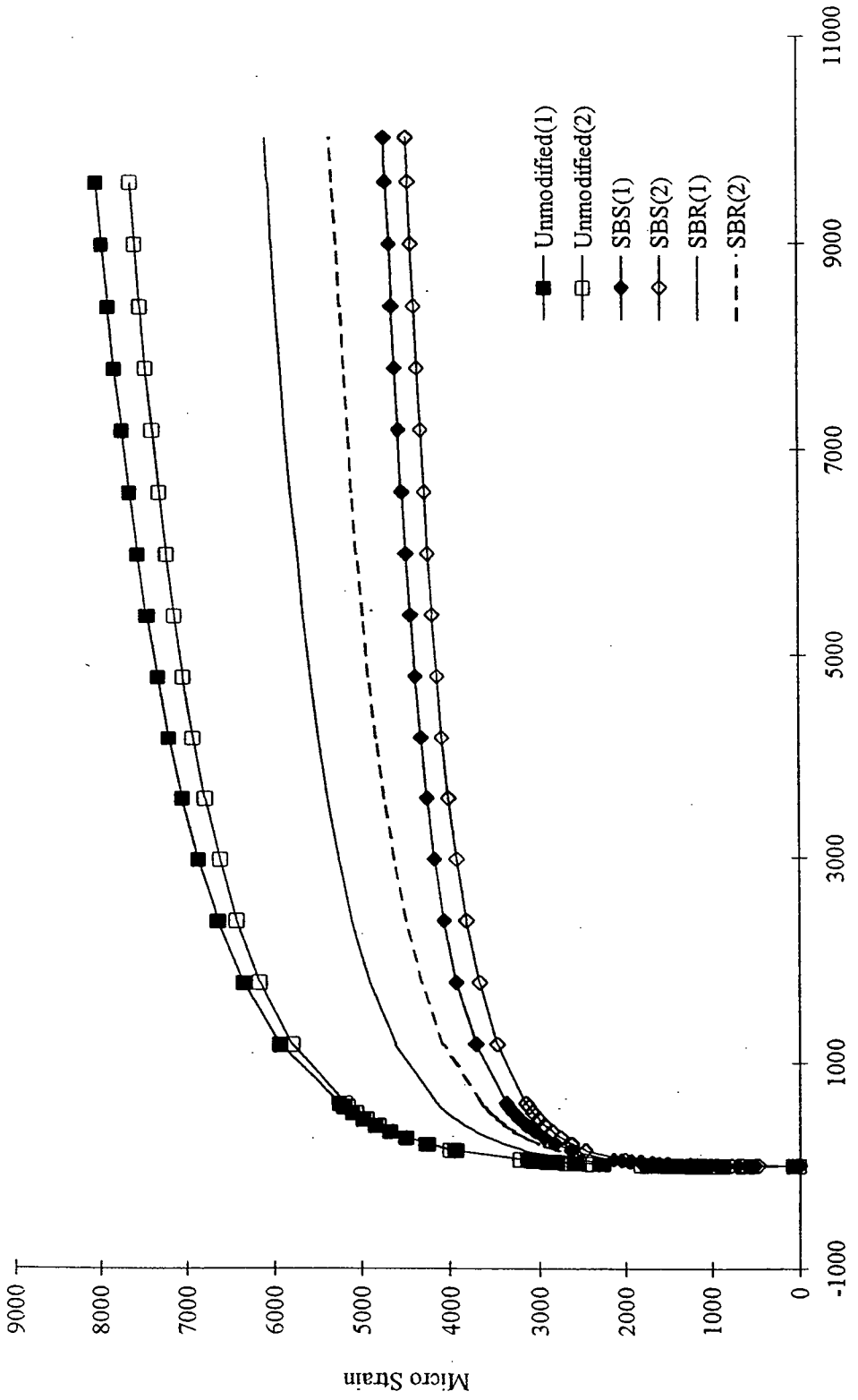

Figure A.8 Creep curves of fine mixes at 60 ^{O}C; effects of asphalt type

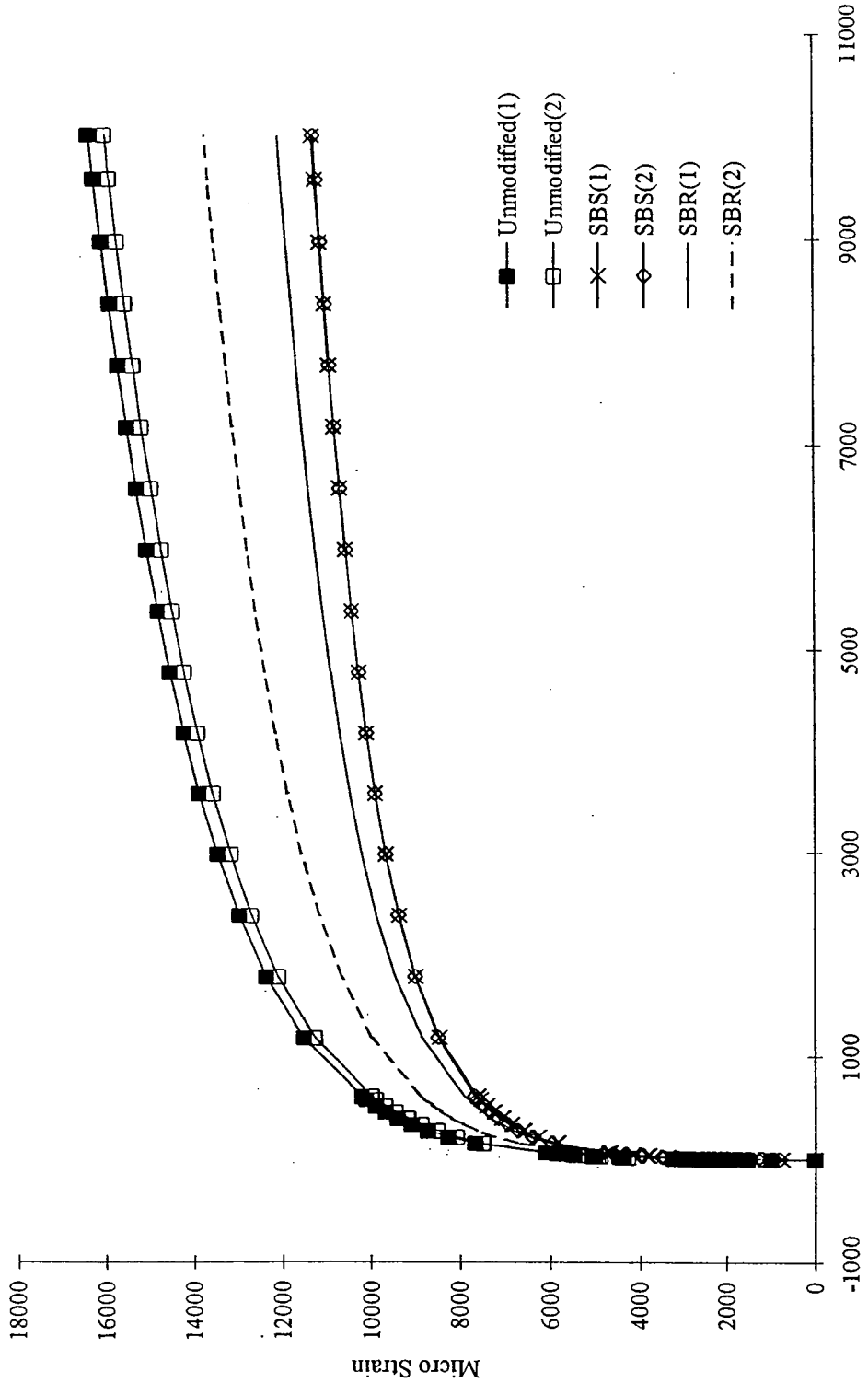

Figure A.9 Creep curves of gravel mixes at 60 ^{O}C; effects of asphalt type

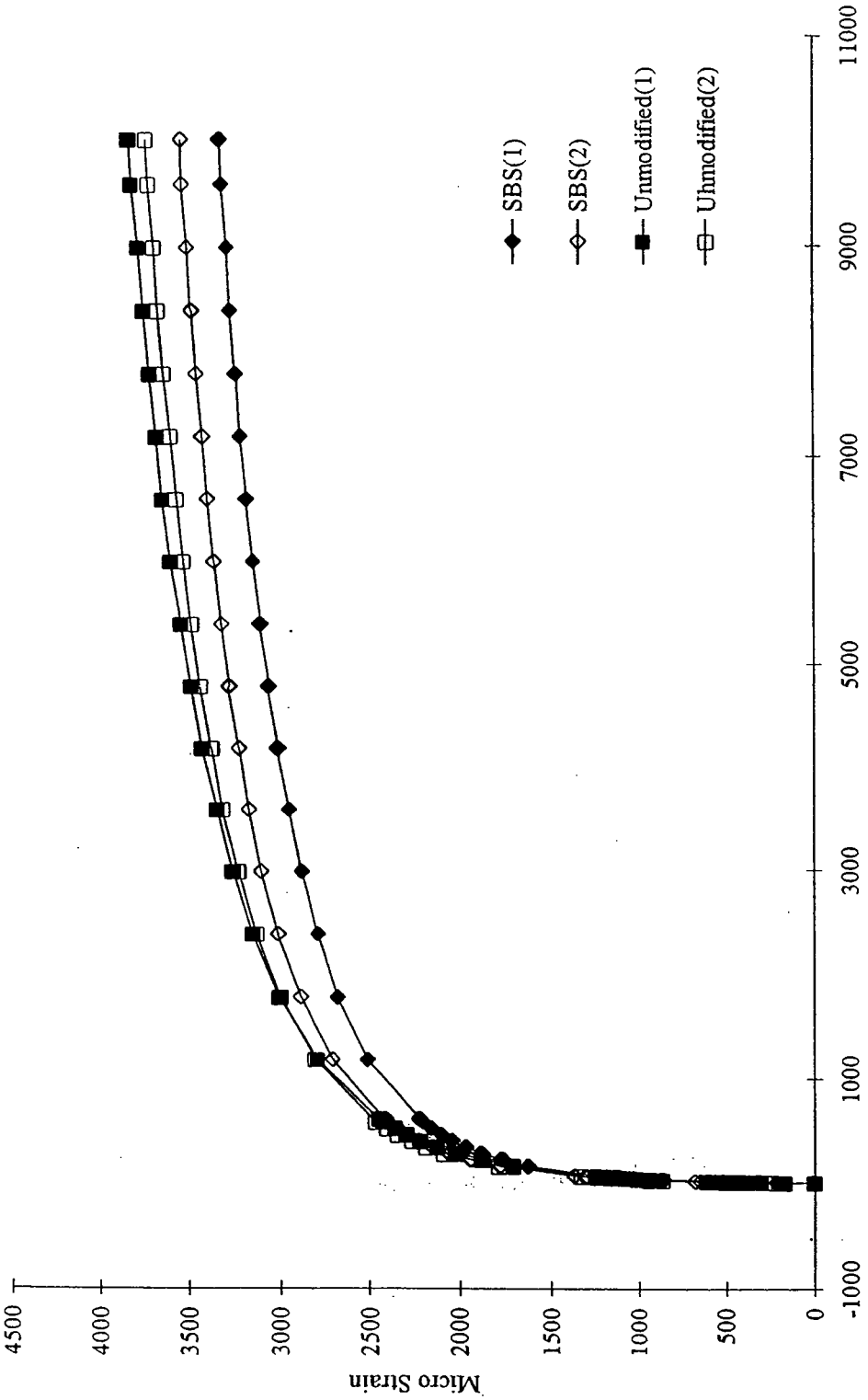

Figure A.10 Creep curves of coarse mixes at 40 ^{O}C; effects of asphalt type

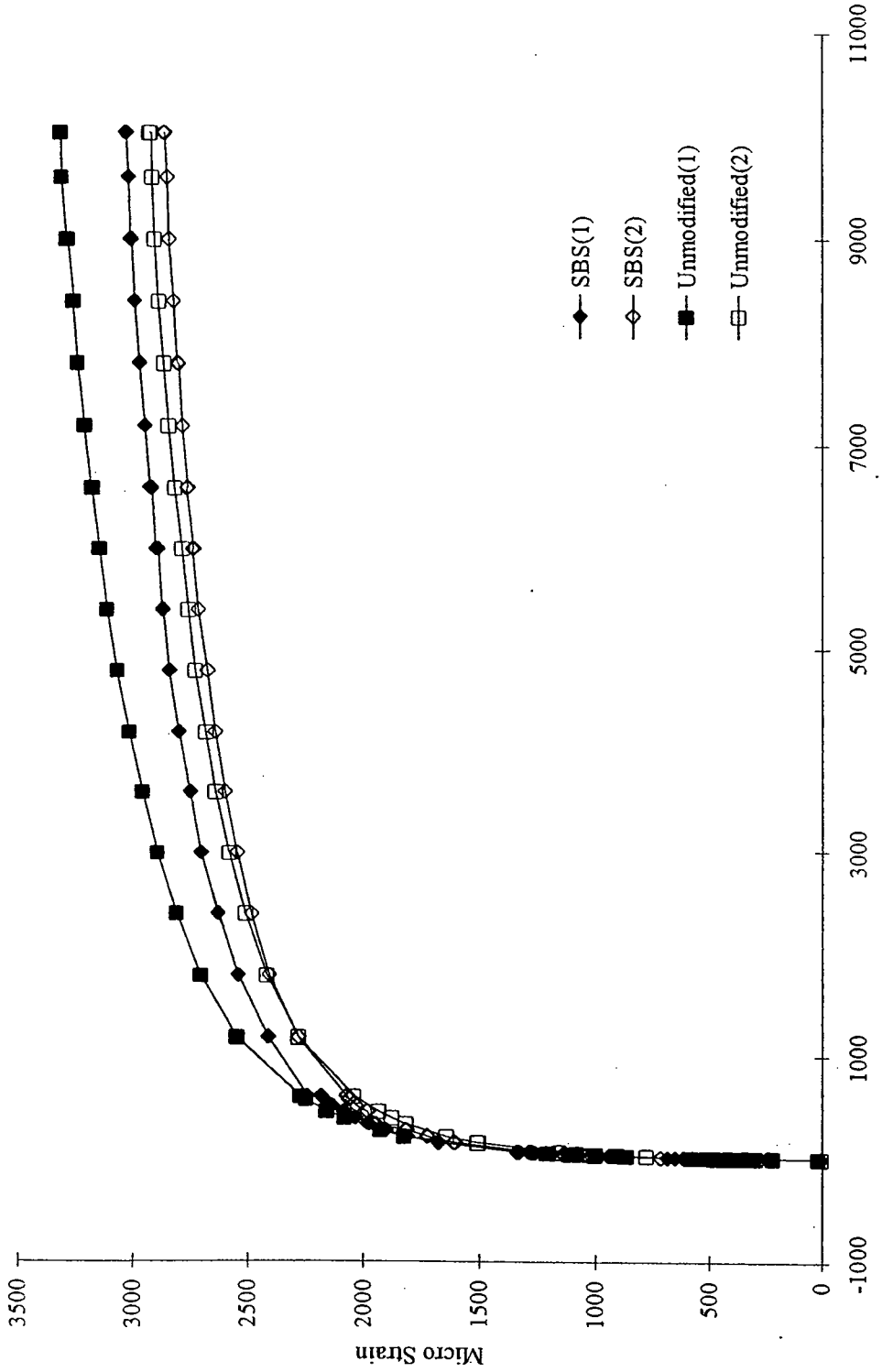

Figure A.11 Creep curves of intermediate mixes at 40 ^{O}C; effects of asphalt type

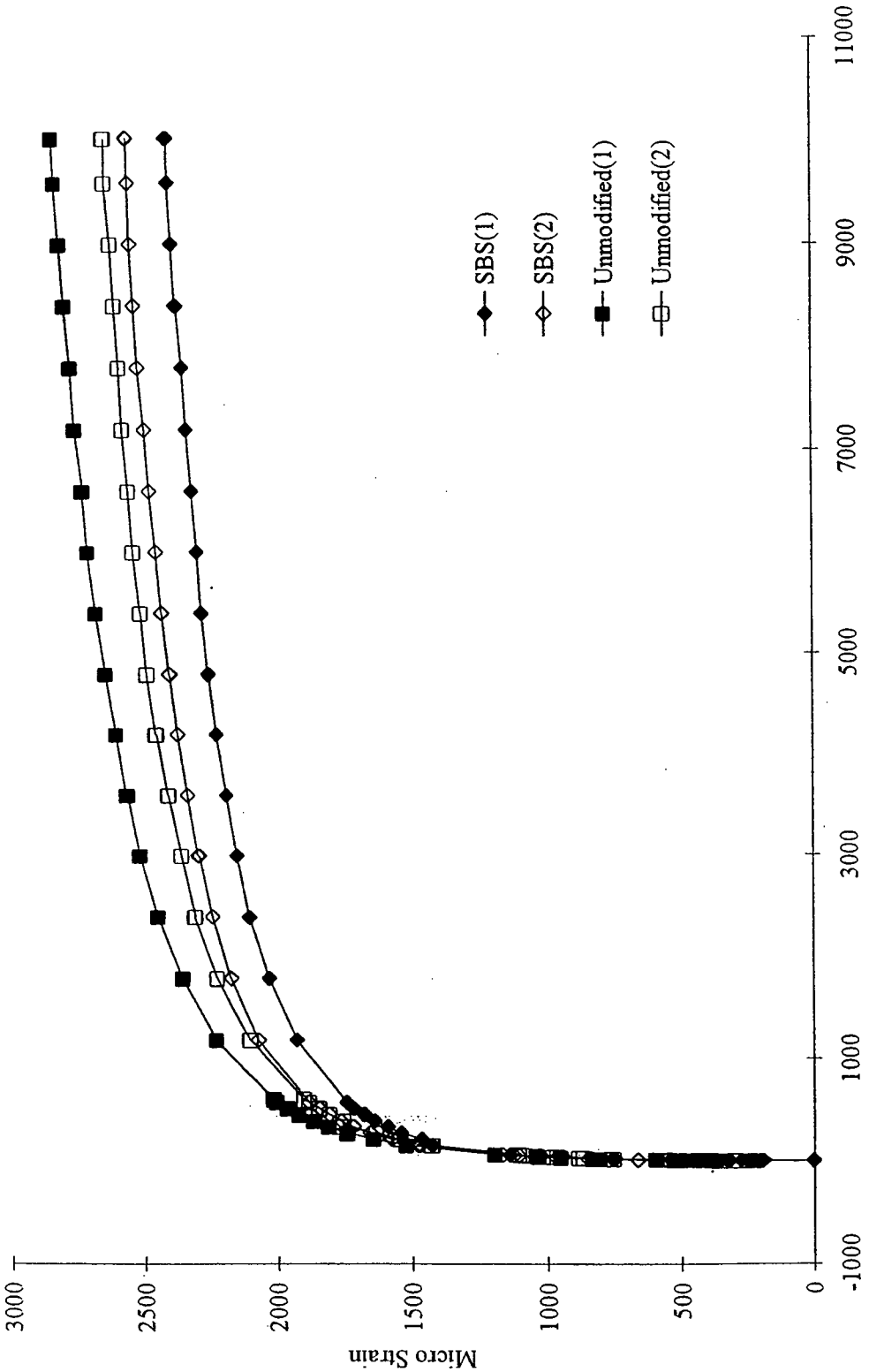

Figure A.12 Creep curves of fine mixes at 40 ^{O}C; effects of asphalt type

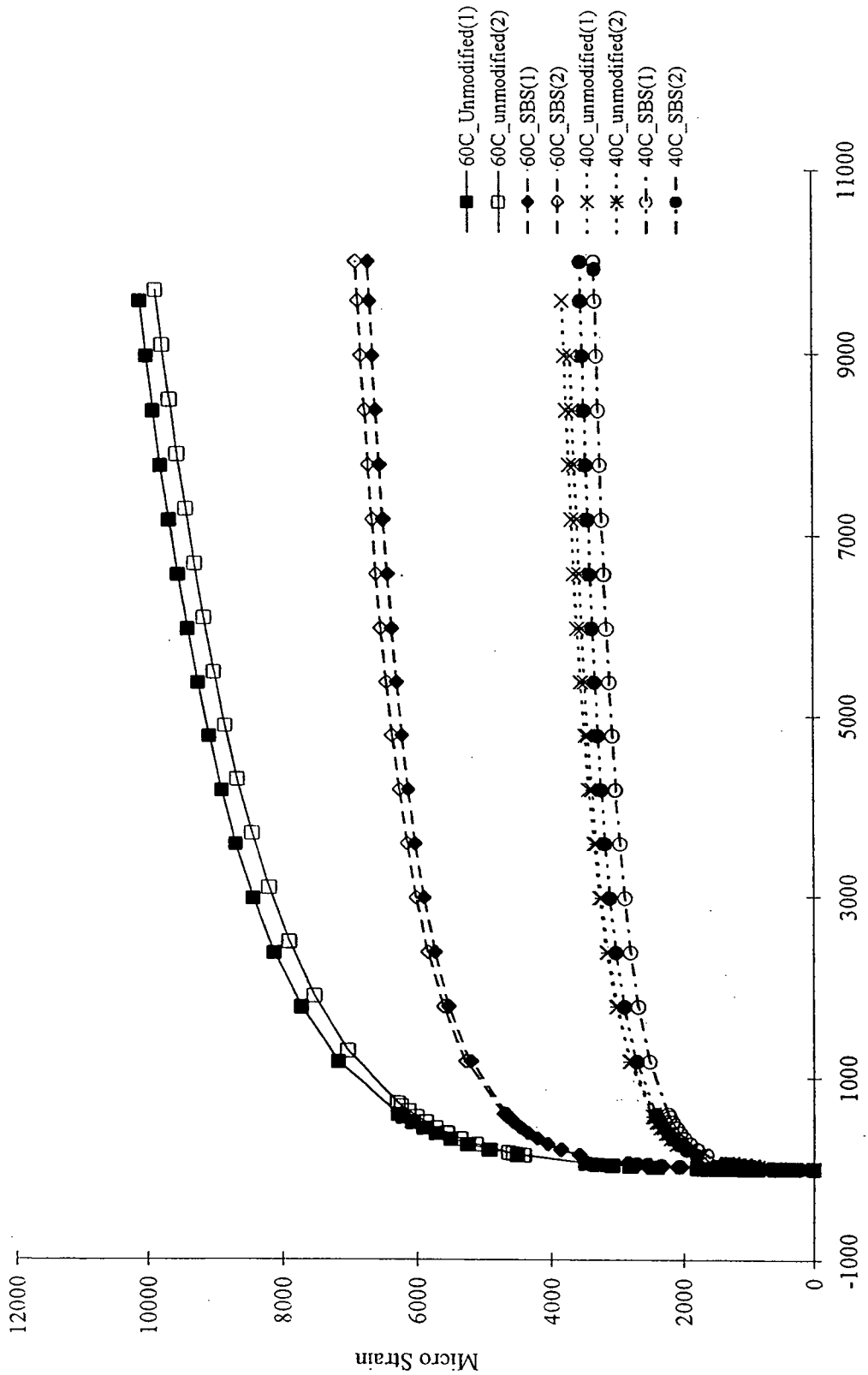

Figure A.13 Creep curves of coarse mixes (unmodified and SBS) at 60 ^{o}C and 40 ^{o}C; effect of binder on temperature dependency

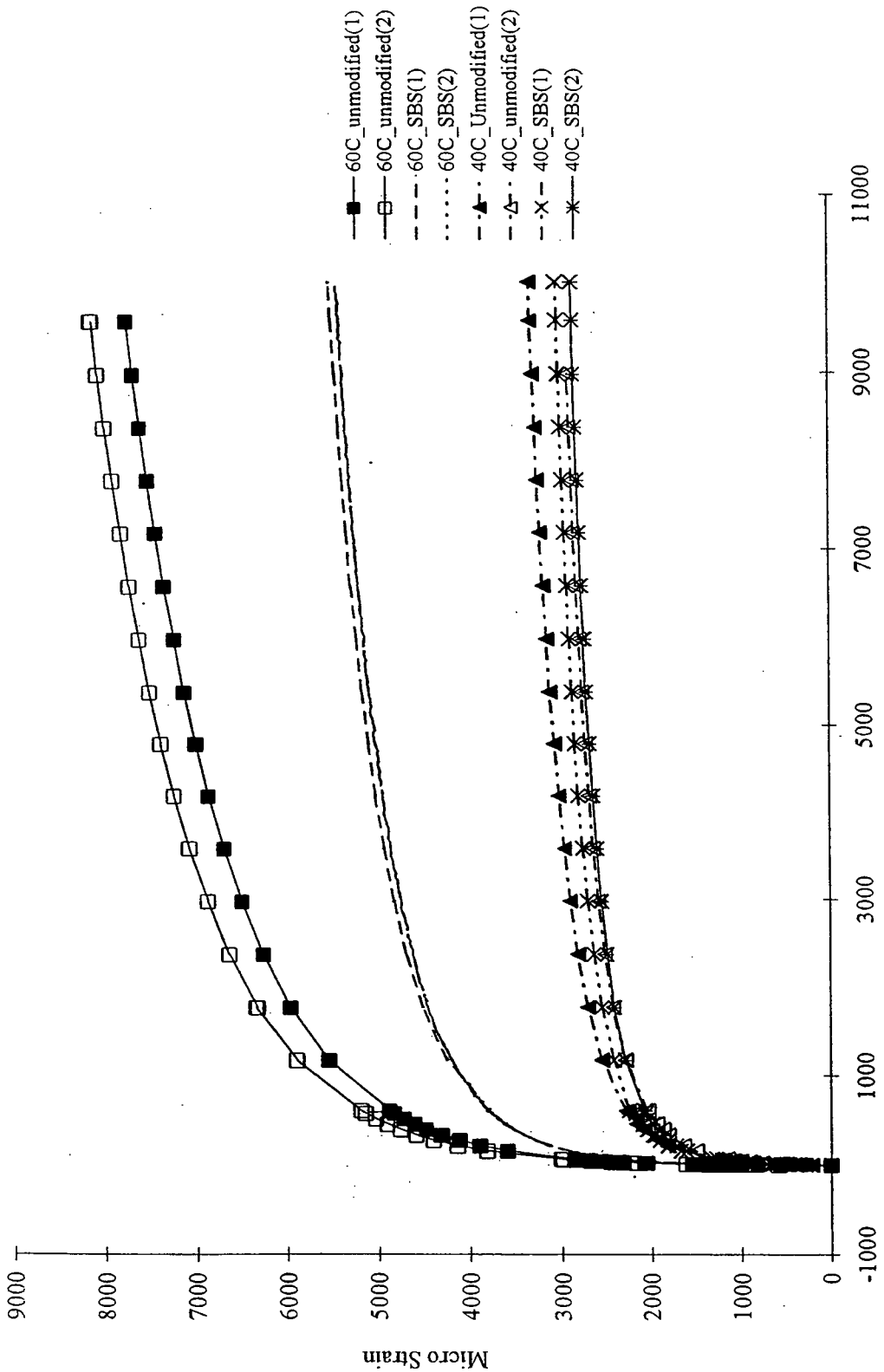

Figure A.14 Creep curves of intermediate mixes (unmodified and SBS) at 60 ^{o}C and 40 ^{o}C; effect of binder on temperature dependency

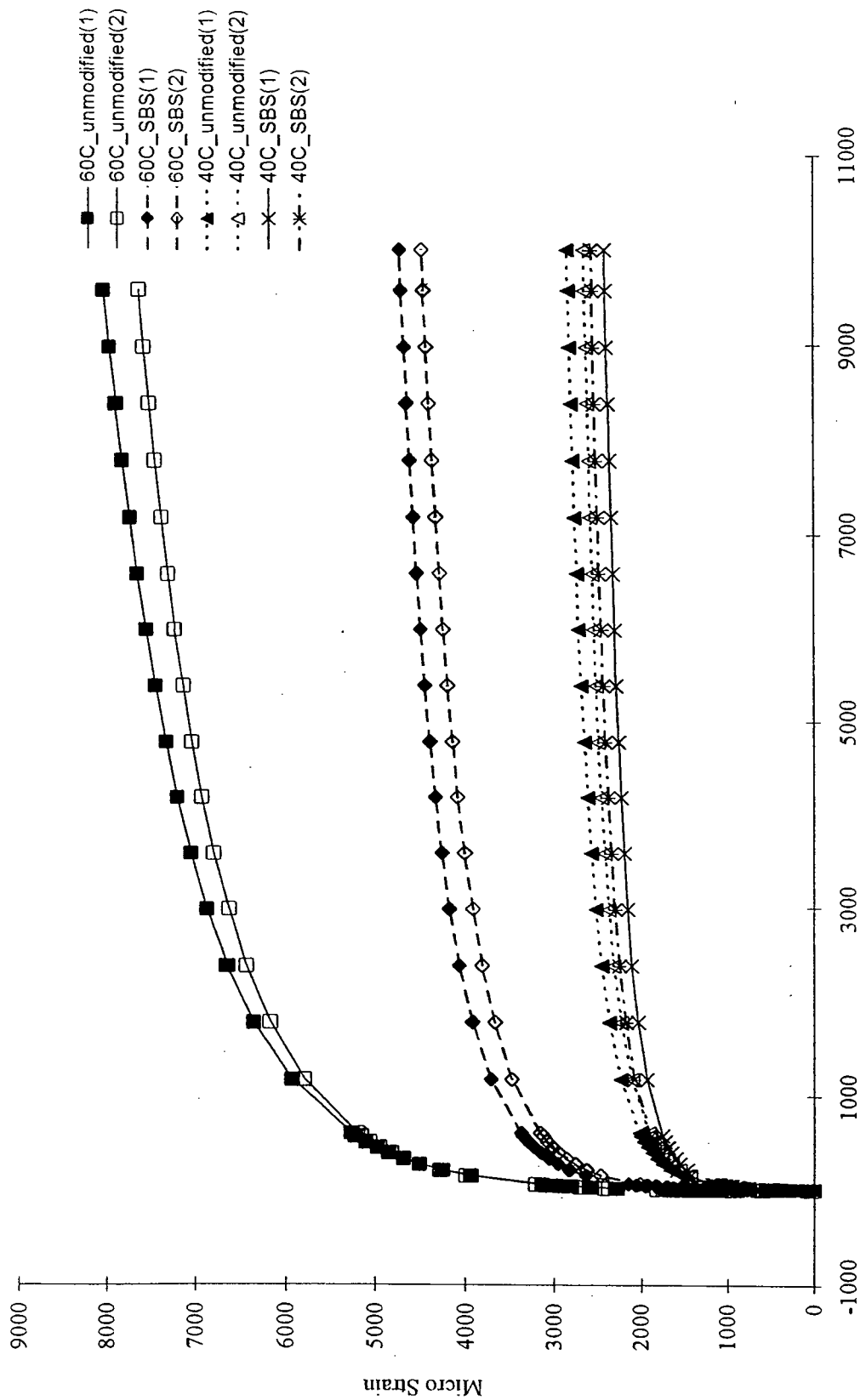

Figure A.15 Creep curves of fine mixes (unmodified and SBS) at 60 ^{o}C and 40 ^{o}C; effect of binder on temperature dependency

APPENDIX B

CREEP CURVES (UNIAXIAL STATIC CREEP TEST)

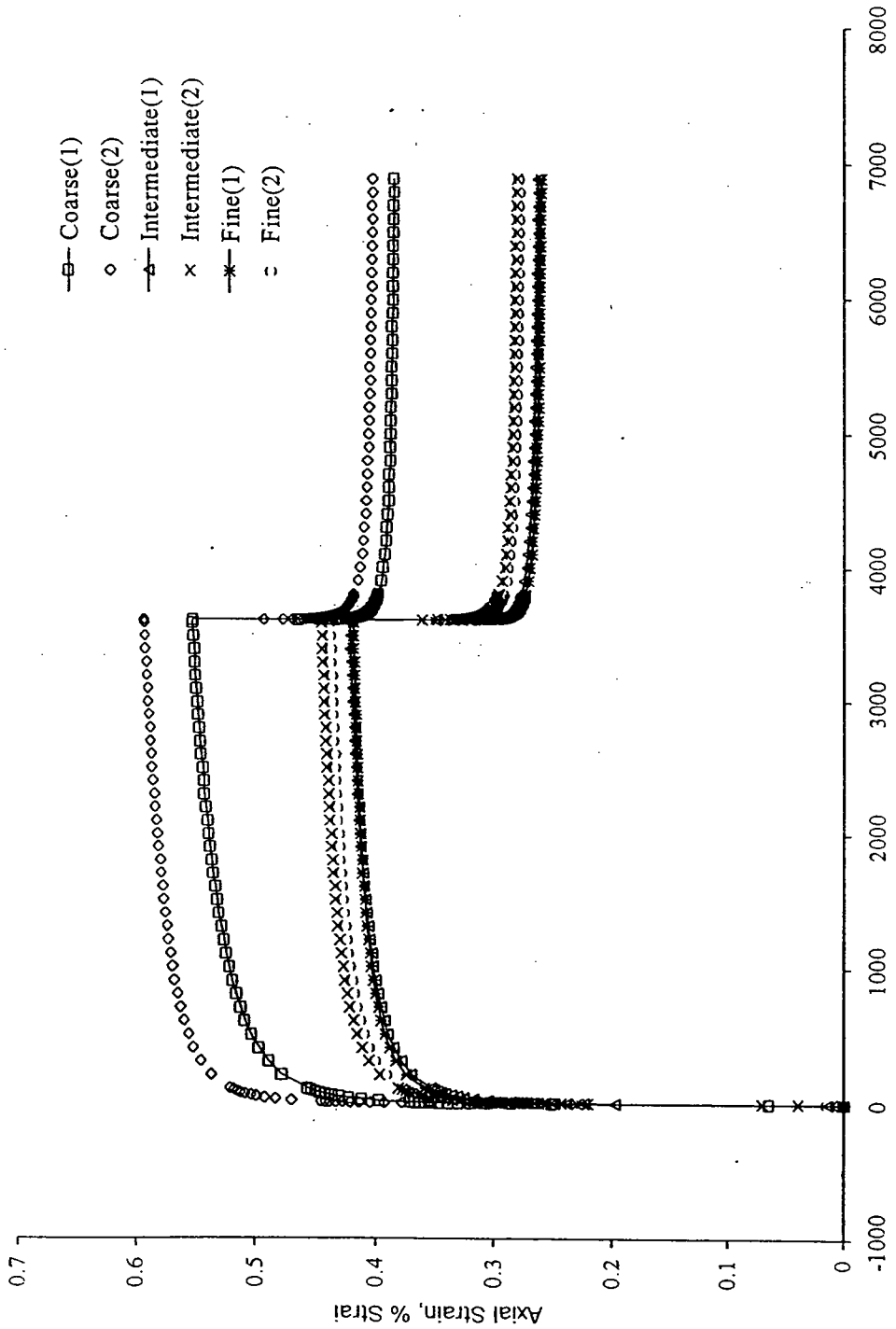

Figure B.1 Creep curves of unmodified mixes at 60 ^{O}C; effect of aggregate gradation

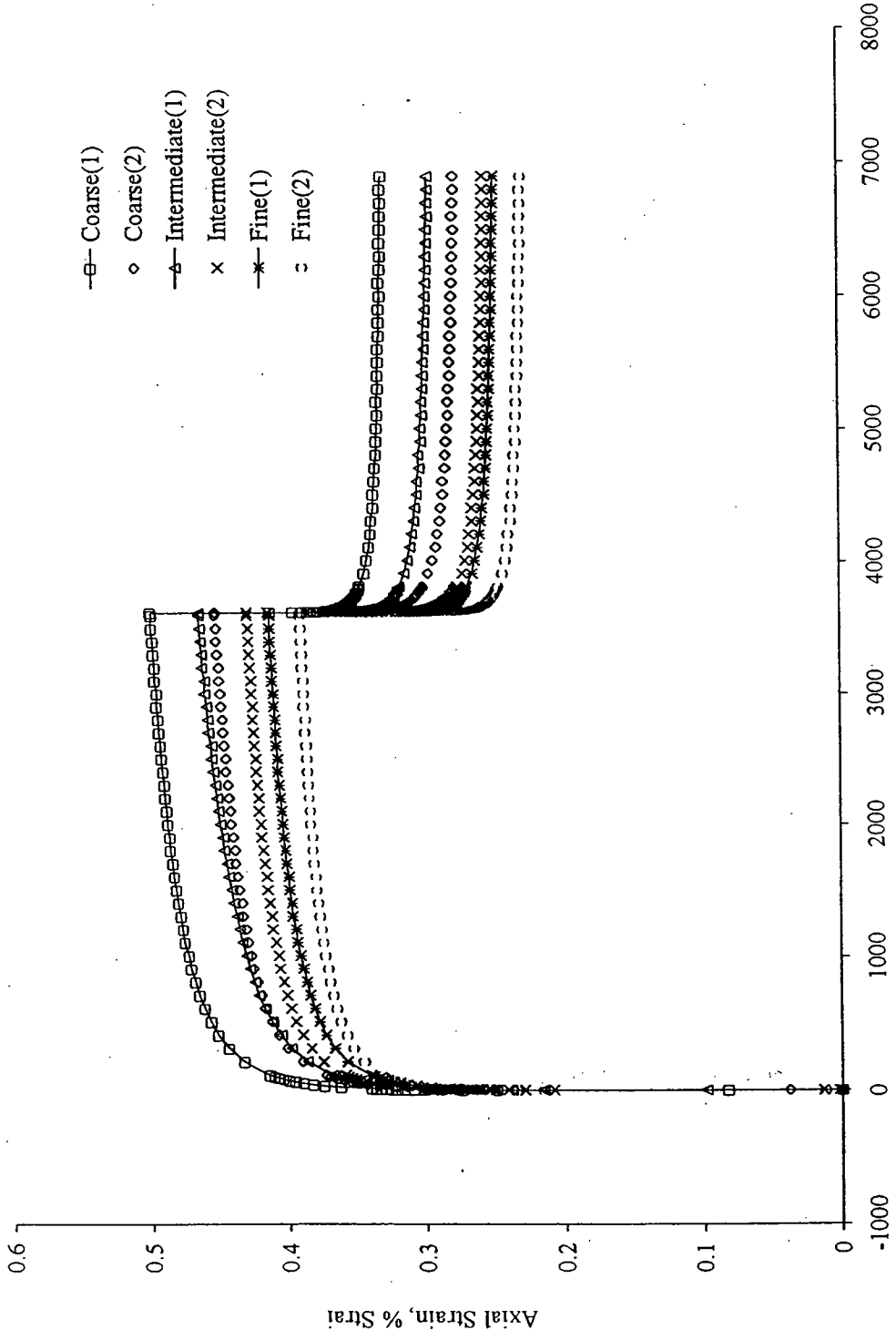

Figure B.2 Creep curves of SBS mixes at 60 ^{O}C; effect of aggregate gradation

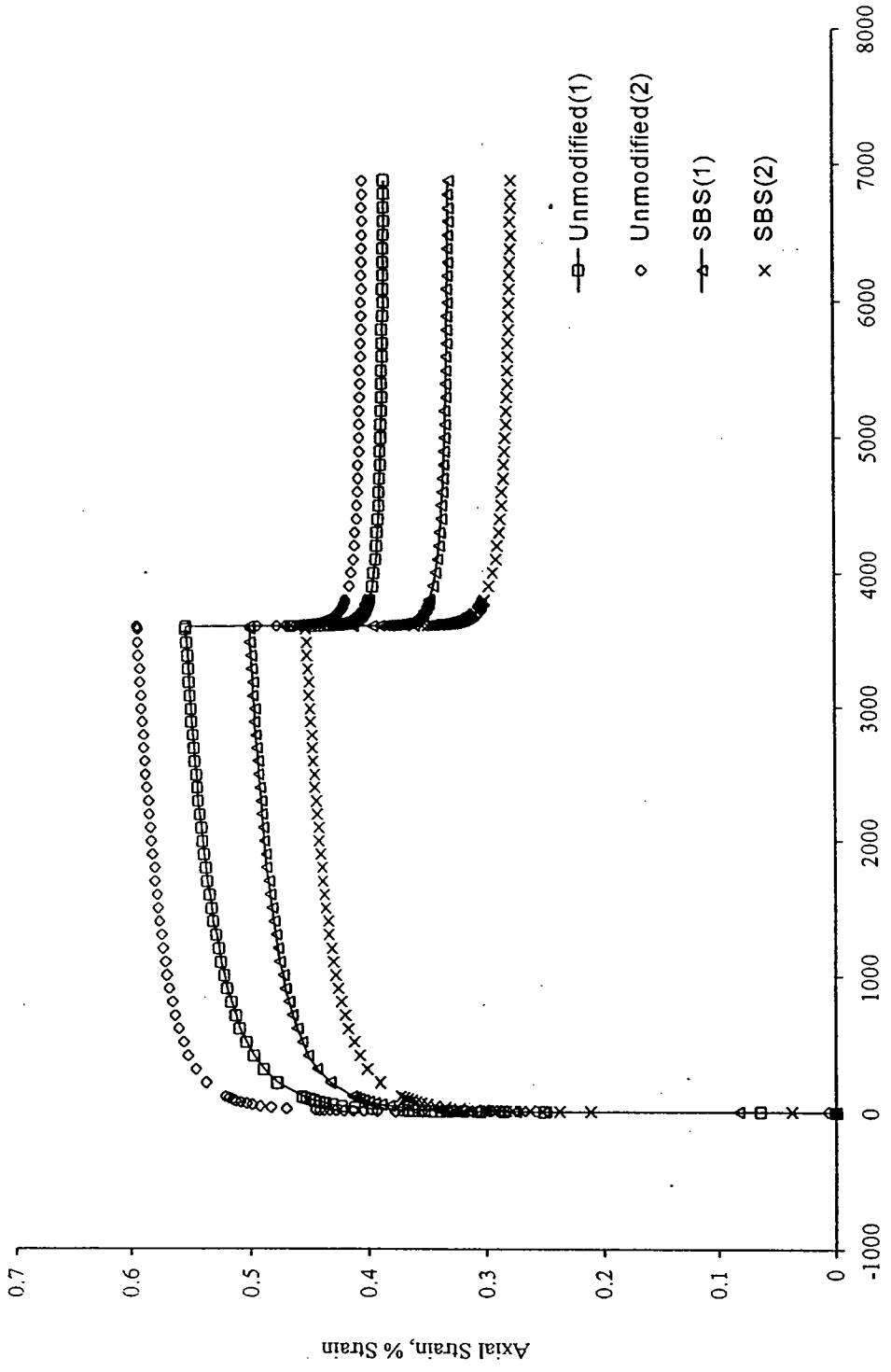

Figure B.3 Creep curves of coarse mixes at 60 ^{O}C; effect of asphalt type

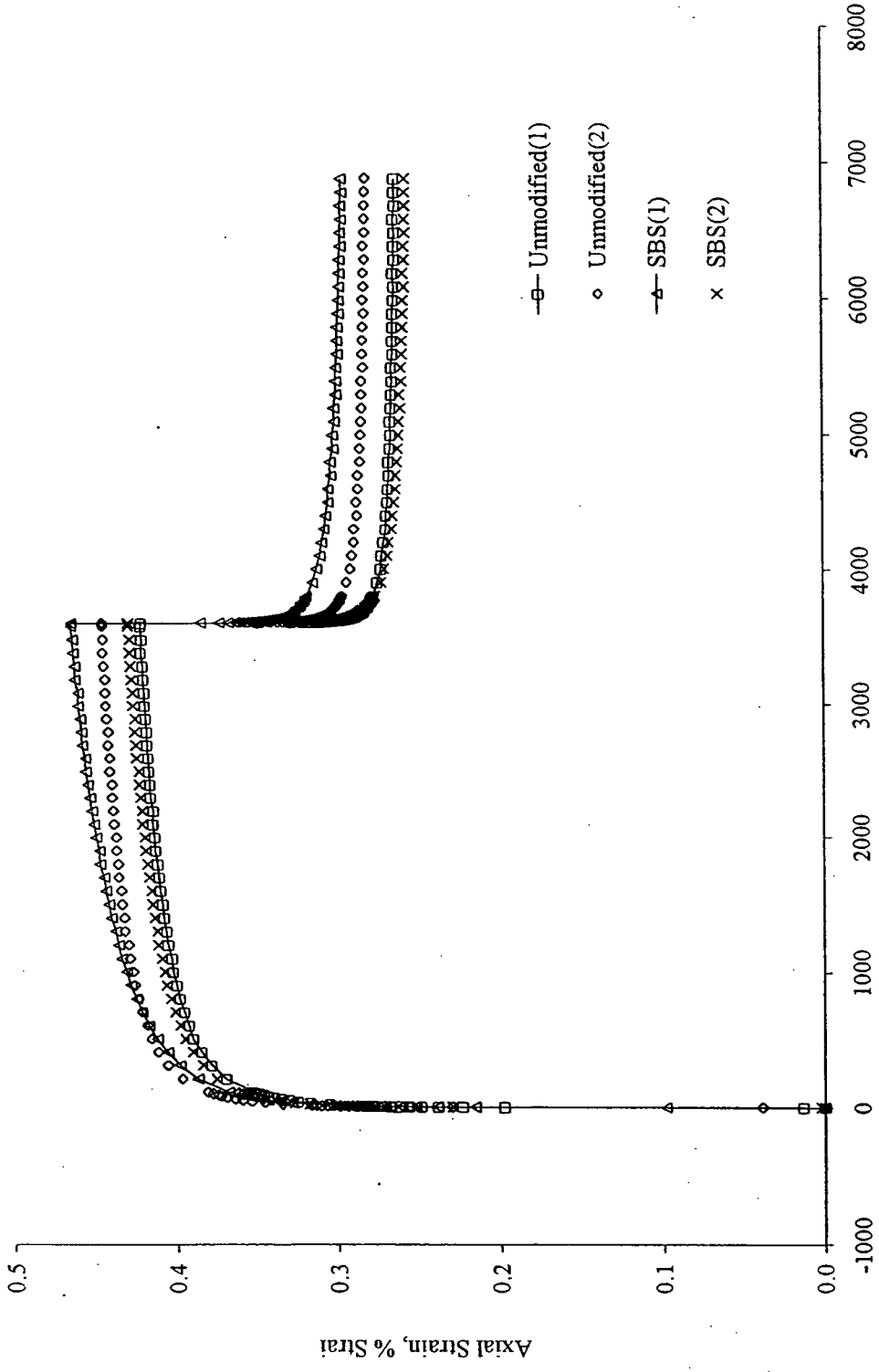

Figure B.4 Creep curves of intermediate mixes at 60 ^{O}C; effect of asphalt type

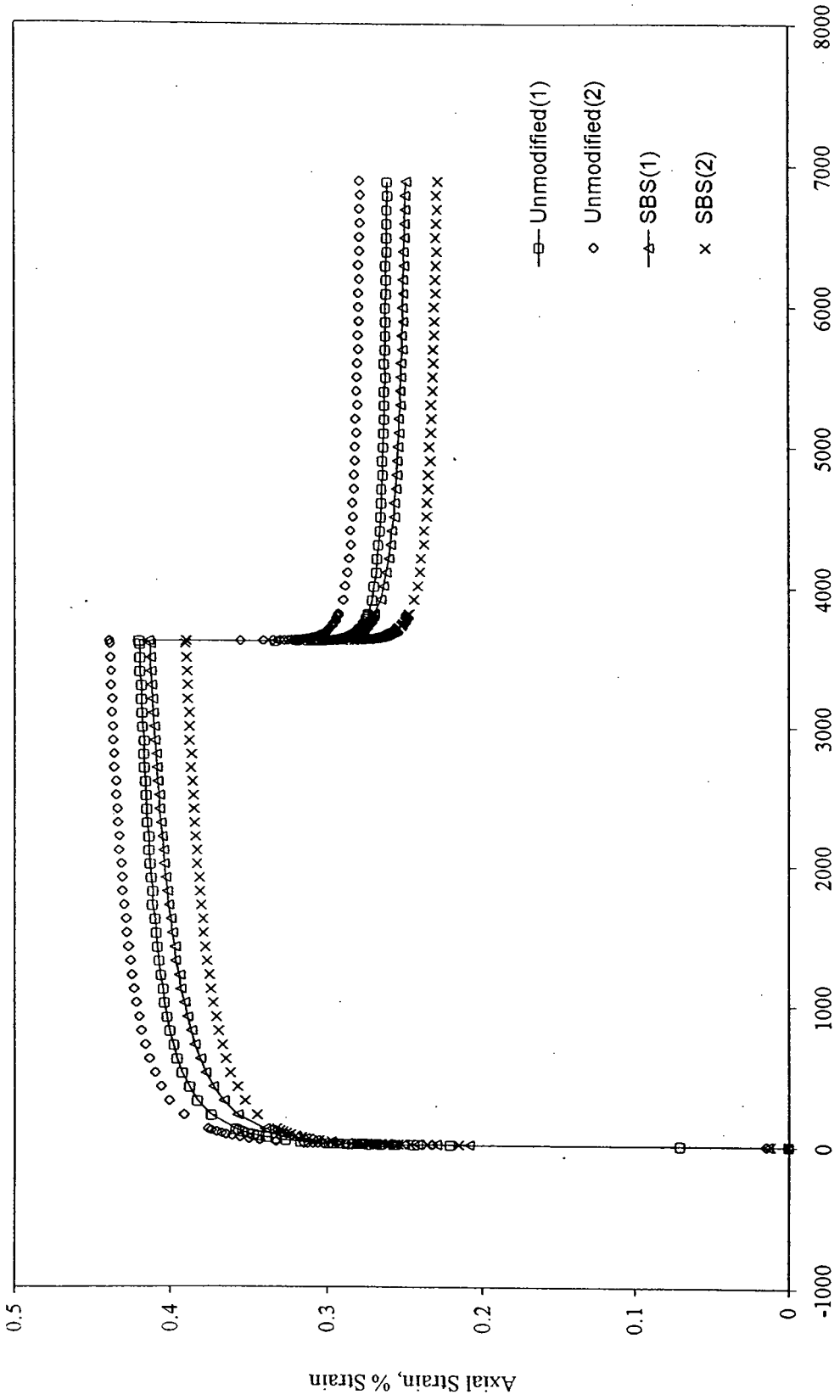

Figure B.5 Creep curves of fine mixes at 60 ^{O}C; effect of asphalt type

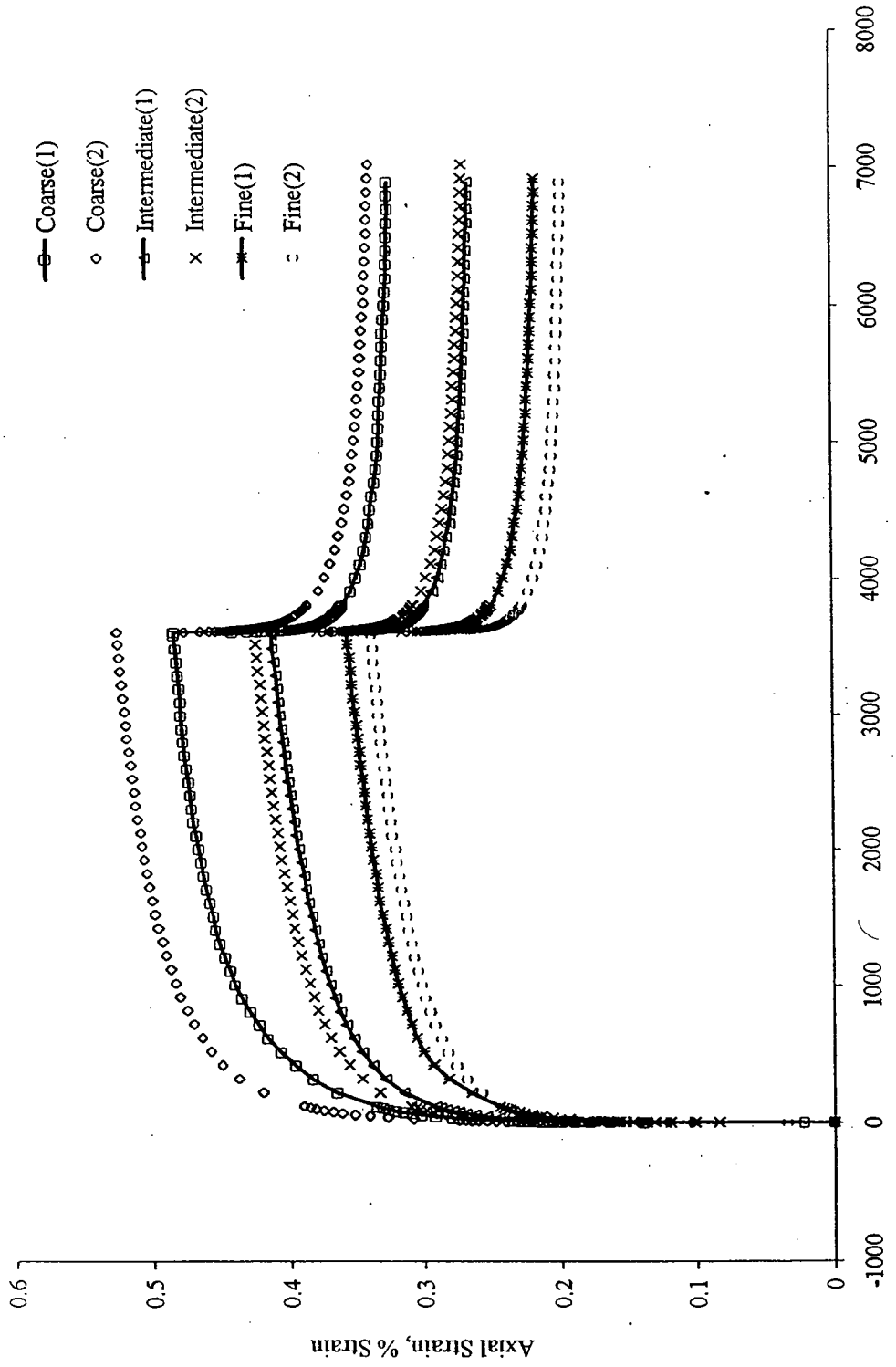

Figure B.6 Creep curves of unmodified mixes at 40 ^{O}C; effect of aggregate gradation

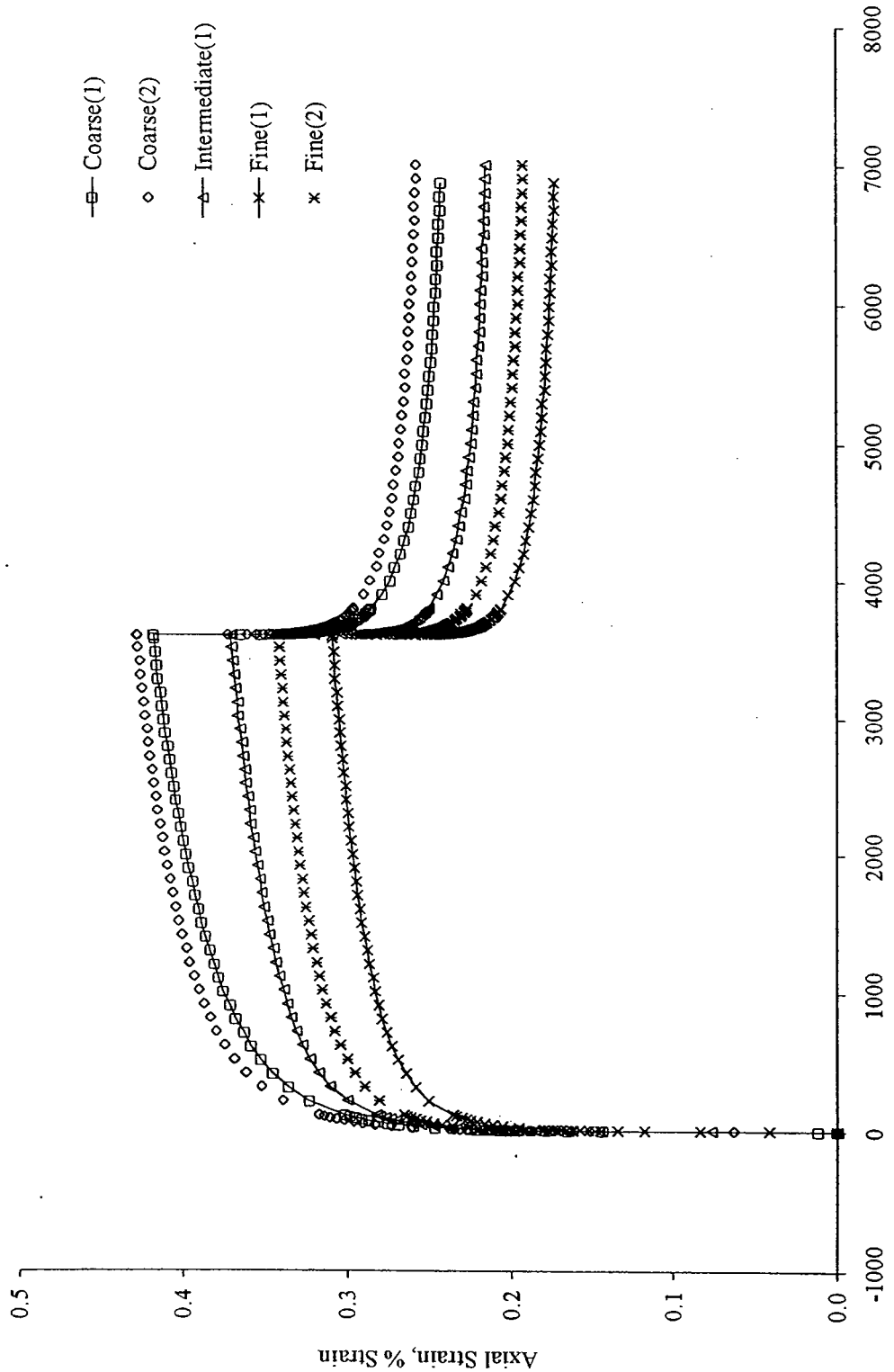

Figure B.7 Creep curves of SBS mixes at 40 ^{O}C; effect of aggregate gradation

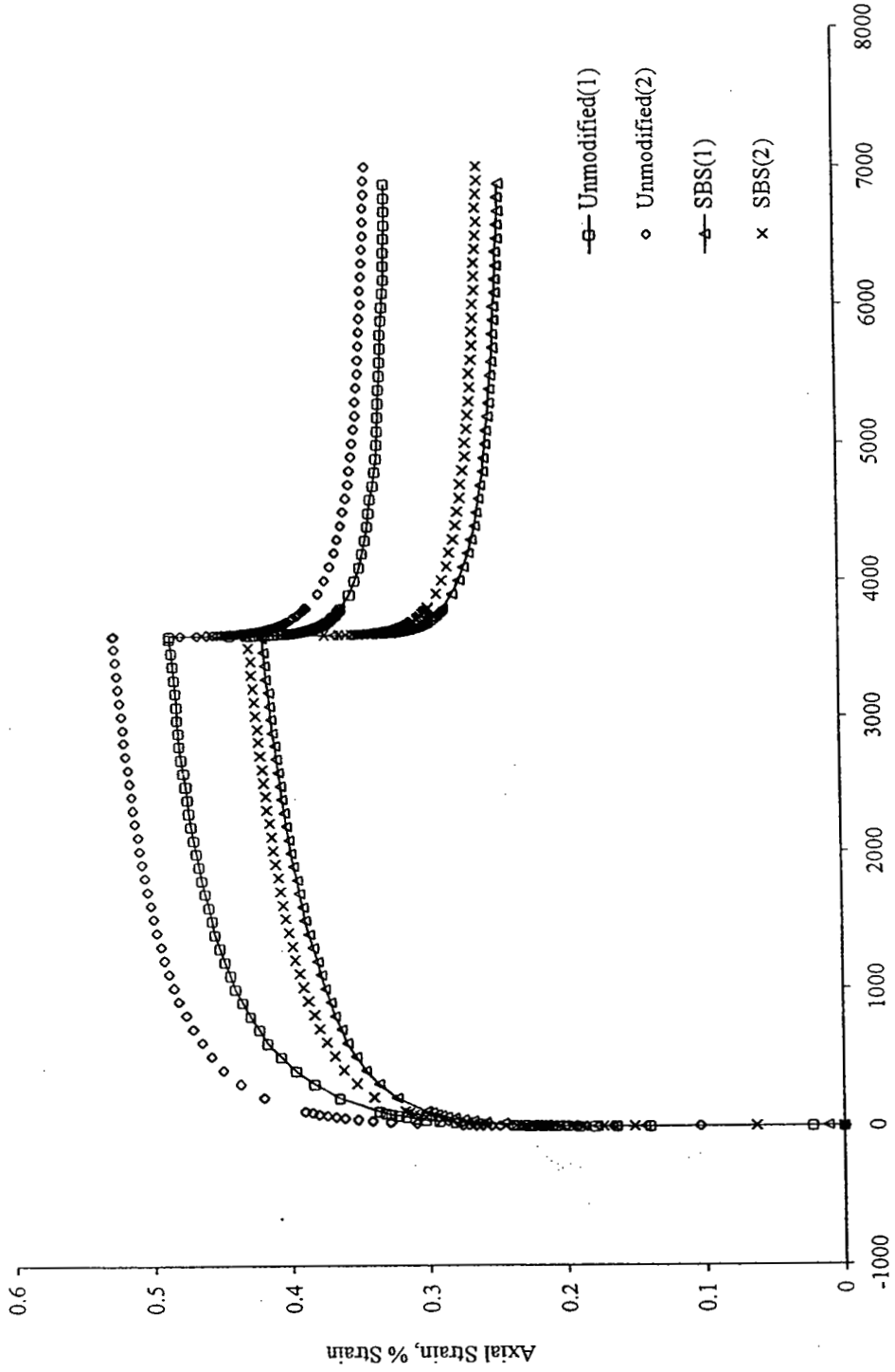

Figure B.8 Creep curves of coarse mixes at 40 ^{o}C; effect of asphalt type

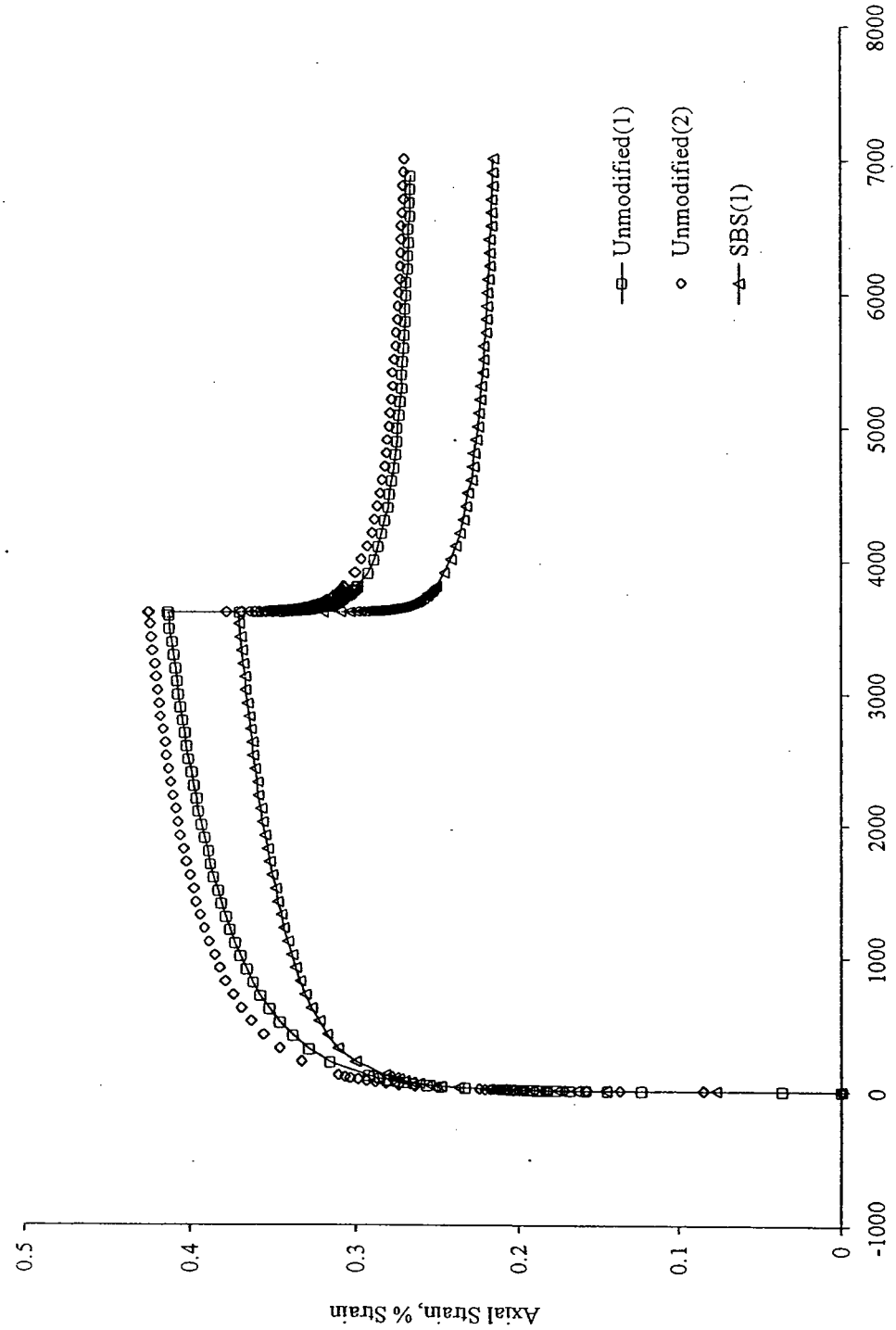

Figure B.9 Creep curves of intermediate mixes at 40 ^{O}C; effect of asphalt type

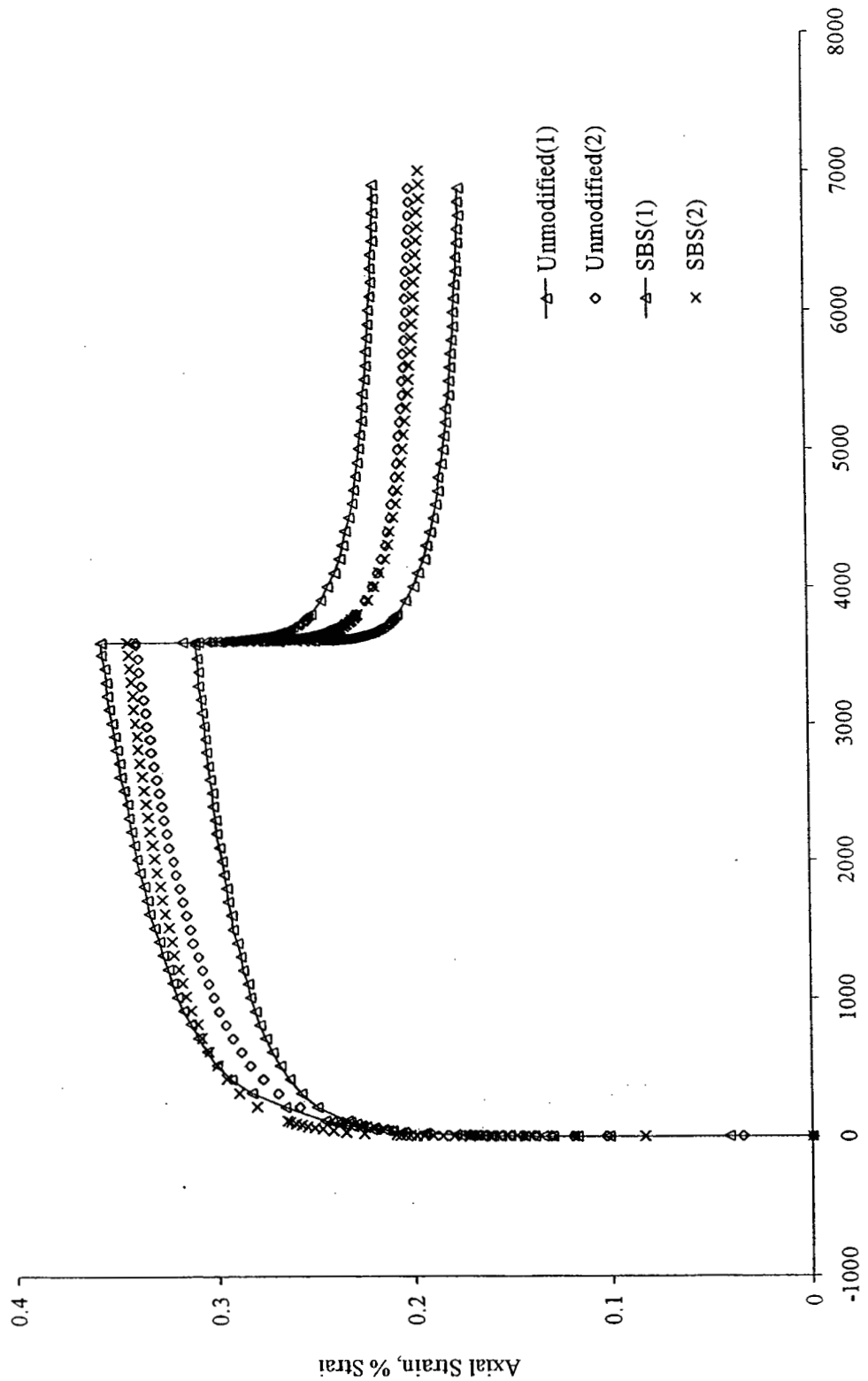

Figure B.10 Creep curves of fine mixes at 40 ^{O}C; effect of asphalt type

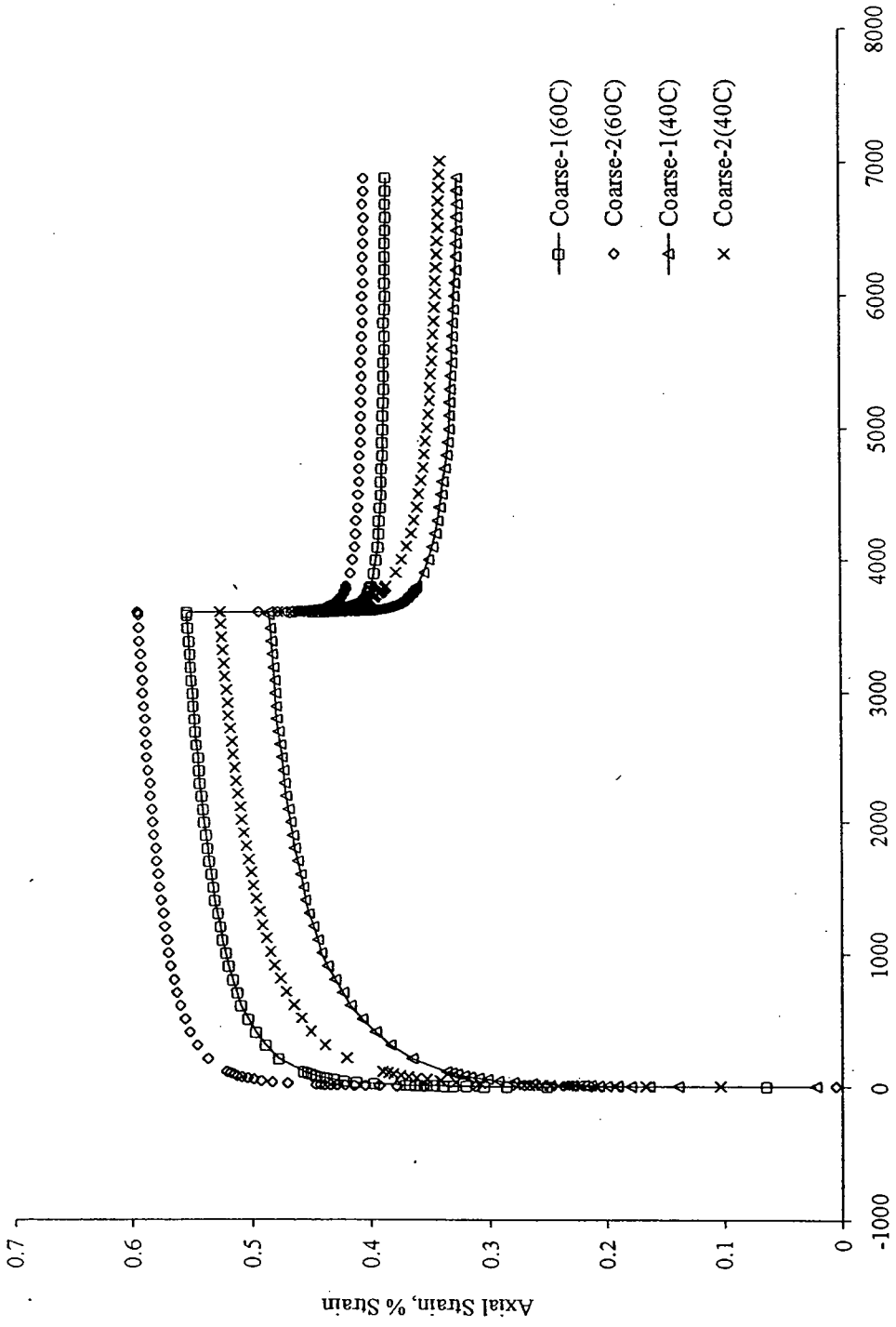

Figure B.11 Creep curves of coarse (unmodified) mixes at 60 ^{O}C and 40 ^{O}C, effect of temperature

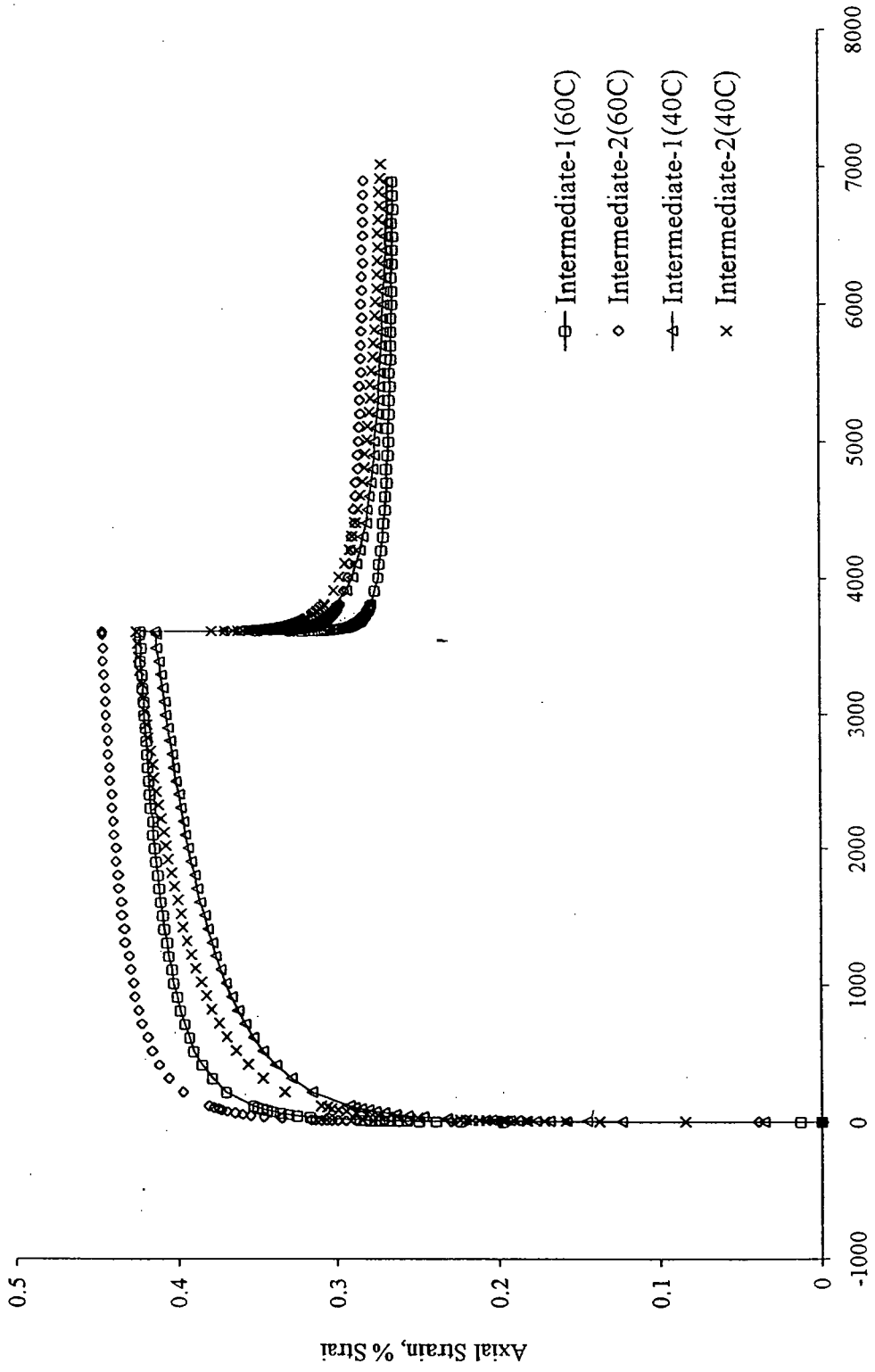

Figure B.12 Creep curves of intermediate (unmodified) mixes at 60 ^{o}C and 40 ^{o}C; effect of temperature

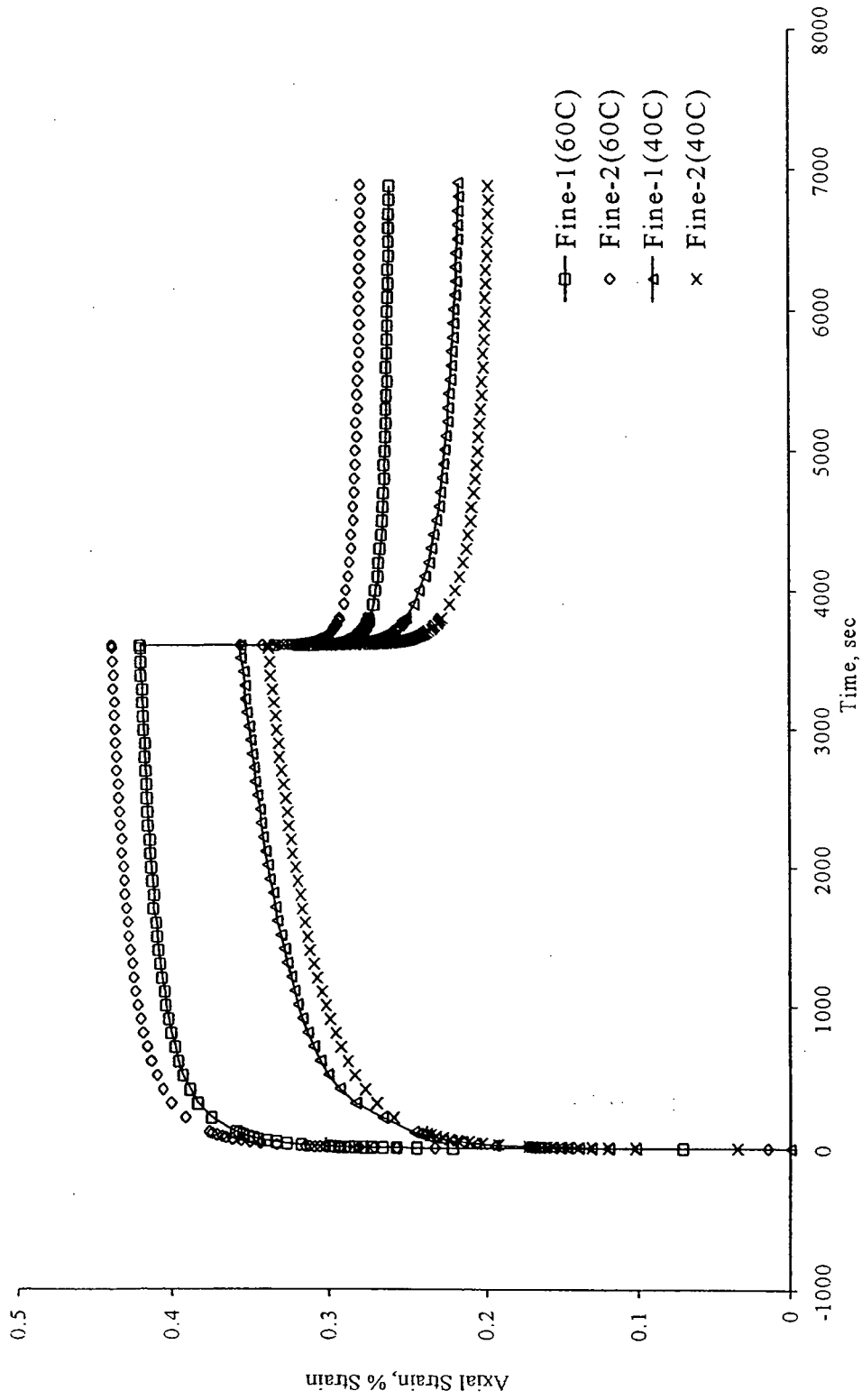

Figure B.13 Creep curves of fine (unmodified) mixes at 60 ^{O}C and 40 ^{O}C; effect of temperature

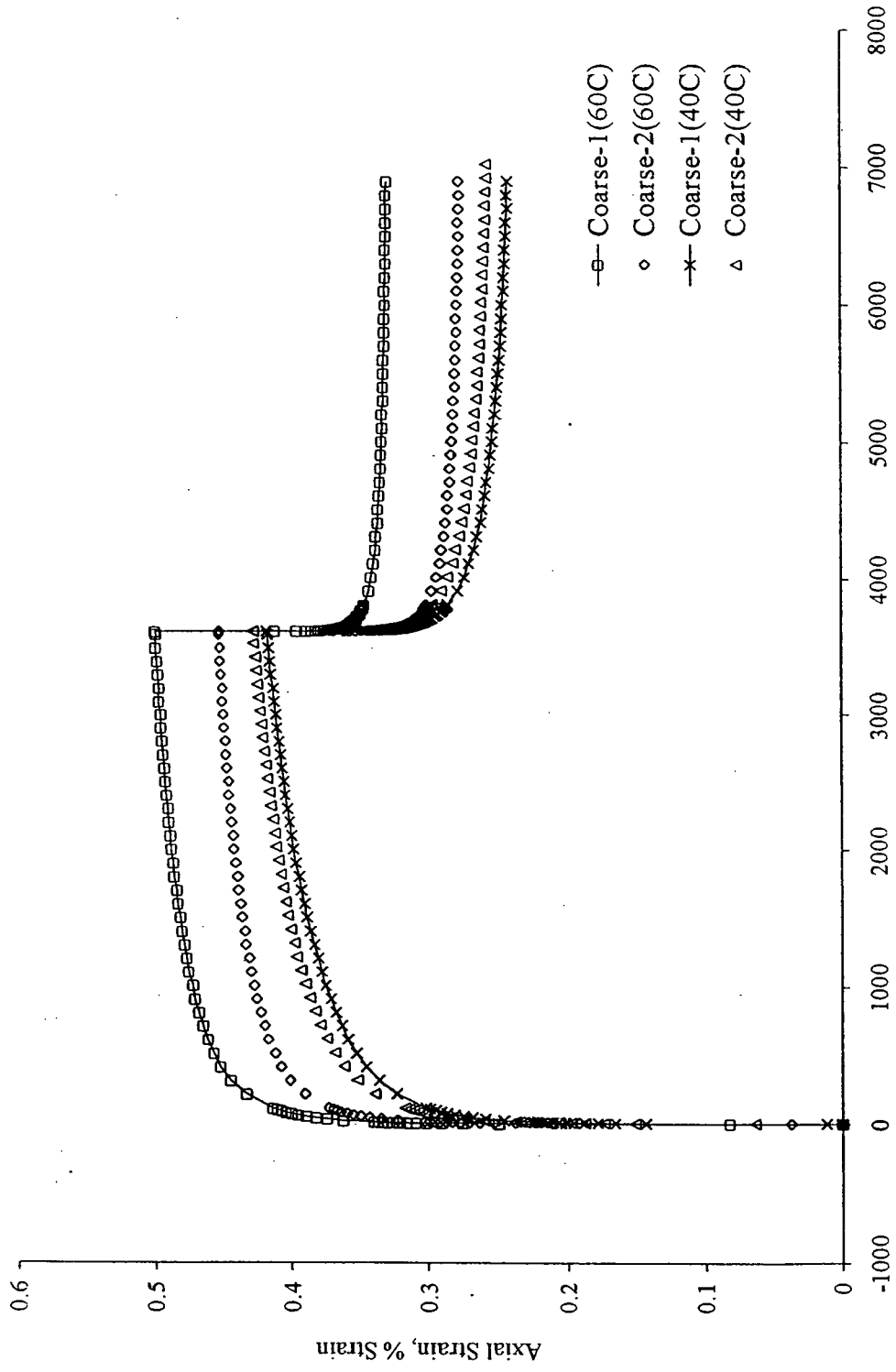

Figure B.14 Creep curves of coarse (SBS) mixes at 60 ^{O}C and 40 ^{O}C

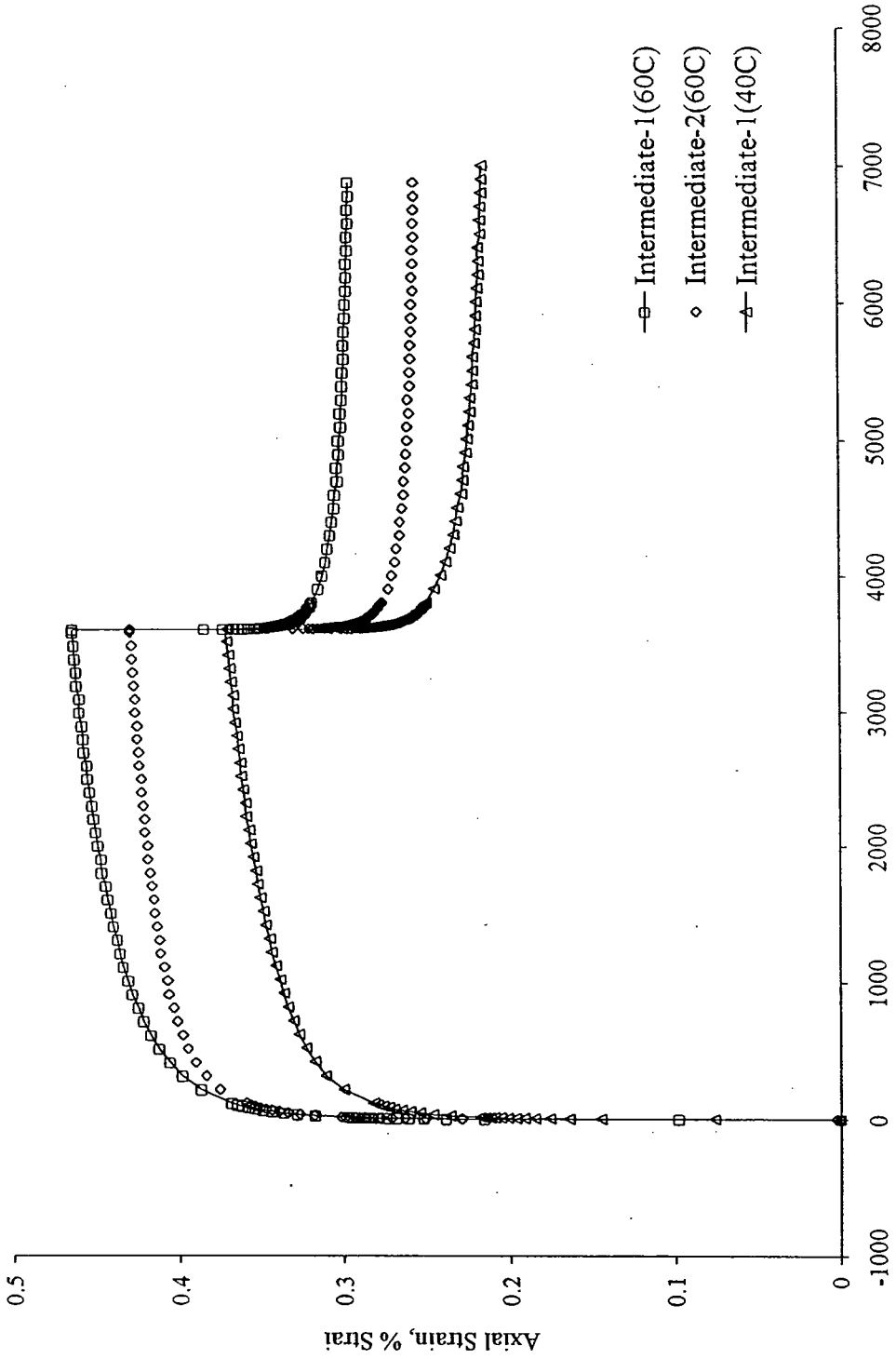

Figure B.15 Creep curves of intermediate (SBS) mixes at 60 ^{o}C and 40 ^{o}C

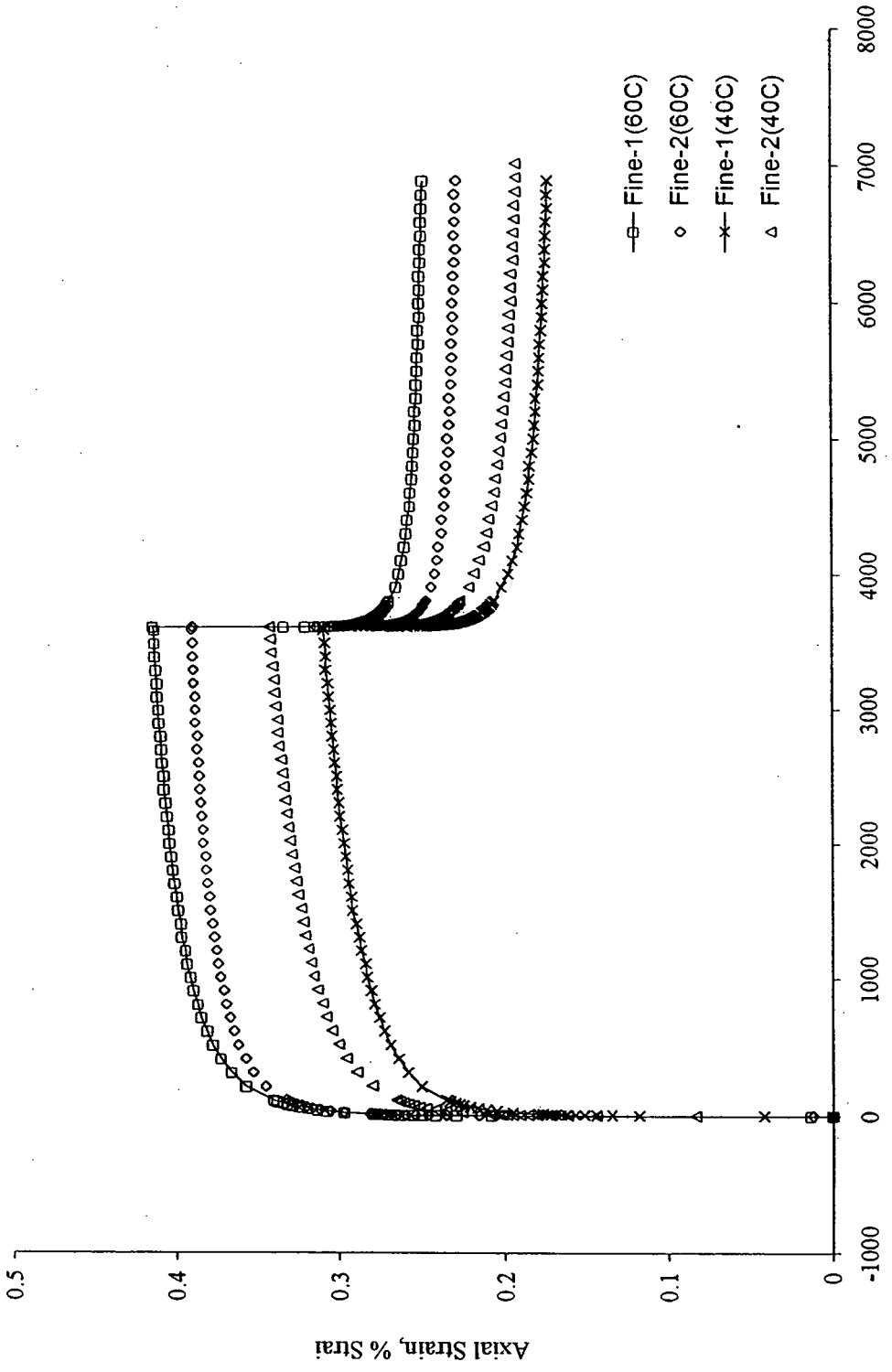

Figure B.16 Creep curves of fine (SBS) mixes at 60 ^{O}C and 40 ^{O}C

APPENDIX C

FATIGUE CURVES (FLEXURAL BEAM FATIGUE TEST)

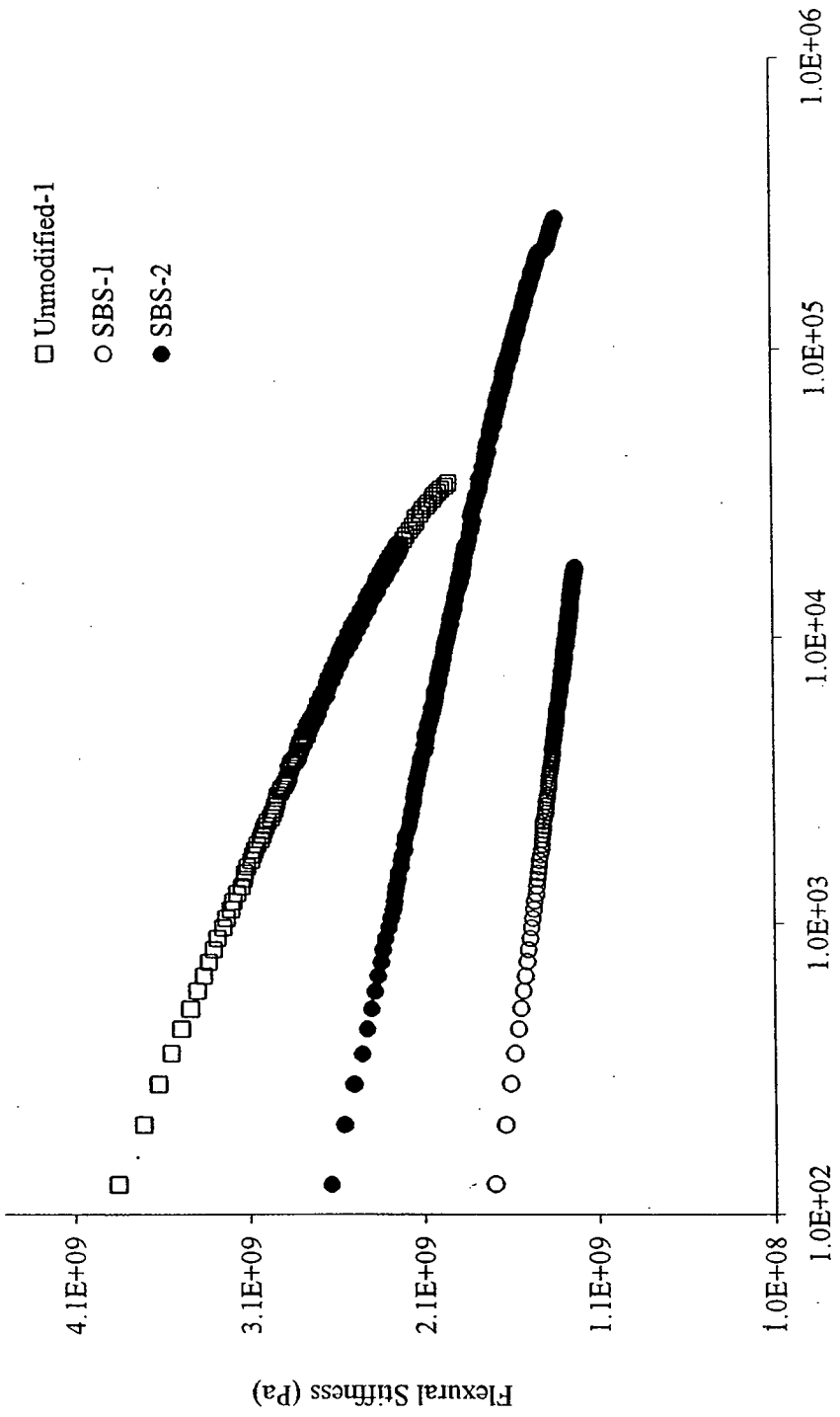

Figure C.1 Flexural stiffness versus number of load repetition for coarse mixes

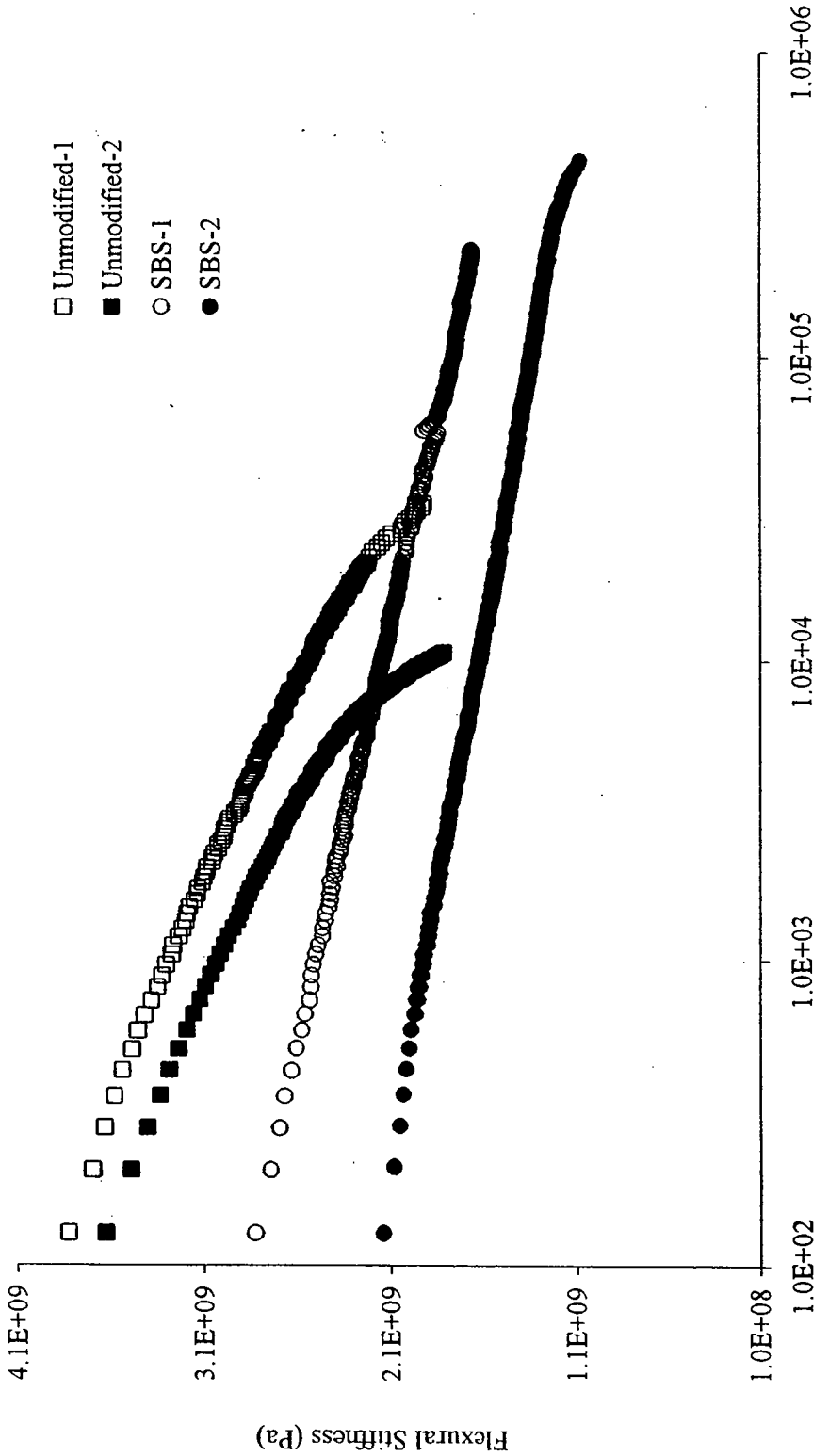

Figure C.2 Flexural stiffness versus number of load repetition for intermediate mixes

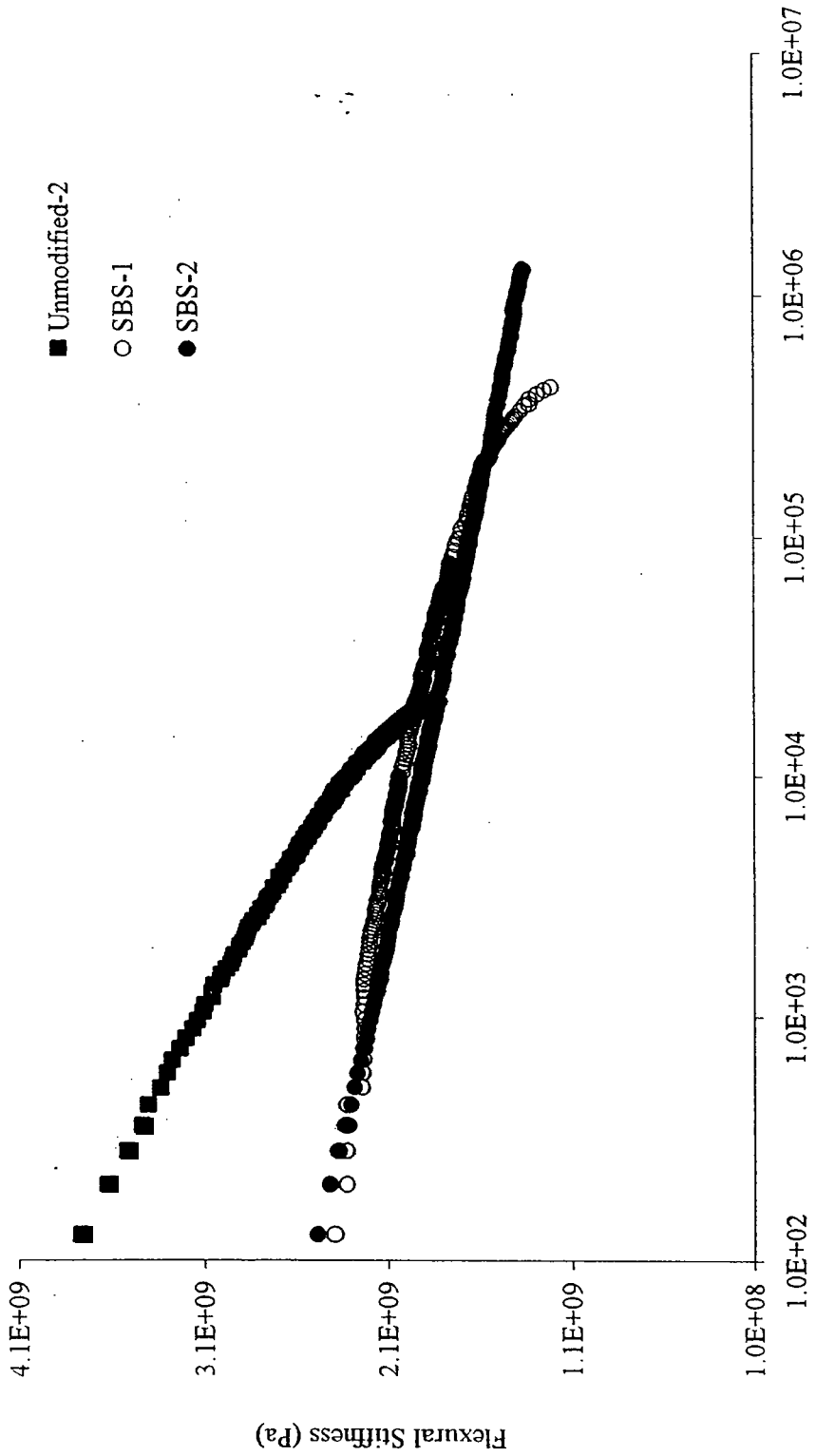

Figure C.3 Flexural stiffness versus number of load repetition for fine mixes